

Large N Conformal Field Theory from Gauge/Gravity Duality

Hasina Tahiridimbisoa Nirina Maurice

February 2017

*A thesis submitted to the Faculty of Science, University of the Witwatersrand, in
fulfillment of the requirements for the degree of Doctor of Philosophy*



UNIVERSITY OF THE
WITWATERSRAND,
JOHANNESBURG

Declaration

I, the undersigned, hereby declare that the work contained in this PhD thesis is my original work, and that any work done by others or by myself previously has been acknowledged and referenced accordingly. This thesis has not been submitted before for any degree or examination in any other university.

A handwritten signature in black ink, appearing to read 'Nirina Maurice Hasina Tahiridimbisoa'.

Nirina Maurice Hasina Tahiridimbisoa,

10 February 2017

Abstract

In this dissertation we exploit the AdS/CFT correspondence to describe a system of strings suspended between giant gravitons. The strings can be in an excited state. The excitations of the strings can be given a particle-like description and are known as magnons. The proposed gauge invariant operators used to construct a complete description of this system belong to the $\mathfrak{su}(2)$ sector of the $\mathcal{N} = 4$ SYM. Using an open spin chain description of the suspended strings, the states of the system we consider enjoy an $SU(2|2)^2$ symmetry. By making use of this symmetry, we compute the all loop anomalous dimensions of these operators. The spectrum of the dilatation operator in the $\mathfrak{su}(2)$ sector of the theory is reproduced in the dual gravity description. In the dual theory, the energies of the magnons are computed using strings in a background LLM geometry and the results are in complete agreement with the anomalous dimensions of the operators we have considered. Using the symmetries enjoyed by our system we achieve a complete determination - up to an overall phase - of the reflection/scattering matrix between a boundary magnon and a bulk magnon. Thus, although the open boundary conditions of the spin chain spoil integrability, the complete determination of the S -matrix is still possible. The two-loop subleading correction to the dilatation operator is also explored. This subleading term corresponds to a correction of the magnon energies. The computation of this subleading term requires consideration of the giant's backreaction on their excitations. We find that this backreaction implies a nontrivial mixing of the dual operators and this mixing is characterized completely.

Acknowledgements

I would like to thank my wife for being always very supportive to me in doing this project. Also I am very grateful for my two sons Mauricio and Joshua for their understanding, patience and sacrifice to complete this work. In addition, I would like to thank my supervisor Professor Robert de Mello Koch for taking most of his time to guide, teach and clarify to me how to do research in the framework of theoretical physics. In a big topic like string theory, it is very easy to get distracted and driven away from the direction to finish this project within the finite time offered for it. However, this is another quality I would like to thank my supervisor because he always helped me on each next move toward this end. I also want to thank Professor Vishnu Jejjala for his series of string theory lectures, which helped illuminate some of my knowledge on string theory. In addition, I would like to thank collectively all my officemates, especially A. L. Mahu, Abdelhamid M. A. Ali, Christopher Mathwin for being wonderful co-authors of the two publications we made and also to Gareth J. Kemp, who always shares and discusses physics with me whenever we meet. Without forgetting Lwazi, Teflon, Randle and my other student friends, having all of you in the office were very supportive and helpful to me to achieve this work.

The author also acknowledges the founding support of the German Academic Exchange Services (DAAD) with the help of the African institute of Mathematical Sciences (AIMS) to make this project possible.

Contents

Declaration	ii
Abstract	iii
Acknowledgments	iv
1 Introduction: Background and general overview	3
1.1 Novel results obtained in this study	7
1.2 The AdS/CFT correspondence	9
1.2.1 AdS space	9
1.2.2 Symmetry argument relating $\mathcal{N} = 4$ SYM theory and type	
IIB superstring theory	10
1.2.3 A heuristic motivation for AdS/CFT	11
1.3 Review of the large N expansion	13
1.4 Zero dimensional Matrix Model	17
1.4.1 Matrix model correlation functions in terms of $\mathcal{Z}[J]$	18
1.4.2 Examples of correlation functions	19
1.4.3 Ribbon graph Feynman diagrams	19
1.4.4 Higher order correlation functions	20
1.5 CFT	22
1.5.1 Introduction to CFT	22
1.5.2 Correlation functions in CFT	26
2 Anomalous Dimensions of Heavy Operators from Magnon Energies	27

2.1	Outline of chapter	27
2.2	Chapter introduction	28
2.3	Giants with open strings attached	34
2.4	Action of the Dilatation Operator	37
2.5	Large N Diagonalization: Asymptotic States	40
2.6	String Theory Description	42
2.7	From asymptotic states to exact eigenstates	48
2.8	S –matrix and boundary reflection matrix	51
2.9	Links to the Double Coset Ansatz and Open String Theory	58
2.10	Summary of chapter	61
3	Interacting double coset magnons	64
3.1	Outline of chapter	64
3.2	Chapter introduction	64
3.3	The two loop dilatation operator	68
3.3.1	Leading contribution	68
3.3.2	Subleading contribution	71
3.4	Example: A 2 giant graviton boundstate with 4 strings attached	75
3.5	Summary of chapter	78
4	Conclusions	80
	Appendices	82
A	Large N eigenstates	83
B	Two loop computation of boundary magnon energy	91
C	The difference between simple states and eigenstates vanishes at large N	93
D	Review of dilatation operator action	96
E	One loop computation of bulk/boundary magnon scattering	99

F Another check of the S–matrix	103
F.1 Numerical one-loop perturbative check of the reflection S –matrix	103
F.2 Setting up the numerical test	104
F.2.1 Solutions for $p_2 = 0$	104
F.2.2 General solutions for $p_2 \neq 0$	105
F.2.3 Numerical plots for the magnitudes	106
F.2.4 Numerical plots for the phase differences	107
F.2.5 Relative errors in the magnitudes	109
G No integrability	111
H Double Coset background	113
I How to compute traces	116
I.1 Projector transformed	117
I.2 Summing over H	117
I.3 Summing over S_m	119
I.3.1 First evaluation	119
I.4 Second evaluation	120
I.5 General result	122
I.6 Illustration of the general result	124
I.7 Results for the 2–brane 4–string system	126
J Gauss graph normalization	128
K The projective null cone in $D = 6$ and CFT in $\mathbb{R}^{1,3}$	133
K.1 Reproducing conformal transformations in $\mathbb{R}^{1,3}$	137
L Review of the two point CFT correlation function	142
References	153

List of Figures

1.1	Illustration of an excited state of 3 giants with strings stretching between them. The black nodes represent the giants and the blue curves represent the strings. The particles excitation of the strings are called magnons.	5
1.2	Illustration of a stack of N $D3$ –branes with strings attached to them.	11
1.3	Gauge field propagator in the ribbon graph notation.	14
1.4	Three-point and four-point vertices in the ribbon graph notation.	14
1.5	Ribbon graphs define a triangulation of a two-dimensional surface.	15
1.6	<i>i</i>) $\Sigma_0 = S^2$ is a two-sphere - <i>ii</i>) $\Sigma_1 = T_2$ is a two dimensional torus and <i>iii</i>) represent a typical Σ_h where h is the genus of the surface (or number of handles).	16
1.7	We illustrate in the above figures how to go from a planar Feynman diagram figure a) to a triangulation of a two-sphere figure b). The next figure shows a typical non-planar Feynman diagram figure c) to a triangulation of a torus figure d).	17

2.1	A cartoon illustrating the R, R_1^k, R_2^k labeling for an example with $k = 4$ open string strings and 3 giant gravitons. The shape of the strings stretching between the giants is not realistic - only the locations of the end points of the open strings is accurate. The giant gravitons are orbiting on the circles shown; the radius shown for each orbit is accurate. They wrap an S^3 which is transverse to the plane on which they orbit. The smaller the radius of the giants orbit, the larger the S^3 it wraps. The size of the S^3 that the giant wraps is given by its momentum, which is equal to the number of boxes in the column which corresponds to the giant. The numbers appearing in the boxes of R_1^4 tell us where the open strings start and the numbers appearing in the boxes of R_2^4 where they end.	36
2.2	The cutoff function used in constructing large N eigenstates	41
2.3	The giant is orbiting on the smaller circle shown. Each red segment is a magnon. The arrows in the figure simply indicate the orientation of the central charge k_i of the i th magnon. The LLM disk is shaded in this and subsequent figures. This is done to distinguish the rim of the LLM disk from the orbits of the giant gravitons.	43
2.4	A bulk magnon subtending an angle θ has a length of $2 \sin \frac{\theta}{2}$	44
2.5	A boundary magnon subtending an angle θ has a length $\sqrt{(1-r)^2 + 4r \sin^2 \frac{\theta}{2}}$	45
2.6	A two strings attached to two giant gravitons state. To distinguish the two strings, one of them has been indicated with dashed lines. Both giants are submaximal and so are moving on circles with a radius $ z < 1$. One of the strings has only two boundary magnons. The second string has two boundary magnons and three bulk magnons. Notice that each open string has a non-vanishing central charge. It is only for the full state that the central charge vanishes. See [1] for closely related observations.	46
2.7	A boundary magnon subtending an angle has a length of $\sqrt{(r-1)^2 + 4r \sin^2 \frac{\theta}{2}}$	47
2.8	A bulk magnon scatters with a boundary magnon. In the process the direction of the momentum of the bulk magnon is reversed.	49

2.9	A bulk magnon scatters with a boundary magnon. In the process the direction of the momentum of the bulk magnon is reversed. Before the scattering the boundary magnon subtends an angle φ_1 and the bulk magnon subtends an angle φ_2 . After the scattering the boundary magnon subtends an angle $\varphi_1 + \varphi_2 + \theta$ and the bulk magnon subtends an angle $-\theta$	50
2.10	A bulk magnon scatters with a boundary magnon. The sum of the momenta of the two magnons is . Here we only show two of the magnons; we indicate them in red before the scattering and in green after the scattering. In the process the direction of the momentum both magnons is reversed.	57
J.1	This Gauss graph is one of the double coset elements defined by the charge $\vec{m} = [2, 4]$. One possible label is $\sigma = (1, 4)(2, 3)$	128
J.2	Above, the two dashed horizontal lines are identified. In doing so, this Gauss graph is another graphic representation of the Gauss graph in Figure J.1	129
J.3	Illustration of a generic Gauss graph label by $\sigma \in H \setminus S_m / H$. Again the two dashed horizontal lines are identified.	129
J.4	Graphical manipulation of the Gauss graph labeled by $\gamma_1 \sigma \gamma_2$ and its relation to the Gauss graph labeled by σ	130
J.5	Above, we have only illustrated the n_{ij} parallel strings stretching from the i 'th giant to the j 'th giant. The $n_{ij} + n_{ij}$ different integers labeling these strings belong respectively to $\{\mathfrak{M}_{i-1} + 1, \dots, \mathfrak{M}_i\}$ for the starting points and $\{\mathfrak{M}_{j-1} + 1, \dots, \mathfrak{M}_j\}$ for the ending points.	131
K.1	This figure gives an illustration of the light cone of the spacetime $\mathbb{R}^{2,4}$. The red section line is identified with the 4-dimensional spacetime $\mathbb{R}^{1,3}$. X^\pm are light cone coordinates defined by $X^\pm = \frac{X^5 \pm X^4}{\sqrt{2}}$	134

LIST OF FIGURES

- K.2 Illustration of the action of $\Lambda \in SO(2, 4)$ followed by rescaling $\lambda(X)$ on a small displacement in the section of the light cone, which is identified to be the 4-dimensional space $\mathbb{R}^{1,3}$ 136

Chapter 1

Introduction: Background and general overview

In this thesis, we consider $\mathcal{N} = 4$ super Yang-Mills theory (SYM) with gauge group $U(N)$. By making a novel use of symmetries present, we compute anomalous dimension of a certain class of operators whose classical dimension goes as $O(N)$ in the large N limit. We will begin by developing the background from $\mathcal{N} = 4$ SYM that is relevant to the study of this thesis. The discussion of the symmetries that play a central role is carried out at the end of this section.

In $\mathcal{N} = 4$ SYM theory there are 6 real scalar spin-0 fields ϕ_i ; one spin-1 gauge field \mathcal{A}_μ and four spin- $\frac{1}{2}$ fermionic fields ψ_I . These quantum fields of the theory are in the adjoint representation of the gauge group so that each field is a $N \times N$ matrix. The operators with classical dimension of order N that we consider are composed using the ϕ_i fields. It is usual to complexify these 6 scalar fields into three complex fields X , Y and Z as

$$X = \phi_5 + i\phi_6, \quad Y = \phi_3 + i\phi_4, \quad Z = \phi_1 + i\phi_2. \quad (1.1)$$

One of the uses of this rewriting is that it allows us to define closed subsectors of the theory that do not mix when the theory is renormalized. In this situation we can study the dilatation operator within a given subsector. In this thesis we will focus on the $\mathfrak{su}(2)$ sector of the theory, defined by focusing on operators

constructed using only the Z and Y fields. The operators we consider will be composed of order N Z 's and order 1 Y 's. It is a challenging problem to evaluate their correlators at large N . This is because one encounters huge combinatoric factors which overpower the usual $\frac{1}{N^2}$ suppressions so that we can not ignore the contribution coming from non-planar diagrams. Accordingly, the usual methods for computing matrix model correlation functions are no longer effective. The usual method for evaluating correlators of a generic $U(N)$ gauge theory is due to 't Hooft [2]. Feynman diagrams are drawn as ribbon graphs and suggest that in the limit $N \rightarrow \infty$ the gauge theory is dual to a free string theory. Accordingly, 't Hooft identified $\frac{1}{N}$ as the string coupling g_s . We will review in Sec. 1.3 't Hooft's proposal concerning the large N limit of a gauge theory.

Although the usual method is not effective in evaluating correlation functions of the operators we consider, it turns out that group representation theory techniques provide a powerful approach to the problem. Group representation theory techniques were first introduced by the authors of [3] to evaluate correlators of operators belonging to the $\frac{1}{2}$ -BPS sector. The study [3] is strongly motivated by the AdS/CFT correspondence.

According to the AdS/CFT correspondence four-dimensional $U(N)$, $\mathcal{N} = 4$ SYM is dual to type IIB superstring theory on the $\text{AdS}_5 \times S^5$ background. This particular gauge/gravity duality is the most studied example of the AdS/CFT correspondence. In general, the AdS/CFT correspondence claims a duality between a gauge theory in a p -dimensional spacetime that enjoys conformal invariance and quantum gravity on $\text{AdS}_{p+1} \times X$, where X is some compact manifold. The AdS/CFT correspondence is a strong/weak duality. In other words if the coupling strength is strong on one side of the correspondence, the dual is weakly coupled. This strong/weak coupling duality is remarkably useful since it allows us to explore strong coupling limits by using the weakly coupled dual theory.

According to the AdS/CFT correspondence, the operators we consider in the gauge theory have a dual interpretation in the gravity description. According to the correspondence, operators with a classical dimension that grows like N as we take $N \rightarrow \infty$ are identified as giant gravitons in the string theory. Giant gravitons are an example of D3-branes in the type IIB superstring theory.

The giant gravitons have a worldvolume with S^3 topology so that they have a vanishing $D3$ monopole moment but a non-vanishing $D3$ dipole moment. In this sense, they are not typical $D3$ –branes and in fact are only stable as a consequence of the background RR flux. The relevant literature discussing giant gravitons includes [4; 5; 6]. In the type IIB superstring theory D-branes are non perturbative objects. To see that D-branes are non-perturbative, it is enough to note that they are described by the Born-Infeld action with a brane tension that is inversely proportional to the string coupling g_s . In the regime where g_s vanishes, the brane tension diverges and all D-branes decouple from the perturbative spectrum.

Giant gravitons expand in the S^5 or AdS_5 geometries. The scaling dimensions in the dual gauge theory correspond to the energies of the giants. In this way the anomalous dimensions of the gauge theory operators give the energy spectrum of the giants.

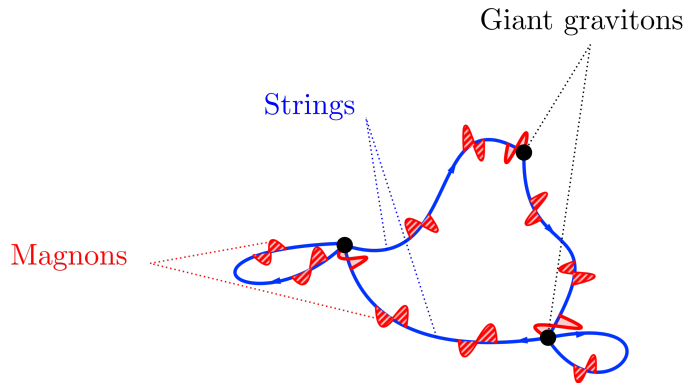


Figure 1.1: Illustration of an excited state of 3 giants with strings stretching between them. The black nodes represent the giants and the blue curves represent the strings. The particles excitation of the strings are called magnons.

A system of excited giant gravitons corresponds to a boundstate of giant gravi-

tons with strings stretching between them. Furthermore, a string suspended between two giant gravitons also can be excited¹ so that a cartoon illustration of some excited state of giants is given in Figure 1.1.

The expansion of the giant graviton expanding in the S^5 geometry is limited by the size of the S^5 . In contrast to this, a giant expanding in the AdS space is not limited. The expansion of the giant is due to a Lorentz force-like coupling to the background RR flux. The magnitude of this force is directly proportional to the angular momentum of the giant. Accordingly, it follows that the restriction on the size of the giant translates into a constraint on the momentum of the giant. The giants trace out non-geodesic motion as a consequence of the force coming from the RR flux. The size of the giant reflects this force and hence the actual orbit followed by the giant in spacetime. The strings attached to the giant are dragged in this non-geodesic motion. In Chapter 2 we will explain in detail how the size of the giants affects their string excitations and the magnon excitations of these strings.

The gauge invariant operators we consider are built from products of traces of fields. A generic local operator we consider takes the form

$$\cdots \text{Tr}(Z^{n_1}YZ^{n_2}\cdots Z) \text{Tr}(Z^{m_1}YZ^{m_2}\cdots Z)\cdots \text{Tr}(Z^{p_1}YZ^{p_2}\cdots Z)\cdots, \quad (1.2)$$

where the total number of Z 's fields is order N and the number of Y fields is order 1. A string in the dual description is constructed using $O(\sqrt{N})$ Z 's. The magnon excitations correspond to the Y fields. The construction of these gauge theory operators uses techniques from group representation theory and they are called restricted Schur polynomials. Relevant background includes [7; 8; 9; 10; 11]. We will postpone the complete description of these operators to Chapter 2.

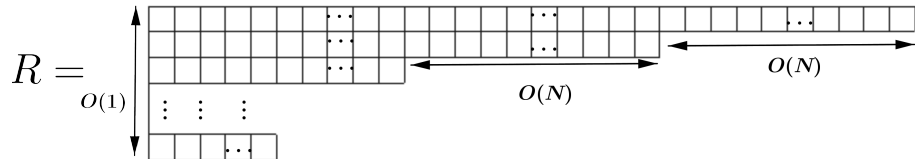
We will now discuss the symmetries we use to compute the anomalous dimensions. Following [12; 13] the string suspended between the giants has an open spin chain interpretation. This spin chain enjoys an $SU(2|2)^2$ symmetry. Understanding the action of this symmetry on the operators we consider will essentially determine the anomalous dimensions, which is our main goal. The

¹The excitations of the open strings can be given a particle-like interpretation as magnons of a spin chain.

details of this argument will be developed in Chapter 2

1.1 Novel results obtained in this study

The purpose of this section is to review the literature relevant to the class of problems considered in this thesis. In this way we are able to situate our results in this field of study. First, the exact correlators of the restricted Schur polynomials, which are the operators we consider in this work, were studied by the authors of [7; 8; 9; 10; 11]. Using these operators the authors of [14; 15; 16; 17; 18; 19] computed the anomalous dimensions in the $\mathfrak{su}(2)$ sector of $\mathcal{N} = 4$ SYM. Further, [19] managed to compute the leading higher loop anomalous dimensions for a class of restricted Schur polynomials. This class of restricted Schur polynomials are labeled by Young diagrams R with order N boxes that have the following shape



In the Young diagram R illustrated above, we assume that there are $p \sim O(1)$ rows. Each row contains order $O(N)$ boxes. The difference in the number of boxes in two different rows is also of order N . We recall that each row of the Young diagram R is identified as a giant graviton. In this way, the Young diagram R labels a boundstate of p giant gravitons. The above limit for the shape of Young diagram R was needed for the analysis of [19]. In this limit, the backreaction of the giant gravitons on their string excitations can be ignored and the action of the leading higher loop dilatation operator is factorized into two separate actions on the Z 's and the Y 's. In this way, one is able to demonstrate that the eigenstates of the leading higher loop dilatation operator are the states of a collection of harmonic oscillators. These harmonic oscillators were introduced by the authors of [16] and generalized in [19]. The rigorous mathematical background needed to solve the eigenvalue problem using the harmonic oscillators is developed in [20]. The eigenstates are called Gauss

graph operators.

The studies described above manage to reproduce the expected state space for excited giant gravitons. They do not however make contact with the semi-classical string physics developed in [21]. The novel results presented in this thesis will provide this link. In particular by giving the open string a description as a gauge theory word composed of $O(\sqrt{N})$ letters we recognize the open string as an open spin chain. Excitations of this open string are then described using the magnon language of [21]. Furthermore, we also compute the reflection/scattering between a boundary magnon and a bulk magnon. These results follow by implementing the $SU(2|2)^2$ symmetry. Details of this first result are summarized in Chapter 2 of this dissertation.

The results that we have obtained for the scattering of open string magnons complement a number of existing results in the literature. The use of the $SU(2|2)^2$ symmetry was pioneered in [12; 13] where the S –matrix of two bulk magnons on a closed string was determined. In addition to this Maldacena and Hofman considered the case of a maximal giant graviton and computed the S –matrix of a boundary magnon and a bulk magnon [22]. The analysis again uses the $SU(2|2)^2$ symmetry. Following these results, the reflection/scattering S –matrix we obtain in Chapter 2 is for the case of a boundary magnon and a bulk magnon, for giant gravitons of any size. In this way, our S –matrix results interpolate between the results in [12; 13] and [22]. Motivated by the Maldacena and Hofman works [22] we also compute the energies of magnon excitations of the strings suspended between submaximal giants. In perfect agreement with general predictions of AdS/CFT, we find that these magnon energies correspond exactly with the anomalous dimensions of the operators we consider on the gauge theory side.

Starting at the subleading two loop anomalous dilatation operator, the back-reaction of the giants on their excitation becomes important and one has to consider this contribution to operator mixing. This contribution results in a mixing of Gauss graph operators under renormalization. This mixing has been computed in detail. A discussion of these results is given in Chapter 3 of this thesis.

To conclude this section, we now outline the remainder of this thesis. The re-

maining sections in Chapter 1 provide a general review and background relevant for the thesis. We start with a broad review of the AdS/CFT correspondence in section 1.2. Then we review, in section 1.3, 't Hooft's argument employing ribbon diagrams for the correlators of a generic $U(N)$ gauge theory. The section 1.4 that follows is focused on a review of the zero-dimensional matrix model correlation functions. Our aim in this section is to explain the complexity of large N but non-planar limits. To conclude this first chapter we consider some basic elements of CFTs. In Chapter 2 we will report the first novel result of this thesis. The contents of Chapter 2 were published in JHEP 03 (2016) 156. Chapter 3 describes further results. These results were published in Phys. Rev. D 93, 0650057 (2016). Finally, we will conclude this dissertation in Chapter 4.

1.2 The AdS/CFT correspondence

1.2.1 AdS space

Classically, gravity is described by General Relativity (GR). According to GR, the equations describing gravity as a curvature of spacetime are the Einstein equations

$$R_{\mu\nu} - \frac{1}{2}g_{\mu\nu}R = \kappa T_{\mu\nu}. \quad (1.3)$$

On the right hand side of this equation, $T_{\mu\nu}$ is the energy momentum tensor. On the left hand side R and $R_{\mu\nu}$ are respectively the Ricci scalar and Ricci tensor. The left hand side of (1.3) describes purely intrinsic geometrical properties of the spacetime.

AdS_5 is a manifold with Lorentzian signature metric. AdS_5 is the maximally symmetric solution to the Einstein equation (1.3), with cosmological constant Λ . To see this, start with the Einstein-Hilbert action

$$S = \frac{1}{16\pi G_5} \int dx^5 \sqrt{|g|} (R - \Lambda), \quad (1.4)$$

and solve the classical equation of motion $\frac{\delta S}{\delta g^{\mu\nu}} = 0$, to find

$$R_{\mu\nu} - \frac{1}{2}g_{\mu\nu}R = -\frac{\Lambda}{2}g_{\mu\nu}, \quad R = \frac{5}{3}\Lambda, \quad R_{\mu\nu} = \frac{\Lambda}{3}g_{\mu\nu}. \quad (1.5)$$

Using global coordinates

$$\begin{aligned} x_0 &= L \cosh \rho \cos \tau, \\ x_5 &= L \cosh \rho \sin \tau, \\ x_i &= L \sinh \rho \hat{x}_i, \quad \sum_{i=1}^4 \hat{x}_i^2 = 1, \end{aligned}$$

the metric of the AdS_5 is

$$ds^2 = L(-\cosh^2 \rho d\tau^2 + d\rho^2 + \sinh^2 \rho d\Omega_3^2). \quad (1.6)$$

Above, $d\Omega_3^2$ is the metric on a three-dimensional sphere S^3 . Having this metric of the AdS_5 space, it is possible to see that the isometry group is $SO(2, 4)$. $SO(2, 4)$ is the connected conformal group in a flat four-dimensional spacetime. Hence, we already have a hint that the AdS_5 space and CFTs in 4–dimensional spacetime might be related.

1.2.2 Symmetry argument relating $\mathcal{N} = 4$ SYM theory and type IIB superstring theory

The $\text{AdS}_5 \times S^5$ spacetime with N units of RR five form flux is an exact background solution of type IIB superstring theory. The AdS/CFT correspondence claims that IIB superstring theory on this background is exactly equivalent to $\mathcal{N} = 4$ super Yang-Mills theory. The first evidence for the correspondence is an exact match of the symmetries enjoyed by these two theories.

First, note that type IIB superstring theory and $\mathcal{N} = 4$ SYM theory are both supersymmetric theories with the same number of supercharges. Further, $\mathcal{N} = 4$ SYM enjoys conformal symmetry, even at the quantum level. Accordingly, we learn that both theories have the same $SO(2, 4)$ symmetry. On the gravity side, this symmetry is realized as the isometry group of the AdS_5 spacetime. In the gauge theory, it is the conformal invariance of the theory.

Another obvious symmetry present in the gravity theory is the $SO(6)$ isometry of the S^5 geometry. In the gauge theory this is identified with the global $SU(4) \sim SO(6)$ R –symmetry that rotates the supercharges.

Although a matching of the symmetries of the two theories is suggestive,

it is certainly not a proof of the correspondence. Indeed, although significant evidence for the conjecture exists, it is still not proved.

1.2.3 A heuristic motivation for AdS/CFT

Following [23; 24] a convenient way to derive the full action of the $D = 4$, $\mathcal{N} = 4$ SYM is to start with $D = 10$, $\mathcal{N} = 1$ SYM and then dimensionally reduce it to $D = 4$. We will not review the full action of the $D = 4$, $\mathcal{N} = 4$ SYM, instead we only present the bosonic part. The bosonic part of the Lagrangian of the $\mathcal{N} = 4$ SYM in 4–dimensional spacetime is²

$$\mathcal{L}_B = \frac{1}{g_{YM}^2} \int d^4x \text{Tr} \left(\frac{1}{2} \mathcal{F}_{\mu\nu} \mathcal{F}^{\mu\nu} + D_\mu \phi_i D^\mu \phi^i + \frac{1}{2} [\phi_i, \phi_j] [\phi^i, \phi^j] \right) \quad (1.7)$$

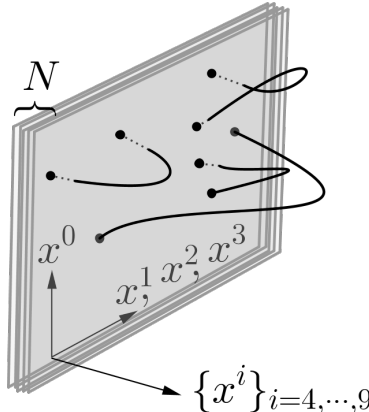


Figure 1.2: Illustration of a stack of N $D3$ –branes with strings attached to them.

One way to motivate the AdS/CFT correspondence considers a system of N parallel, coincident $D3$ –branes in Type IIB string theory. This system admits two possible descriptions. Since the $D3$ –branes are massive charged objects, they act as a source for supergravity fields. In particular, the $D3$ –branes deform

²Repeated indices are summed. This summation includes the spacetime indices μ, ν, \dots and the indices on the bosonic fields.

the spacetime thereby producing a nontrivial spacetime geometry. Further, they are charged so that they source N units of RR 5-form flux. The supergravity description can be trusted at weak string coupling (when quantum corrections can be neglected) and in the limit that we have a very large number N of $D3$ –branes ensuring a spacetime geometry that is approximately flat. The second possible description for the system understands the $D3$ –branes as boundary conditions for open strings. In this second description, both open and closed strings play a role. Note that in the first description, only closed strings appear. To motivate the correspondence, we now take a low energy limit and require equivalence of the two descriptions in this limit.

The low energy limit of the first description captures two decoupled systems. First, we have long wavelength supergravity modes propagating in the region away from the branes, where spacetime is approximately flat. Since these modes have a very large wavelength they are not able to resolve the $D3$ –branes and they do not even detect the presence of these branes. The second system is comprised of all of the modes of the Type IIB string theory close to the stack of branes. These modes are red-shifted to a low energy due to the huge gravitational potential they experience in the local vicinity of the $D3$ –branes. The local geometry in the vicinity of the $D3$ –branes is the $\text{AdS}_5 \times S^5$ spacetime. So, in summary, the low energy limit has produced two decoupled sectors: (i) long wavelength supergravity modes propagating in 10–dimensional Minkowski spacetime and (ii) all of the modes of Type IIB superstring theory in the $\text{AdS}_5 \times S^5$ geometry.

Now consider the description invoking both open and closed strings in the Type IIB string theory. The low energy limit of the closed string states gives long wavelength supergravity modes propagating in 10–dimensional Minkowski spacetime. The low energy limit of the open string states is $\mathcal{N} = 4$ SYM theory. Further, in the low energy limit, the interaction mixing the closed and open string sectors vanish and the two sectors again decouple. So, in summary, the low energy limit has produced two decoupled sectors: (i) long wavelength supergravity modes propagating in 10–dimensional Minkowski spacetime and (ii) 3+1 dimensional $\mathcal{N} = 4$ SYM theory.

Since we believe these two descriptions are equivalent, their low energy

physics should also be equivalent. We are then lead to conclude that Type IIB superstring theory on $\text{AdS}_5 \times S^5$ is dual to $\mathcal{N} = 4$ SYM theory.

With this discussion in hand, we have a new insight into how to interpret the matrix valued fields of the SYM theory. The SYM theory describes the low energy limit (i.e. the zero modes) of the open string system. The six scalar fields of the theory describe directions transverse to the $D3$ –branes, while the gauge fields describe directions parallel to the $D3$ –branes. Recall that we are considering N $D3$ –branes stacked on top of each other. The matrix indices which run from 1 to N label which brane inside the stack the open string is connected to. Diagonal elements of the matrix field describe open strings that start and end on the same $D3$, while off diagonal elements of the matrix field describe strings that stretch between two different $D3$ –branes.

1.3 Review of the large N expansion

We review in this section the arguments [2] showing that the correlators of a generic $U(N)$ gauge theory are dominated by the planar diagrams of the theory. To start with, consider the pure $U(N)$ gauge theory with the Lagrangian

$$\mathcal{L} = -\frac{1}{4g_{YM}^2} \text{tr}(\mathcal{F}_{\mu\nu}\mathcal{F}^{\mu\nu}), \quad (1.8)$$

where

$$\mathcal{F}_{\mu\nu}^a_b = \partial_\mu \mathcal{A}_\nu^a - \partial_\nu \mathcal{A}_\mu^a - i[\mathcal{A}_\mu, \mathcal{A}_\nu]^a_b. \quad (1.9)$$

Introduce $\lambda = Ng_{YM}^2$, which is the so-called 't Hooft coupling. In terms of λ ,

$$\mathcal{L} = -\frac{1}{4} \frac{N}{\lambda} \text{tr}(\mathcal{F}_{\mu\nu}\mathcal{F}^{\mu\nu}). \quad (1.10)$$

The Feynman rules are written in terms of ribbon graph diagrams. The double lines keep track of the two $U(N)$ indices present on the (matrix valued) field. The Feynman rules are

1. For the propagator

$$\begin{array}{c} a \xrightarrow{\quad} c \\ b \xleftarrow{\quad} d \end{array} \sim \frac{\lambda}{N} \delta_{ac} \delta_{bd}$$

Figure 1.3: Gauge field propagator in the ribbon graph notation.

2. For the three-point and four-point vertices, one finds

$$\begin{array}{c} i \xrightarrow{\quad} j \\ n \xleftarrow{\quad} k \\ \quad \quad \quad l \\ \quad \quad \quad m \end{array} \sim \frac{N}{\lambda} \delta_{ij} \delta_{kl} \delta_{mn},$$

$$\begin{array}{c} a \xrightarrow{\quad} b \\ h \xleftarrow{\quad} c \\ \quad \quad \quad d \\ \quad \quad \quad e \\ \quad \quad \quad f \\ \quad \quad \quad g \end{array} \sim \frac{N}{\lambda} \delta_{ab} \delta_{cd} \delta_{ef} \delta_{gh}$$

Figure 1.4: Three-point and four-point vertices in the ribbon graph notation.

Using the above Feynman rules it is possible determine the N and λ dependence of an amplitude \mathcal{M} of some connected diagram without external legs. One can argue that the resulting Feynman diagram is a triangulation of a 2-dimensional surface

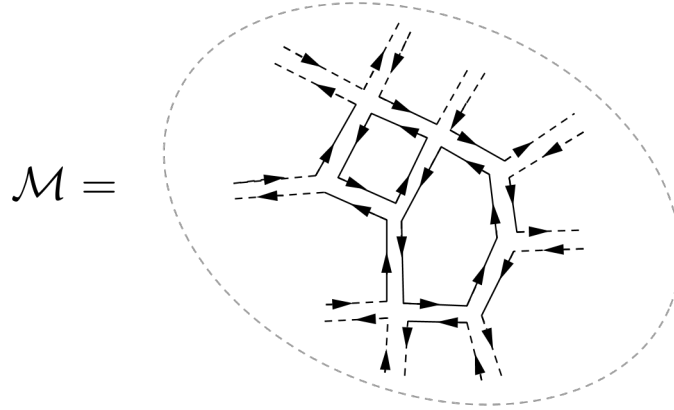


Figure 1.5: Ribbon graphs define a triangulation of a two-dimensional surface.

Each polygon in this diagram contributes a factor $\sum_{i=1}^N \delta_i^i = N$. Let E be the total number of edges (propagators), V the total number of vertices and F the total number of faces (closed loops or closed polygons) in the connected diagram. The dependence on N and λ of the amplitude \mathcal{M} is

$$\mathcal{M} \sim \left(\frac{N}{\lambda}\right)^V \left(\frac{\lambda}{N}\right)^E N^F = N^{V-E+F} \lambda^{E-V}. \quad (1.11)$$

The power of N is the famous Euler characteristic

$$\chi = V - E + F.$$

This Euler characteristic is a topological number which only depends on the topology of the diagram. Each connected diagram gives a triangulation of a closed two dimensional connected and oriented manifold Σ_h , with the Euler characteristic given by χ above. The following figures illustrate some typical examples of the Σ_h 's.

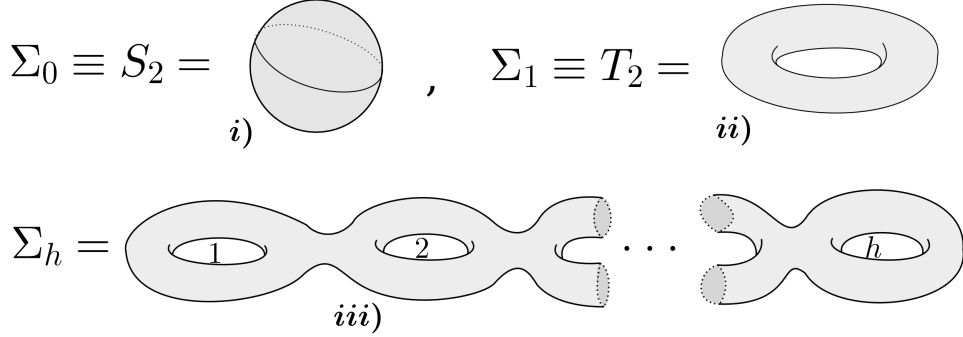


Figure 1.6: *i*) $\Sigma_0 = S^2$ is a two-sphere - *ii*) $\Sigma_1 = T_2$ is a two dimensional torus and *iii*) represent a typical Σ_h where h is the genus of the surface (or number of handles).

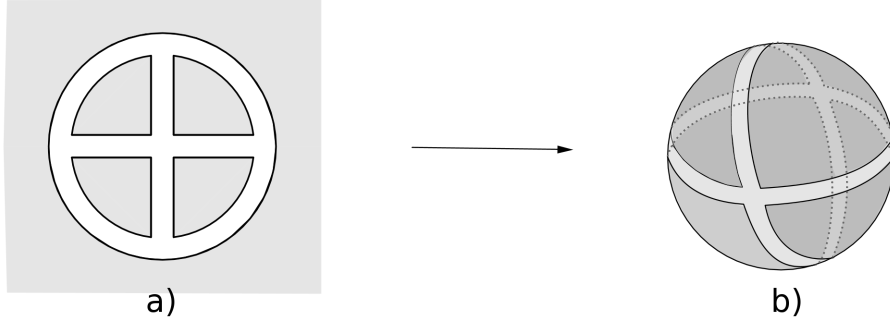
The Euler characteristic is given by

$$\chi(\Sigma_h) = 2 - 2h, \quad (1.12)$$

where h is the number of handles on the surface Σ_h . The amplitude of each connected diagram without external legs is

$$\mathcal{M} \propto N^{2-2h} \lambda^{E-V}. \quad (1.13)$$

It was 't Hooft [2], who first noted this connection between the power of N multiplying the amplitude \mathcal{M} and the Euler characteristic of Σ_h .



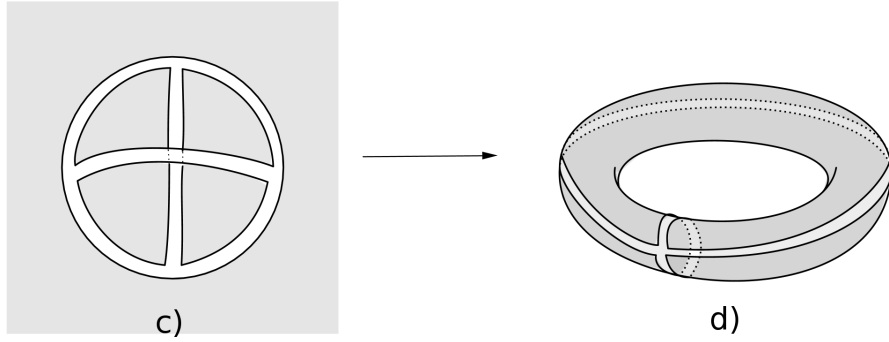


Figure 1.7: We illustrate in the above figures how to go from a planar Feynman diagram figure a) to a triangulation of a two-sphere figure b). The next figure shows a typical non-planar Feynman diagram figure c) to a triangulation of a torus figure d).

The limit $N \rightarrow \infty$ with λ fixed defines a systematic large N expansion of the theory. This limit is known as the 't Hooft limit. It is clear that at large N the only diagrams that contribute are those with $h = 0$. Their contribution in the amplitude goes like N^2 . These diagrams are known as planar diagrams because they can be drawn on a two dimensional plane without self-crossing. The geometry of the Σ_h 's, see Fig1.6, are also encountered in the quantum theory of fundamental strings. In fact, it is attractive to identify these figures as the world-sheets of quantum strings. For more details and a review on the connection between gauge theory and string theory one is referred to [25; 26; 27; 28].

1.4 Zero dimensional Matrix Model

In this section we consider a zero dimensional toy model to compute correlation functions of certain operators constructed from $N \times N$ Hermitian matrices. Our motivation for studying this toy model is to learn about the N dependence of the correlation functions of matrices. This study will illustrate how ribbon graph Feynman diagrams emerge in the theory. Here our focus is on the free theory for simplicity. To begin our discussion, we start by defining the generating function

of the correlation functions of the theory.

1.4.1 Matrix model correlation functions in terms of $\mathcal{Z}[J]$

Let J and M be two $N \times N$ Hermitian matrices. Consider the generating function

$$\mathcal{Z}[J] = \int [dM] e^{-\frac{1}{2} \text{tr}(M^2) + \text{tr}(MJ)}, \quad \mathcal{Z}[J=0] = 1, \quad (1.14)$$

By completing the square followed by a change of variable, one can show that this generating function is simply

$$\mathcal{Z}[J] = e^{\frac{1}{2} \text{tr}(J^2)}. \quad (1.15)$$

A general matrix model correlation function is

$$\langle M_{j_1}^{i_1} M_{j_2}^{i_2} \cdots M_{j_n}^{i_n} \rangle = \int [dM] M_{j_1}^{i_1} M_{j_2}^{i_2} \cdots M_{j_n}^{i_n} e^{-\frac{1}{2} \text{tr}(M^2)}. \quad (1.16)$$

We adopt the Einstein summation convention

$$(MJ)_k^i = \sum_j^N M_j^i J_k^j \equiv M_j^i J_k^j,$$

so that the trace of matrix is simply written as

$$\text{tr}(M) = M_i^i.$$

Accordingly, the generating function (1.14) becomes

$$\mathcal{Z}[J] = \int [dM] e^{-\frac{1}{2} M_j^i M_i^j + M_k^l J_l^k}. \quad (1.17)$$

This last equation leads to the relation

$$\langle M_j^i M_l^k \rangle = \frac{\partial^2}{\partial J_i^j \partial J_k^l} \mathcal{Z}[J] \Big|_{J=0}. \quad (1.18)$$

Using $\mathcal{Z}[J] = e^{\frac{1}{2} \text{tr}(J^2)}$ and the identity

$$\frac{\partial}{\partial J_k^l} e^{\frac{1}{2} \text{tr}(J^2)} = J_l^k e^{\frac{1}{2} \text{tr}(J^2)},$$

a straightforward calculation yields

$$\langle M_j^i M_l^k \rangle = \delta_l^i \delta_j^k. \quad (1.19)$$

(1.19) is enough to evaluate any correlation function of matrices. The only extra ingredient one needs is Wick's theorem.

1.4.2 Examples of correlation functions

Consider the following correlator

$$\begin{aligned}
 \langle \text{tr}(M^4) \rangle &= \langle M_j^i M_k^j M_l^k M_i^l \rangle = \frac{\partial^4}{\partial J_i^j \partial J_j^k \partial J_k^l \partial J_i^l} e^{\frac{1}{2} \text{tr}(J^2)} \Big|_{J=0}, \\
 &= \frac{\partial^3}{\partial J_i^j \partial J_j^k \partial J_k^l} \left(J_i^l e^{\frac{1}{2} \text{tr}(J^2)} \right) \Big|_{J=0}, \\
 &= \frac{\partial^2}{\partial J_i^j \partial J_j^k} \left[(\delta_l^l \delta_i^k + J_l^k J_i^l) e^{\frac{1}{2} \text{tr}(J^2)} \right] \Big|_{J=0}, \\
 &= \frac{\partial}{\partial J_i^j} \left[(0 + \delta_k^l \delta_i^j J_l^k + \delta_k^k \delta_l^j J_i^l + \delta_l^l \delta_i^k J_k^j + J_i^l J_l^k J_k^j) e^{\frac{1}{2} \text{tr}(J^2)} \right] \Big|_{J=0}, \\
 &= \delta_i^i + \delta_k^k \delta_j^j \delta_i^i + \delta_l^l \delta_k^k \delta_j^j, \\
 &= N + 2N^3.
 \end{aligned} \tag{1.20}$$

The general pattern resulting from this calculation is summarized in terms of Wick's theorem [29]. In terms of the Wick contraction notation the example (1.20) becomes

$$\begin{aligned}
 :M_j^i M_k^j M_l^k M_i^l: &\equiv \overbrace{M_j^i M_k^j} \overbrace{M_l^k M_i^l} + \overbrace{M_j^i M_k^j} \overbrace{M_l^k M_i^l} + \overbrace{M_j^i M_k^j} \overbrace{M_l^k M_i^l}, \\
 &= \delta_k^k \delta_j^j \delta_i^i + \delta_k^k \delta_j^j \delta_i^i + \delta_l^l \delta_k^k \delta_j^j = N + 2N^3.
 \end{aligned}$$

In the above notation, each Wick contracted matrices reflects the way each pair of derivatives with respect to J act on the matrices. This can be summarized by Feynman rules using the ribbon graph language.

1.4.3 Ribbon graph Feynman diagrams

The rules for ribbon graphs are

- For each matrix M appearing in a correlation function, draw a pair of dots associated respectively to the upper- and lower-index of the matrix.
- For each Wick contraction connect the two pairs of dots for the two Wick contracted matrices with a pair of lines.
- For each repeated index we sum over, connect the associated dots with a line.

- For each diagram associate a number N^l where l is the total number of closed loops in the diagram.
- Finally, sum over all the possible diagrams to produce the final answer.

Using these rules, reconsider the example in (1.20)

$$\begin{aligned}
 :M_j^i M_k^j M_l^k M_i^l: &= \dots i \dots j \dots k \dots l \dots l \dots i \dots + \dots i \dots j \dots k \dots l \dots l \dots i \dots \\
 &\quad N^3 \qquad \qquad \qquad N \\
 &+ \dots i \dots j \dots k \dots k \dots l \dots l \dots i \dots \\
 &\quad N^3 \\
 &= N + 2N^3
 \end{aligned}$$

In the above diagrams, the dotted horizontal lines do not represent anything. They are included for clarity as we now explain. The ribbons beneath the dotted horizontal lines represent the Wick contractions and the ones above represent the summation that appears in the trace.

1.4.4 Higher order correlation functions

The above techniques are no longer effective for correlation functions of operators constructed using order N matrices. The difficulty is a consequence of the huge number of Feynman diagrams that can be drawn. In this section, we explain how this problem arises in the evaluation of higher order correlators. To start with, it is helpful to consider two independent Hermitian $N \times N$ matrices M and K and define

$$Z = \frac{1}{\sqrt{2}}(M + iK), \quad \Rightarrow \quad Z^\dagger = \frac{1}{\sqrt{2}}(M - iK). \quad (1.21)$$

It is a simple exercise to check that

$$\langle Z_j^i Z_l^\dagger \rangle = \delta_l^i \delta_j^k, \quad \langle Z_j^i Z_l^k \rangle = \langle Z_l^\dagger \rangle = 0. \quad (1.22)$$

To see the general pattern for the correlators of n pairs of Z and Z^\dagger matrices, consider the cases $n = 2$, $n = 3$ and the indices of the matrices are not summed (i.e. we do not take their trace).

- Case for $n = 2$

$$\begin{aligned}
 \langle Z_{j_1}^{i_1} Z_{j_2}^{i_2} Z_{l_1}^{\dagger k_1} Z_{l_2}^{\dagger k_2} \rangle &= Z_{j_1}^{i_1} \overbrace{Z_{j_2}^{i_2} Z_{l_1}^{\dagger k_1} Z_{l_2}^{\dagger k_2}}^{\text{Ribbon}} + Z_{j_1}^{i_1} \overbrace{Z_{j_2}^{i_2} Z_{l_1}^{\dagger k_1} Z_{l_2}^{\dagger k_2}}^{\text{Ribbon}} \\
 &= \delta_{l_1}^{i_1} \delta_{l_2}^{i_2} \delta_{j_1}^{k_1} \delta_{j_2}^{k_2} + \delta_{l_2}^{i_1} \delta_{l_1}^{i_2} \delta_{j_2}^{k_1} \delta_{j_1}^{k_2}, \\
 &= \sum_{\sigma \in S_2} \delta_{l_{\sigma(1)}}^{i_1} \delta_{l_{\sigma(2)}}^{i_2} \delta_{j_{\sigma^{-1}(1)}}^{k_1} \delta_{l_{\sigma^{-1}(2)}}^{k_2}
 \end{aligned}$$

- Case for $n = 3$

$$\begin{aligned}
 \langle Z_{j_1}^{i_1} Z_{j_2}^{i_2} Z_{j_3}^{i_3} Z_{l_1}^{\dagger k_1} Z_{l_2}^{\dagger k_2} Z_{l_3}^{\dagger k_3} \rangle &= Z_{j_1}^{i_1} \overbrace{Z_{j_2}^{i_2} \overbrace{Z_{j_3}^{i_3} Z_{l_1}^{\dagger k_1} Z_{l_2}^{\dagger k_2} Z_{l_3}^{\dagger k_3}}^{\text{Ribbon}}}^{\text{Ribbon}} + Z_{j_1}^{i_1} \overbrace{Z_{j_2}^{i_2} \overbrace{Z_{j_3}^{i_3} Z_{l_1}^{\dagger k_1} Z_{l_2}^{\dagger k_2} Z_{l_3}^{\dagger k_3}}^{\text{Ribbon}}}^{\text{Ribbon}} \\
 &\quad + Z_{j_1}^{i_1} \overbrace{Z_{j_2}^{i_2} \overbrace{Z_{j_3}^{i_3} Z_{l_1}^{\dagger k_1} Z_{l_2}^{\dagger k_2} Z_{l_3}^{\dagger k_3}}^{\text{Ribbon}}}^{\text{Ribbon}} + Z_{j_1}^{i_1} \overbrace{Z_{j_2}^{i_2} \overbrace{Z_{j_3}^{i_3} Z_{l_1}^{\dagger k_1} Z_{l_2}^{\dagger k_2} Z_{l_3}^{\dagger k_3}}^{\text{Ribbon}}}^{\text{Ribbon}} \\
 &\quad + Z_{j_1}^{i_1} \overbrace{Z_{j_2}^{i_2} \overbrace{Z_{j_3}^{i_3} Z_{l_1}^{\dagger k_1} Z_{l_2}^{\dagger k_2} Z_{l_3}^{\dagger k_3}}^{\text{Ribbon}}}^{\text{Ribbon}} + Z_{j_1}^{i_1} \overbrace{Z_{j_2}^{i_2} \overbrace{Z_{j_3}^{i_3} Z_{l_1}^{\dagger k_1} Z_{l_2}^{\dagger k_2} Z_{l_3}^{\dagger k_3}}^{\text{Ribbon}}}^{\text{Ribbon}}, \\
 &= \delta_{l_1}^{i_1} \delta_{l_2}^{i_2} \delta_{l_3}^{i_3} \delta_{j_1}^{k_1} \delta_{j_2}^{k_2} \delta_{j_3}^{k_3} + \delta_{l_2}^{i_1} \delta_{l_1}^{i_2} \delta_{l_3}^{i_3} \delta_{j_2}^{k_1} \delta_{j_1}^{k_2} \delta_{j_3}^{k_3} + \delta_{l_2}^{i_1} \delta_{l_3}^{i_2} \delta_{l_1}^{i_3} \delta_{j_3}^{k_1} \delta_{j_1}^{k_2} \delta_{j_2}^{k_3} \\
 &\quad + \delta_{l_1}^{i_1} \delta_{l_3}^{i_2} \delta_{l_2}^{i_3} \delta_{j_1}^{k_1} \delta_{j_3}^{k_2} \delta_{j_2}^{k_3} + \delta_{l_3}^{i_1} \delta_{l_2}^{i_3} \delta_{l_1}^{i_2} \delta_{j_2}^{k_1} \delta_{j_3}^{k_2} \delta_{j_1}^{k_3} + \delta_{l_3}^{i_1} \delta_{l_2}^{i_2} \delta_{l_1}^{i_3} \delta_{j_3}^{k_1} \delta_{j_2}^{k_2} \delta_{j_1}^{k_3}, \\
 &= \sum_{\sigma \in S_3} \delta_{l_{\sigma(1)}}^{i_1} \delta_{l_{\sigma(2)}}^{i_2} \delta_{l_{\sigma(3)}}^{i_3} \delta_{j_{\sigma^{-1}(1)}}^{k_1} \delta_{j_{\sigma^{-1}(2)}}^{k_2} \delta_{j_{\sigma^{-1}(3)}}^{k_3}.
 \end{aligned}$$

From these two examples, it is clear that the general formula is

$$\langle Z_{j_1}^{i_1} Z_{j_2}^{i_2} \cdots Z_{j_n}^{i_n} Z_{l_1}^{\dagger k_1} Z_{l_2}^{\dagger k_2} \cdots Z_{l_n}^{\dagger k_n} \rangle = \sum_{\sigma \in S_n} \delta_{l_{\sigma(1)}}^{i_1} \delta_{l_{\sigma(2)}}^{i_2} \cdots \delta_{l_{\sigma(n)}}^{i_n} \delta_{j_{\sigma^{-1}(1)}}^{k_1} \delta_{j_{\sigma^{-1}(2)}}^{k_2} \cdots \delta_{j_{\sigma^{-1}(n)}}^{k_n}. \quad (1.23)$$

Above, S_n is the permutation group of n different objects. This group has $n!$ elements. If $n \sim O(N)$ the summation in (1.23) is not easy to perform. This is due to the fact that the number of terms to be summed, which is $N!$ is huge. This leads to huge combinatoric factors that overpower the $\frac{1}{N^2}$ suppression of higher genus ribbon graphs. It is due to this combinatorics problem that ribbon diagrams of all genus contribute and ribbon graph techniques are no longer effective.

1.5 CFT

1.5.1 Introduction to CFT

Using the AdS/CFT correspondence, one hopes to learn about quantum gravity in AdS space, by asking questions in the CFT. There are also other important motivations to study CFT. The study of critical phenomena is intimately connected to conformal symmetries. Further, in Wilson's renormalization group (RG) scheme, CFTs are the endpoints of any RG flow and hence they are important to understand the space of all QFTs.

One example of a conformal transformation is a scaling transformation. Consider a quantum mechanical system where one chooses to fix the units by setting $\hbar = 1$. The usual commutation relation between position x and momentum p is

$$[x, p] = i. \quad (1.24)$$

To keep our units fixed, the action of the scaling transformation on x and p must be

$$\begin{cases} x \rightarrow \lambda x, \\ p \rightarrow \lambda^{-1} p. \end{cases} \quad (1.25)$$

Since in special relativity, time and energy have to be treated on the same footing as space and momentum, similar scaling transformations apply to time and energy.

It is not difficult to apply this transformation to QFT by doing simple dimensional analysis. Toward this end, consider a non-interacting massless and real scalar field in D -dimensional spacetime, with the action

$$S = \int d^D x \partial_\mu \phi \partial^\mu \phi. \quad (1.26)$$

A physical observable in this theory is the field ϕ . In units where $\hbar = 1$, the action S is dimensionless. It follows that the scalar field has classical dimension $[\phi] = L^{-\Delta_\phi}$, $\Delta_\phi = \frac{D-2}{2}$. A scale transformation acts as

$$\begin{cases} x^\mu \rightarrow x'^\mu = \lambda x^\mu, \\ \phi(x) \rightarrow \phi'(\lambda x) = |\lambda|^{-\Delta_\phi} \phi(x). \end{cases} \quad (1.27)$$

Using (1.27) it is straight forward to show that $S[\phi] = S'[\phi']$, i.e. the free and massless real scalar field action is scale invariant.

The above description is classical. The field fluctuates at the quantum level. Quantum corrections to the above description can be understood using the Wilsonian RG scheme, [30]. RG scheme provides a rigorous demonstration that there are only a finite number of Lagrangians (i.e QFTs) that one can write down at low energy. In this way QFTs are just effective theories summarizing the degrees of freedom that are present at very short distance scales. As one flows from the UV to the IR regime, all possible interactions are organized into a finite number of marginal and relevant interactions. The change of a coupling constant as function of energy scale is formulated in terms of the β -function of the theory

$$\frac{\partial g_a(\mu)}{\partial \log(\mu)} = \beta_a(g_a). \quad (1.28)$$

If all of the β -functions of the theory vanish, the theory is a CFT. One example of a theory that is conformal invariant at classical and quantum level is the $\mathcal{N} = 4$ SYM theory.

Conformal transformations are coordinate transformations satisfying

$$\Lambda_\rho^\mu \Lambda_\sigma^\nu \eta_{\mu\nu} = \Omega(x)^2 \eta_{\rho\sigma}. \quad (1.29)$$

$SO(2, d)$ is the conformal group in d -dimensions. Appendix K considers the group $SO(2, 4)$. To work out the generators of the conformal group, perform an infinitesimal transformation

$$x^\mu \rightarrow x'^\mu = x^\mu + \zeta^\mu(x). \quad (1.30)$$

It follows that

$$\Lambda_\nu^\mu = \frac{\partial x'^\mu}{\partial x^\nu} = \delta_\nu^\mu + \partial_\nu \zeta^\mu. \quad (1.31)$$

Close to the identity we have

$$\Omega(x)^2 = 1 + 2\varpi(x) + O(\varpi^2). \quad (1.32)$$

Plugging (1.31) and (1.32) into (1.29) at first order in $\zeta(x)$ one finds

$$\partial_\mu \zeta_\nu + \partial_\nu \zeta_\mu = 2\eta_{\mu\nu} \varpi(x), \quad \varpi(x) = \frac{1}{d} \partial_\rho \zeta^\rho. \quad (1.33)$$

This equation is called the conformal Killing vector equation. With some non-trivial manipulations, one shows that this equation implies

$$\partial_\rho \partial_\sigma \partial_\nu \zeta_\mu = 0. \quad (1.34)$$

Thus, the general solution for ζ_μ is at most quadratic in x^μ . The unique solution consistent with the above equation is

$$\zeta^\mu = \epsilon^\mu + \omega^{\mu\nu} x_\nu + \lambda x^\mu + \epsilon'^\mu x_\rho x^\rho - 2\epsilon'_\rho x^\rho x^\mu, \quad (1.35)$$

where the parameters ϵ^μ , $\omega^{\mu\nu} = -\omega^{\nu\mu}$, λ and ϵ'^μ are constant independent of x^σ . Setting the parameters $\lambda = 0$ and $\epsilon'^\mu = 0$, the conformal Killing vector equation (1.33) reduces to

$$\partial_\mu \zeta_\nu + \partial_\nu \zeta_\mu = 0. \quad (1.36)$$

In addition, the scaling factor also becomes $\Omega(x) = 1$, so that (1.29) becomes

$$\Lambda_\rho^\mu \Lambda_\sigma^\nu \eta_{\mu\nu} = \eta_{\rho\sigma}. \quad (1.37)$$

Hence, this subgroup is the Poincaré group. The parameters λ and ϵ'^μ in (1.35) are respectively the parameters for scale and special conformal transformations. ϵ^μ and $\omega^{\mu\nu}$ are respectively the parameters for spacetime translations and Lorentz transformations. The total number of conformal group parameters in d dimensions can be summarized as follows

- d for ϵ^μ (spacetime translation)
- $\frac{d(d-1)}{2}$ for $\omega^{\mu\nu} = -\omega^{\nu\mu}$ (boosts+rotations)
- 1 for λ (scaling transformation)
- d for ϵ'^μ (special conformal transformations).

In total, one counts $\frac{(d+2)(d+1)}{2}$ generators of the conformal group. A finite conformal transformation is

$$\Lambda = e^{i\epsilon^\mu P_\mu + \frac{i}{2}\omega^{\mu\nu} L_{\mu\nu} + i\lambda D + i\epsilon'^\mu K_\mu}. \quad (1.38)$$

To work out the form of the generators P_μ , $M_{\mu\nu}$, D and K_μ one can expand this finite transformation about the identity to yield

$$\begin{aligned} x'^\rho &= \left(1 + i\epsilon^\mu P_\mu + \frac{i}{2} \omega^{\mu\nu} L_{\mu\nu} + i\lambda D + i\epsilon'^\mu K_\mu \right)_\sigma^\rho x^\sigma \\ &= x^\rho + \delta x^\rho. \end{aligned}$$

Comparing this small change δx^ρ with (1.35) we find

$$P_\mu = -i\partial_\mu, \quad (1.39)$$

$$M_{\mu\nu} = -i(x_\mu\partial_\nu - x_\nu\partial_\mu), \quad (1.40)$$

$$D = ix_\mu\partial^\mu, \quad (1.41)$$

$$K_\mu = -i(x_\rho x^\rho \partial_\mu - 2x_\mu x_\sigma \partial^\sigma) \quad (1.42)$$

These generators obey

$$\begin{cases} i[M_{\mu\nu}, M_{\alpha\beta}] = \eta_{\nu\alpha}M_{\mu\beta} + \eta_{\mu\beta}M_{\nu\alpha} - \eta_{\nu\beta}M_{\mu\alpha} - \eta_{\mu\alpha}M_{\nu\beta}, \\ i[D, P_\mu] = P_\mu, \\ i[M_{\mu\nu}, K_\alpha] = \eta_{\nu\alpha}K_\mu - \eta_{\mu\alpha}K_\nu, \\ i[M_{\mu\nu}, P_\alpha] = \eta_{\nu\alpha}P_\mu - \eta_{\mu\alpha}P_\nu, \\ i[P_\mu, K_\nu] = 2\eta_{\mu\nu}D + 2M_{\mu\nu}, \\ i[D, K_\mu] = -K_\mu. \end{cases} \quad (1.43)$$

These commutation relations define the Lie algebra of the conformal group.

Let $\eta_{MN} = \text{diag}(-1, 1, \dots, 1, -1)$ ³ be the metric of $\mathbb{R}^{2,d}$. The isometry group of this space is the group $SO(2, d)$ which is generated by

$$L_{MN} = -i(X_M\partial_N - X_N\partial_M).$$

The Lie algebra $\mathfrak{so}(2, d)$ satisfied by these generators is

$$i[L_{MN}, L_{RS}] = \eta_{NR}L_{MS} + \eta_{MS}L_{NR} - \eta_{NS}L_{MR} - \eta_{MR}L_{NS}. \quad (1.44)$$

³Capital Latin indices M, N, \dots take value in $0, 1, 2, \dots, d, d+1$. This signature of the metric also follows from our adopted signature for the metric $\eta_{\mu\nu}$ of the d -dimensional physical spacetime.

The isomorphism between the algebra (1.43) and the algebra (1.44) is as follows

$$\left. \begin{array}{l} P_\mu = L_{d+1,\mu} + L_{d,\mu}, \\ K_\mu = L_{d+1,\mu} - L_{d,\mu}, \\ D = L_{d+1,d}, \\ M_{\mu\nu} = L_{\mu\nu}. \end{array} \right\} \Rightarrow [L_{MN}] = \begin{bmatrix} (M_{\mu\nu}) & \frac{P^\mu - K^\mu}{2} & -\frac{P^\mu + K^\mu}{2} \\ -\frac{P_\mu - K_\mu}{2} & 0 & D \\ \frac{P_\mu + K_\mu}{2} & -D & 0 \end{bmatrix}. \quad (1.45)$$

This demonstrates that the conformal group is indeed $SO(2, d)$. In this way the non linear action of the conformal group on the physical spacetime coordinates $x^\mu \in \mathbb{R}^{1,d-1}$ can be realized as linear Lorentz rotations on the coordinates $X^M \in \mathbb{R}^{2,d}$.

1.5.2 Correlation functions in CFT

The observable in CFTs are correlators of local operators. Requiring the full conformal symmetry, the two point correlation of two local operators \mathcal{O}_1 and \mathcal{O}_2 is

$$\langle \mathcal{O}_1(x) \mathcal{O}_2(y) \rangle = \frac{\delta_{\Delta_1, \Delta_2}}{|x - y|^{\Delta_1 + \Delta_2}}, \quad (1.46)$$

where the Δ_i 's give the scaling dimension of the operators \mathcal{O}_i . We review the derivation of this two point correlation function of local operator in Appendix L. Operators in the CFT are labeled by the eigenvalues of the dilatation operator D and the Lorentz spin operator $M_{\mu\nu}$. These two operators commute

$$[D, M_{\mu\nu}] = 0. \quad (1.47)$$

Thus, D and $M_{\mu\nu}$ are simultaneously diagonalizable. Primary operators are defined by

$$[K_\mu, \mathcal{O}^A(0)] = 0. \quad (1.48)$$

The representation to which the primary operator belongs is given by

$$\begin{aligned} [D, \mathcal{O}^A(0)] &= -i\Delta_{\mathcal{O}} \mathcal{O}^A(0), \\ [M_{\mu\nu}, \mathcal{O}^A(0)] &= i\{\Sigma_{\mu\nu}\}_B^A \mathcal{O}^B(0). \end{aligned}$$

For a review of CFT see the textbook [31]. For an introductory review of CFT and its application to string theory see [32]. Recent developments and new ideas can be found in [33; 34; 35; 36; 37; 38; 39; 40; 41; 42; 43; 44; 45].

Chapter 2

Anomalous Dimensions of Heavy Operators from Magnon Energies

2.1 Outline of chapter

In this chapter we study spin chains with boundaries that are dual to open strings suspended between systems of giant gravitons and dual giant gravitons. Motivated by a geometrical interpretation of the central charges of $\mathfrak{su}(2|2)$, we propose a simple and minimal all loop expression that interpolates between the anomalous dimensions computed in the gauge theory and energies computed in the dual string theory. The discussion makes use of a description in terms of magnons, generalizing results for a single maximal giant graviton. The symmetries of the problem determine the structure of the magnon boundary reflection/scattering matrix up to a phase. We compute a reflection/scattering matrix element at weak coupling and verify that it is consistent with the answer determined by symmetry. We find the reflection/scattering matrix does not satisfy the boundary Yang-Baxter equation so that the boundary condition on the open spin chain spoils integrability. We also explain the interpretation

of the double coset ansatz in the magnon language. The work discussed in this chapter was reported in JHEP 03 (2016) 156.

2.2 Chapter introduction

In this chapter we will connect two distinct results that have been achieved in the context of gauge/gravity duality. The first result, which is motivated by the Penrose limit in the $AdS_5 \times S^5$ geometry [46], is the natural language for the computation of anomalous dimensions of single trace operators in the planar limit provided by integrable spin chains (see [47] for a thorough review). For the spin chain models we study, using only the symmetries of the system, one can determine the exact large N anomalous dimensions and the two magnon scattering matrix. Using integrability one can go further and determine the complete scattering matrix of spin chain magnons[12; 13]. The second results which we will use are the powerful methods exploiting group representation theory, which allow one to study correlators of operators whose classical dimension is of order N . In this case, the large N limit is not captured by summing the planar diagrams. Our results allow a rather complete understanding of the anomalous dimensions of gauge theory operators that are dual to giant graviton branes with open strings suspended between them. These results generalize the analysis of [21] to systems that include non-maximal giant gravitons and dual giant gravitons. The boundary magnons of an open string attached to a maximal giant graviton are fixed in place - they can not hop between sites of the open string. In the case of non maximal giant gravitons and dual giant gravitons there are non-trivial interactions between the open string and the brane, allowing the boundary magnons to move away from the string endpoints.

The operators we focus on are built mainly out of one complex $U(N)$ adjoint scalar Z , and a much smaller number M of impurities given by a second complex scalar field Y , which are the “magnons” that hop on the lattice of the Z s. The dilatation operator action on these operators matches the Hamiltonian of a spin chain model comprising of a set of defects that scatter from each other. The spin chain models enjoy an $SU(2|2)^2$ symmetry. The symmetries of the system determines the energies of impurities, as well as the two impurity scattering

matrix[12; 13]. The $\mathfrak{su}(2|2)$ algebra includes two sets of bosonic generators ($R^a{}_b$ and $L^\alpha{}_\beta$) that each generate an $SU(2)$ group. The action of the generators is summarized in the relations

$$[R^a{}_b, T^c] = \delta^c_b T^a - \frac{1}{2} \delta^a_b T^c, \quad [L^\alpha{}_\beta, T^\gamma] = \delta^\gamma_\beta T^\alpha - \frac{1}{2} \delta^\alpha_\beta T^\gamma \quad (2.1)$$

where T is any tensor transforming as advertised by its index. The algebra also includes two sets of super charges Q_a^α and S_β^b . These close the algebra

$$\{Q_a^\alpha, S_\beta^b\} = \delta_a^b L^\alpha{}_\beta + \delta_\beta^\alpha R^a{}_b + \delta_a^b \delta_\beta^\alpha C, \quad (2.2)$$

where C is a central charge, and

$$\{Q_a^\alpha, Q_b^\beta\} = 0, \quad \{S_\alpha^a, S_\beta^b\} = 0. \quad (2.3)$$

We will realize this algebra on states that include magnons. When the magnons are well separated, each magnon transforms in a definite representation of $\mathfrak{su}(2|2)$ and the full state transforms in the tensor product of these individual representations. Acting on the i th magnon we can have a centrally extended representation[12; 13]

$$\{Q_a^\alpha, S_\beta^b\} = \delta_a^b L^\alpha{}_\beta + \delta_\beta^\alpha R^a{}_b + \delta_a^b \delta_\beta^\alpha C, \quad (2.4)$$

$$\{Q_a^\alpha, Q_b^\beta\} = \epsilon^{\alpha\beta} \epsilon_{ab} \frac{k_i}{2}, \quad \{S_\alpha^a, S_\beta^b\} = \epsilon_{\alpha\beta} \epsilon^{ab} \frac{k_i^*}{2}. \quad (2.5)$$

The total multimagnon state must be in a representation for which the central charges k_i , k_i^* vanish. Thus the multi magnon state transforms under the representation with

$$C = \sum_i C_i, \quad \sum_i k_i = 0 = \sum_i k_i^*. \quad (2.6)$$

A key ingredient to make use of the $\mathfrak{su}(2|2)$ symmetry entails determining the central charges k_i , k_i^* and hence the representations of the individual magnons. There is a natural geometric description of the system, first obtained by an inspired argument in [48] and later put on a firm footing in [22], which gives an elegant and simple description of these central charges. The two dimensional spin chain model that is relevant for planar anomalous dimensions is dual to the

worldsheet theory of the string moving in the dual $AdS_5 \times S^5$ geometry. This string is a small deformation of a $\frac{1}{2}$ –BPS state. A convenient description of the $\frac{1}{2}$ –BPS sector (first anticipated in [49]) is in terms of the LLM coordinates introduced in [50], which are specifically constructed to describe $\frac{1}{2}$ –BPS states built mainly out of Z s. In the LLM coordinates, there is a preferred LLM plane on which states that are built mainly from Z s orbit with a radius $r = 1$ (in convenient units). Consider a closed string state dual to a single trace gauge theory operator built mainly from Z s, but also containing a few magnons M . The closed string solution looks like a polygon with vertices on the unit circle. The sides of the polygon are the magnons. The specific advantage of these coordinates is that they make the analysis of the symmetries particularly simple and allow a perfect match to the $SU(2|2)$ superalgebra of the gauge theory described above. Matching the gauge theory and gravity descriptions in this way implies a transparent geometrical understanding of the k_i and k_i^* , as we now explain. The commutator of two supersymmetries in the dual gravity theory contains $NS-B_2$ gauge field transformations. As a consequence of this gauge transformation, strings stretched in the LLM plane acquire a phase which is the origin of the central charges k_i and k_i^* . It follows that we can immediately read off the central charges for any particular magnon from the sketch of the closed string worldsheet on the LLM plane: the straight line segment corresponds to a complex number which is the central charge [22].

The gauge theory operators that correspond to closed strings have a bare dimension that grows, at most, as \sqrt{N} . We are interested in operators whose bare dimension grows as N when the large N limit is taken. These operators include systems of giant graviton branes. The key difference as far as the sketch of the state on the LLM plane is concerned, is that the giant gravitons can orbit on circles of radius $r < 1$ while dual giant gravitons orbit on circles of radius $r > 1$. The magnons populating open strings which are attached to the giant gravitons can be divided into boundary magnons (which sit closest to the ends of the open string) and bulk magnons. The boundary magnons will stretch from a giant graviton located at $r \neq 1$ to the unit circle, while bulk magnons stretch between points on the unit circle. We will also consider the case below that the entire open string is given by a single magnon, in which case it will stretch

between two points with $r \neq 1$.

The computation of correlators of the corresponding operators in the field theory is highly non-trivial. Indeed, as a consequence of the fact that we now have order N fields in our operators, the number of ribbon graphs that can be drawn is huge. These enormous combinatoric factors easily overpower the usual $\frac{1}{N^2}$ suppression of non-planar diagrams so that both planar and non-planar diagrams must be summed to capture even the leading large N limit of the correlator [51]. This problem can be overcome by employing group representation theory techniques. The article [3] showed that it is possible to compute the correlation functions of operators built from any number of Z s exactly, by using the Schur polynomials as a basis for the local operators of the theory. In [52] these results were elegantly explained by pointing out that the organization of operators in terms of Schur polynomials is an organization in terms of projection operators. Completeness and orthogonality of the basis follows from the completeness and orthogonality of the underlying projectors. With these insights [3; 52], many new directions opened up. A basis for the local operators which organizes the theory using the quantum numbers of the global symmetries was given in [53; 54]. Another basis, employing projectors related to the Brauer algebra was put forward in [55] and developed in a number of interesting works [56; 57; 58; 59; 60; 61; 62]. For the systems we are interested in, the most convenient basis to use is provided by the restricted Schur polynomials. Inspired by the Gauss Law which will arise in the world volume description of the giant graviton branes, the authors of [63] suggested operators in the gauge theory that are dual to excited giant graviton brane states. This inspired idea was pursued both in the case that the open strings are described by an open string word [7; 8; 9] and in the case of minimal open strings, with each open string represented by a single magnon [10; 11]. The operators introduced in [7; 10] are the restricted Schur polynomials. Further, significant progress was made in understanding the spectrum of anomalous dimensions of these operators in the studies [8; 9; 64; 14; 15; 16; 20; 17]. Extensions which consider orthogonal and symplectic gauge groups and other new ideas, have also been achieved [65; 66; 67; 68; 69; 70].

In this chapter we will connect the string theory description and the gauge

theory description of the operators corresponding to systems of excited giant graviton branes. Our study gives a concrete description of the central charges k_i and some of the consequences of the $\mathfrak{su}(2|2)$ symmetry. We will see that the restricted Schur polynomials provide a natural description of the quantum brane states. For the open strings we find a description in terms of open spin chains with boundaries and we explain precisely what the boundary interactions are. The double coset ansatz of the gauge theory, which solves the problem of minimal open strings consisting entirely of a single magnon, also has an immediate and natural interpretation in the same framework.

There are closely related results which employ a different approach to the questions considered in this chapter. A collective coordinate approach to study giant gravitons with their excitations has been pursued in [71; 72; 73; 74; 1]. This technique employs a complex collective coordinate for the giant graviton state, which has a geometric interpretation in terms of the fermion droplet (LLM) description of half BPS states [49; 50]. The motivation for this collective coordinate starts from the observation that within semiclassical gravity, we think of the D-branes as being localized in the dual spacetime geometry. It might seem however, that since in the field theory the operators we write down have a precise \mathcal{R} -charge and a fixed energy, they are dual to a delocalized state. Indeed, since gauge/gravity duality is a quantum equivalence it is subject to the uncertainty principle of quantum mechanics. The \mathcal{R} -charge of an operator is the angular momentum of the dual states in the gravity theory, so that by the uncertainty principle, the dual giant graviton-branes must be fully delocalized in the conjugate angle in the geometry. The collective coordinate parametrizes coherent states, which do not have a definite \mathcal{R} -charge and so may permit a geometric interpretation of the position of the D-brane as the value of the collective coordinate. With the correct choice for the coherent states, mixing between different states of a definite \mathcal{R} -charge would be taken into account and so when diagonalizing the dilatation operator (for example) the mixing between states with different choices of the values of the collective coordinate might be suppressed. This computation would be, potentially, much simpler than a direct computation utilizing operators with a definite \mathcal{R} -charge. Of course, by diagonalizing the dilatation operator for operators dual to giant graviton brane

plus open string states, one would expect to recover the collective coordinates, but this may only be possible after a complicated mixing problem in degenerate perturbation theory is solved. Some of the details that have emerged from our study do not support this semiclassical reasoning. Specifically, we find that the brane states are given by restricted Schur polynomials and these do not receive any corrections when the perturbation theory problem is solved, so that there does not seem to be any need to solve a mixing problem which constructs localized states from delocalized ones. Our large N eigenstates do have a definite \mathcal{R} –charge. The nontrivial perturbation theory problem involves mixing between operators corresponding to the same giant graviton branes, but with different open string words attached. Thus, it is an open string state mixing problem, solved with a discrete Fourier transform, as it was for the closed string. However, there is general agreement between the approaches: the Fourier transform solves a collective coordinate problem which diagonalizes momentum, rather than position.

For an interesting recent study of anomalous dimensions, at finite N , using a very different approach, see [75].

This chapter is organized as follows: In section 2.3 we recall the relevant facts about the restricted Schur polynomials. The action of the dilatation operator on these restricted Schur polynomials is studied in section 2.4 and the eigenstates of the dilatation operator are constructed in section 2.5. Section 2.6 provides the dual string theory interpretation of these eigenstates and perfect agreement between the energies of the string theory states and the corresponding eigenvalues of the dilatation operator is demonstrated. In sections 2.7 and 2.8 we consider the problem of magnon scattering, both in the bulk and off the boundary magnons. We have checked that the magnon scattering matrix we compute is consistent with scattering results obtained in the weak coupling limit of the theory. One important conclusion is that the spin chain is not integrable. In section 2.9 we review the double coset ansatz and describe the dual string theory interpretation of these results. Our conclusions and some discussion is given in section 2.10. Some technical details are collected in the appendices

2.3 Giants with open strings attached

In this section we will review the gauge theory description of the operators dual to giant graviton branes with open string excitations. In this description, each open string is described by a word with order \sqrt{N} letters. Most of the letters are the Z field. There are however $M \sim O(1)$ impurities which are the magnons of the spin chain. For simplicity we will usually take all of the impurities to be a second complex matrix Y . This idea was first applied in [76] to reproduce the spectrum of small fluctuations of giant gravitons [77]. The description was then further developed in [78; 79; 80; 81; 82]. The articles [80; 81; 82] in particular developed this description to the point where interesting dynamical questions¹ could be asked and answered. The open string words are then inserted into a sea of Z s which make up the giant graviton brane(s). Concretely, the operators we consider are

$$\begin{aligned} O(R, R_1^k, R_2^k; \{n_i\}_1, \{n_i\}_2, \dots, \{n_i\}_k) \\ = \frac{1}{n!} \sum_{\sigma \in S_{n+k}} \chi_{R, R_1^k, R_2^k}(\sigma) Z_{i_{\sigma(1)}}^{i_1} \cdots Z_{i_{\sigma(n)}}^{i_n} (W_k)_{i_{\sigma(n+1)}}^{i_{n+1}} \cdots (W_2)_{i_{\sigma(n+k-1)}}^{i_{n+k-1}} (W_1)_{i_{\sigma(n+k)}}^{i_{n+k}} \end{aligned} \quad (2.7)$$

where the open string words are

$$(W_I)_j^i = (YZ^{n_1} YZ^{n_2 - n_1} Y \cdots YZ^{n_{M_I} - n_{M_I-1}} Y)_j^i. \quad (2.8)$$

We have used the notation $\{n_i\}_I$ in (2.7) to describe the integers $\{n_1, n_2, \dots, n_{M_I}\}$ which appear in the I th open string word. This is a lattice notation, which lists the number of Z s appearing to the left of each of the Y s, starting from the second Y : the Z s form a lattice and the n_i give a position in this lattice. This notation is particularly convenient when we discuss the action of the dilatation operator. We will also find an occupation notation useful. The occupation notation lists the number of Z s between consecutive Y s, and is indicated by placing the n_i in brackets. Thus, for example $O(R, R_1^1, R_2^1, \{n_1, n_2, n_3\}) = O(R, R_1^1, R_2^1, \{(n_1), (n_2 - n_1), (n_3 - n_2)\})$. R is a Young diagram with $n+k$ boxes. A bound state of p_s giant gravitons and p_a dual giant gravitons is described by a Young diagram R with p_a rows, each containing order N boxes

¹For example, one could consider the force exerted by the string on the giant

and p_s columns, each containing order N boxes. $\chi_{R, R_1^k, R_2^k}(\sigma)$ is a restricted character [7] given by

$$\chi_{R, R_1^k, R_2^k}(\sigma) = \text{Tr}_{R, R_1^k, R_2^k}(\Gamma_R(\sigma)) \quad (2.9)$$

R^k is a Young diagram with n boxes, that is, it is a representation of S_n . The irreducible representation R of S_{n+k} is reducible if we restrict to the S_n subgroup. R^k is one of the representations that arise upon restricting. In general, any such representation will be subduced more than once. Above we have used the subscripts 1 and 2 to indicate this. We have in mind a Gelfand-Tsetlin like labeling to provide a systematic way to describe the possible R^k we might consider. In this labeling, we use the transformation of the representation under the chain of subgroups $S_{n+k} \supset S_{n+k-1} \supset S_{n+k-2} \supset \dots \supset S_n$. This is achieved by labeling boxes in R . Dropping the boxes with labels $\leq i$, we obtain the representation of S_{n+k-i} to which R^k belongs. We have to spell out how this chain of subgroups are embedded in S_{n+k} . Think of S_q as the group which permutes objects labeled $1, 2, 3, \dots, q$. Here we have $q = n+k$ and the objects we have in mind are the Z fields or the open string words. We associate an integer to an object by looking at the upper indices in (2.7); as an example, the open string described by W_2 is object number $n+k-1$. To go from S_{n+k-i} to $S_{n+k-i-1}$, we keep only the permutations that fix $n+k-i$. We can put the states in R_1^k and R_2^k into a 1-to-1 correspondence. The trace $\text{Tr}_{R_1^k, R_2^k}$ sums the column index over R_1^k and the row index over R_2^k . If we associate the row and column indices with the endpoints of the open string, we can associate the endpoints of the open string I with the box labeled I in R_1^k and R_2^k . The numbers appearing in the boxes of R_1^k literally tell us where the k open strings start and the numbers in R_2^k where the k open strings end. See Figure 2.1 for an example

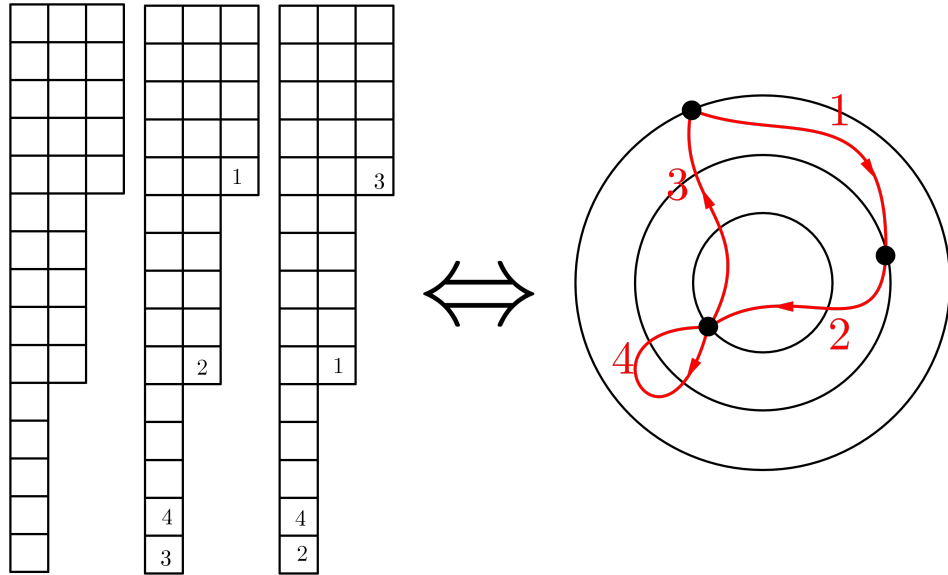


Figure 2.1: A cartoon illustrating the R, R_1^k, R_2^k labeling for an example with $k = 4$ open string strings and 3 giant gravitons. The shape of the strings stretching between the giants is not realistic - only the locations of the end points of the open strings is accurate. The giant gravitons are orbiting on the circles shown; the radius shown for each orbit is accurate. They wrap an S^3 which is transverse to the plane on which they orbit. The smaller the radius of the giants orbit, the larger the S^3 it wraps. The size of the S^3 that the giant wraps is given by its momentum, which is equal to the number of boxes in the column which corresponds to the giant. The numbers appearing in the boxes of R_1^4 tell us where the open strings start and the numbers appearing in the boxes of R_2^4 where they end.

of this labeling. Each Y in an open string word is a magnon. We will take the number of magnons $M_I = O(1) \forall I$. The $Z_{\sigma(j)}^i$ with $1 \leq j \leq n$ belong to the system of giants and the Z s appearing in W_I belong to the I th open string. It is clear that $n \sim O(N)$.

Each giant graviton is associated with a long column and each dual giant graviton with a long row in the Young diagrams labeling the restricted Schur

polynomial. Our notation for the Young diagrams is to list row lengths. Thus a Young diagram that has two columns, one of length n_1 and the second of length n_2 with $n_2 < n_1$ is denoted $(2^{n_2}, 1^{n_1-n_2})$, while a Young diagram with two rows, one of length n_1 and one of length n_2 ($n_1 > n_2$) is denoted (n_1, n_2) .

We want to use the results of [7; 8; 9] to study correlation functions of these operators. The correlators are obtained by summing all contractions between the Z s belonging to the giants, and by grouping the open string words in pairs and summing only the planar diagrams between the fields in each pair of the open string words. To justify the planar approximation for the open string words we take $n_i \geq 0$ and $\sum_{i=1}^L n_i \leq O(N)$. For a nice careful discussion of related issues, see [83].

We can put these operators into correspondence with normalized states

$$O(R, R_1^k, R_2^k; \{n_i\}_1, \{n_i\}_2, \dots, \{n_i\}_k) \leftrightarrow |R, R_1^k, R_2^k; \{n_i\}_1, \{n_i\}_2, \dots, \{n_i\}_k\rangle \quad (2.10)$$

by using the usual state-operator correspondence available for any conformal field theory. In what follows we will mainly use the state language.

2.4 Action of the Dilatation Operator

The one loop dilatation operator, in the $SU(2)$ sector, is [84; 85]

$$D = -\frac{g_{YM}^2}{8\pi^2} \text{Tr} \left([Y, Z] \left[\frac{d}{dY}, \frac{d}{dZ} \right] \right) \quad (2.11)$$

Our goal in this section is to review the action of this dilatation operator on the restricted Schur polynomials, which was constructed in general in [8; 9]. When we act with D on $O(R, R_1^k, R_2^k; \{n_i\}_1, \{n_i\}_2, \dots, \{n_i\}_k)$ the derivative with respect to Y will act on a Y belonging to a specific open string word. Thus, in the large N limit we can decompose the action of D into a sum of terms, with each individual term being the action on a specific open string. If we act on a magnon belonging to the bulk of the open string word, then the only contribution comes by acting with the derivative respect to Z on a field that is immediately adjacent to the magnon. We act only on the adjacent Z fields because to capture the large N limit we should use the planar approximation for

the open string word contractions. To illustrate the action on a bulk magnon, consider the operator corresponding to a single giant graviton with a single open string attached. The giant has momentum n so that R is a single column with $n+1$ boxes: $R = 1^{n+1}$. Further, $R_1^1 = R_2^1 = 1^n$. The open string has three magnons and hence we can describe the $|1^{n+1}, 1^n, 1^n; \{n_1, n_2\}\rangle$. The action on the bulk magnon at large N is

$$D_{\text{bulk magnon}}|1^{n+1}, 1^n, 1^n; \{(n_1), (n_2)\}\rangle = \frac{g_{YM}^2 N}{8\pi^2} \left[2|1^{n+1}, 1^n, 1^n; \{(n_1), (n_2)\}\rangle - |1^{n+1}, 1^n, 1^n; \{(n_1-1), (n_2+1)\}\rangle - |1^{n+1}, 1^n, 1^n; \{(n_1+1), (n_2-1)\}\rangle \right] \quad (2.12)$$

If we act on a magnon which occupies either the first or last position of the open string word, we realize one of the four possibilities listed below.

1. The derivative with respect to Z acts on the Z adjacent to the Y , belonging to the open string and the coefficient of the product of derivatives with respect to Y and Z replaces these fields in the same order. None of the labels of the state change. This term has a coefficient of 1 [8; 9].
2. The derivative with respect to Z acts on the Z adjacent to the Y , belonging to the open string word and the coefficient of the product of derivatives with respect to Y and Z replaces these fields in the opposite order. In this case, a Z has moved out of the open string word and into its own slot in the restricted Schur polynomial - a hop off interaction in the terminology of [8]. In the process the Young diagrams labeling the excited giant graviton grows by a single box. If the string is attached to a giant graviton, the column the endpoint of the relevant open string belongs to inherits the extra box. If the string is attached to a dual giant graviton, the row the endpoint of the relevant open string belongs to inherits the extra box. The coefficient of this term is given by minus one times the square root of the factor associated with the open string box divided by N [8; 9]. We remind the reader that a box in row i and column j is assigned the factor $N - i + j$.
3. The derivative with respect to Z acts on a Z belonging to the giant and the coefficient of the product of derivatives with respect to Y and Z replaces

these fields in the opposite order. In this case, a Z has moved from its own slot in the restricted Schur polynomial and onto the open string word - a hop on interaction in the terminology of [8]. In the process the Young diagrams labeling the giant graviton shrinks by a single box. The details of which column/row shrinks is exactly parallel to the discussion in point 2 above. The coefficient of this term is given by minus one times the square root of the factor associated with the open string box divided by N [8; 9].

4. The derivative with respect to Z acts on a Z belonging to the giant and the coefficient of the product of derivatives with respect to Y and Z replaces these fields in the same order. This is a kissing interaction in the terminology of [8]. None of the labels of the state change. The coefficient of this term is given by the factor associated with the open string box divided by N [8; 9].

For the example we are considering the dilatation operator has the following large N action on the magnons closest to the string endpoints

$$D_{\text{first magnon}}|1^{n+1}, 1^n, 1^n; \{(n_1), (n_2)\}\rangle = \frac{g_{YM}^2 N}{8\pi^2} \left[\left(1 + 1 - \frac{n}{N}\right) |1^{n+1}, 1^n, 1^n; \{(n_1), (n_2)\}\rangle - \sqrt{1 - \frac{n}{N}} (|1^{n+2}, 1^{n+1}, 1^{n+1}; \{(n_1 - 1), (n_2)\}\rangle - |1^n, 1^{n-1}, 1^{n-1}; \{(n_1 + 1), (n_2)\}\rangle) \right] \quad (2.13)$$

and

$$D_{\text{last magnon}}|1^{n+1}, 1^n, 1^n; \{(n_1), (n_2)\}\rangle = \frac{g_{YM}^2 N}{8\pi^2} \left[\left(1 + 1 - \frac{n}{N}\right) |1^{n+1}, 1^n, 1^n; \{(n_1), (n_2)\}\rangle - \sqrt{1 - \frac{n}{N}} (|1^{n+2}, 1^{n+1}, 1^{n+1}; \{(n_1), (n_2 - 1)\}\rangle - |1^n, 1^{n-1}, 1^{n-1}; \{(n_1), (n_2 + 1)\}\rangle) \right] \quad (2.14)$$

There are a few points worth noting: The complete action of the dilatation operator can be read from the Young diagram labels of the operator. The factors of the boxes in the Young diagram for the endpoints of a given open string determine the action of the dilatation operator on that open string. When the labels $R_1^k \neq R_2^k$, the string end points are on different giant gravitons and the two endpoints are associated with different boxes in the Young diagram so that the action of the dilatation operator on the two boundary magnons

is distinct. To determine these endpoint interactions we must go beyond the planar approximation. Notice that for a maximal giant graviton we have $n = N$. In this case, most of the boundary magnon terms in the Hamiltonian vanish and the boundary magnons are locked in place at the string endpoints. The giant graviton brane is simply supplying a Dirichlet boundary condition for the open string. For non-maximal giants, all of the boundary magnon terms are non-zero and, for example, Z fields that belong to the open string can wander into slots describing the giant. Alternatively, since the split between open string and brane is probably not very sharp, we might think that the magnons can wander from the string endpoints into the bulk of the open string. The coefficient of these hopping terms is modified by the presence of the giant graviton, so that the boundary magnons do not behave in the same way as the bulk magnons do.

As a final example, consider a dual giant graviton which carries momentum n . In this case, R is a single row of n boxes and we have

$$D_{\text{first magnon}}|n+1, n, n; \{(n_1), (n_2)\}\rangle = \frac{g_{YM}^2 N}{8\pi^2} \left[\left(1 + 1 + \frac{n}{N}\right) |n+1, n, n; \{(n_1), (n_2)\}\rangle - \sqrt{1 + \frac{n}{N}} (|n+2, n+1, n+1; \{(n_1-1), (n_2)\}\rangle - |n, n-1, n-1; \{(n_1+1), (n_2)\}\rangle) \right] \quad (2.15)$$

In the Appendix A we discuss the action of the dilatation operator at two loops.

2.5 Large N Diagonalization: Asymptotic States

We are now ready to construct eigenstates of the dilatation operator. We will not construct exact large N eigenstates. Rather, we focus on states for which all magnons are well separated. From these states we can still obtain the anomalous dimensions. In section 2.7 we will describe how one might use these asymptotic states to construct exact eigenstates, following [12; 13]. In the absence of integrability however, this can not be carried to completion and our states are best thought of as very good approximate eigenstates.

The Z s in the open string word define a lattice on which the Y s hop. Our construction entails taking a Fourier transform on this lattice. The boundary

interactions allow Z s to move onto and out of the lattice, so the lattice size is not fixed. To implement this idea, we introduce the phases

$$q_a = e^{\frac{i2\pi k_a}{J}} \quad (2.16)$$

with $k_q = 0, 1, \dots, J-1$ as well as a cut off function whose form is shown in figure 2.2. The eigenstate with two magnons is then given by

$$\begin{aligned} |\psi(q_1)\rangle &= \sum_{m_2=0}^{n+J} \sum_{m_1=0}^{m_2} f(m_2) q_1^{m_1-m_2} |1^{n+J+m_1-m_2+1}, 1^{n+J+m_1-m_2}, 1^{n+J+m_1-m_2}; \{m_2 - m_1\}\rangle \\ &+ \sum_{m_1=0}^{m_2+J} \sum_{m_2=0}^n f(m_2) f(J - m_1 + m_2) \\ &\times q_1^{m_1-m_2} |1^{n+J+m_1-m_2+1}, 1^{n+J+m_1-m_2}, 1^{n+J+m_1-m_2}; \{m_2 - m_1\}\rangle \end{aligned} \quad (2.17)$$

For a detailed discussion of the construction, we refer the reader to Appendix A. At large N it is now simple to show that

$$\begin{aligned} D|\psi(q_1)\rangle &= 2 \frac{g_{YM}^2}{8\pi^2} \left(1 + \left[1 - \frac{n}{N} \right] - \sqrt{1 - \frac{n}{N}} (q_1 + q_1^{-1}) \right) \\ &= 2g^2 \left(1 + \left[1 - \frac{n}{N} \right] - \sqrt{1 - \frac{n}{N}} (q_1 + q_1^{-1}) \right) \end{aligned} \quad (2.18)$$

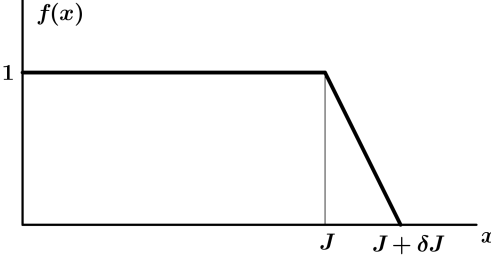


Figure 2.2: The cutoff function used in constructing large N eigenstates

Since both magnons are boundary magnons, the above formula shows that boundary magnons carry momentum and it characterizes their anomalous di-

mension. The analysis for the dual giant graviton of momentum n leads to

$$\begin{aligned} D|\psi(q_1)\rangle &= 2\frac{g_{YM}^2}{8\pi^2} \left(1 + \left[1 + \frac{n}{N} \right] - \sqrt{1 + \frac{n}{N}}(q_1 + q_1^{-1}) \right) |\psi(q_1)\rangle \\ &= 2g^2 \left(1 + \left[1 + \frac{n}{N} \right] - \sqrt{1 + \frac{n}{N}}(q_1 + q_1^{-1}) \right) |\psi(q_1)\rangle \end{aligned} \quad (2.19)$$

For the generalizations to states with more magnons and further details, the reader should consult Appendix A. This completes our discussion of the large N asymptotic eigenstates. We will now consider the dual string theory description of these states.

2.6 String Theory Description

The string theory description of the gauge theory operators is most easily developed using the limit introduced by Maldacena and Hofman [22], in which the spectrum on both sides of the correspondence simplifies. The limit considers operators of large \mathcal{R} charge J and scaling dimension Δ holding $\Delta - J$ and the 't Hooft coupling λ fixed. Both sides of the correspondence enjoy an $SU(2|2) \times SU(2|2)$ supersymmetry with novel central extensions as realized by Beisert in [12; 13]. Once the central charge of the spin-chain/worldsheet excitations have been determined, their spectrum and constraints on their two body scattering are determined. A powerful conclusion argued for in [22] using the physical picture developed in [48] is that there is a natural geometric interpretation for these central charges in the classical string theory. This geometric interpretation also proved useful in the analysis of maximal giant gravitons in [21]. In this section we will argue that it is also applicable to the case of non-maximal giant and dual giant gravitons.

Giant gravitons carry a dipole moment under the RR five form flux F_5 . When they move through the spacetime, the Lorentz force like coupling to F_5 causes them to expand in directions transverse to the direction in which they move [85]. The giant graviton orbits on a circle inside the S^5 and wraps an S^3 transverse to this circle but also contained in the S^5 . Using the complex coordinates $x = x_5 + ix_6$, $y = x_3 + ix_4$ and $z = x_1 + ix_2$ the S^5 is described by

$$|z|^2 + |x|^2 + |y|^2 = 1 \quad (2.20)$$

in units with the radius of the S^5 equal to 1. The giant is orbiting in the $1 - 2$ plane on the circle $|z| = r$. The size to which the giant expands is determined by canceling the force causing them to expand, due to the coupling to the F_5 flux, against the D3 brane tension, which causes them to shrink. Since the coupling to the F_5 flux depends on their velocity, the size of the giant graviton is determined by its angular momentum n as [4; 5; 6]

$$|x|^2 + |y|^2 = \frac{n}{N} \quad (2.21)$$

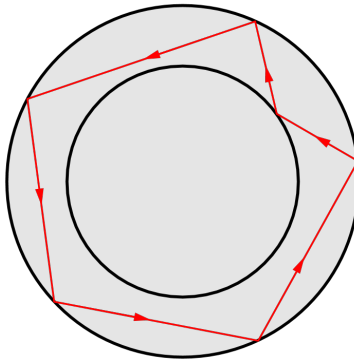


Figure 2.3: The giant is orbiting on the smaller circle shown. Each red segment is a magnon. The arrows in the figure simply indicate the orientation of the central charge k_i of the i th magnon. The LLM disk is shaded in this and subsequent figures. This is done to distinguish the rim of the LLM disk from the orbits of the giant gravitons.

Using (2.20) we see that the giant graviton orbits on a circle of radius [86]

$$r = \sqrt{1 - \frac{n}{N}} < 1 \quad (2.22)$$

Consider now the worldsheet geometry for an open string attached to a giant graviton. Following [22], we will describe this worldsheet solution using LLM coordinates [50]. The worldsheet for this solution, in these coordinates, is shown in Figure 2.3. The figure shows an open string with 6 magnons. Each magnon corresponds to a directed line segment in the figure. The first and last magnons connect to the giant which is orbiting on the smaller circle shown. Between the

magnons we have a collection of $O(\sqrt{N})$ Zs. These are pushed by a centrifugal force to the circle $|z| = 1$ giving the string worldsheet the shape shown in the figure 2.3.

In the limit that the magnons are well separated, each magnon transforms in a definite $SU(2|2)$ representation. The open string itself transforms as the tensor product of the individual magnon representations. The representation of each individual magnon is specified by giving the values of the central charges k_i , k_i^* appearing in (2.5). Regarding the plane shown in Figure 2.3 as the complex plane, k is given by the complex number determined by the vector describing the directed segment corresponding to the magnon. In particular, the magnitude of k is given by the length of the line corresponding to the magnon. The energy of the magnon, which transforms in a short representation, is determined by supersymmetry to be[12; 13]

$$E = \sqrt{1 + 2\lambda|k|^2} = 1 + \lambda|k|^2 - \frac{1}{2}\lambda^2|k|^4 + \dots \quad (2.23)$$

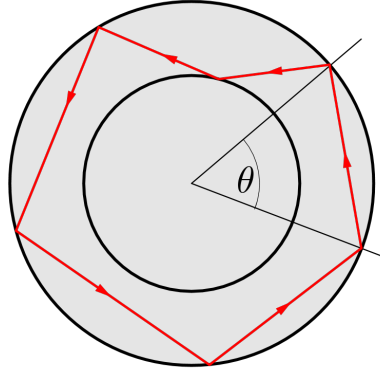


Figure 2.4: A bulk magnon subtending an angle θ has a length of $2 \sin \frac{\theta}{2}$.

For a magnon which subtends an angle θ as shown in figure 2.4, we find [22]

$$E = 1 + 4\lambda \sin^2 \frac{\theta}{2} + O(\lambda^2) = 1 + \lambda(2 - e^{i\theta} - e^{-i\theta}) + O(\lambda^2). \quad (2.24)$$

This is in perfect agreement with the field theory answer (A.12) if we set $\lambda = g^2$ and

$$q = e^{i \frac{2\pi k}{J}} = e^{i\theta} \quad \theta = \frac{2\pi k}{J} \quad (2.25)$$

Thus the angle that is subtended by the magnon is equal to its momentum, which is the well known result obtained in [22]. Consider now the boundary magnon, as shown in Figure 2.5. The circle on which the giant orbits has a radius given by

$$r = \sqrt{1 - \frac{n}{N}} \quad (2.26)$$

The large circle has a radius of 1 in the units we are using. Thus, the length of the boundary magnon is given by the length of the diagonal of the isosceles trapezium shown in Figure 2.5. Consequently

$$\begin{aligned} E &= 1 + \lambda((1-r)^2 + 4r \sin^2 \frac{\theta}{2}) + O(\lambda^2) \\ &= 1 + \lambda(1 + r^2 - r(e^{i\theta} + e^{-i\theta})) + O(\lambda^2) \end{aligned} \quad (2.27)$$

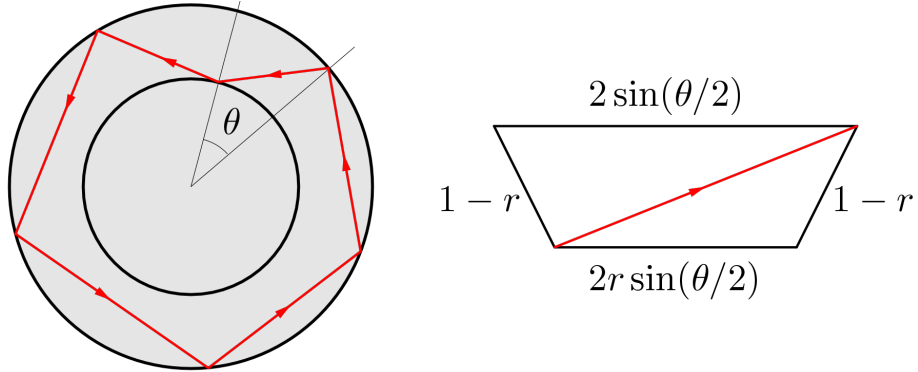


Figure 2.5: A boundary magnon subtending an angle θ has a length $\sqrt{(1-r)^2 + 4r \sin^2 \frac{\theta}{2}}$.

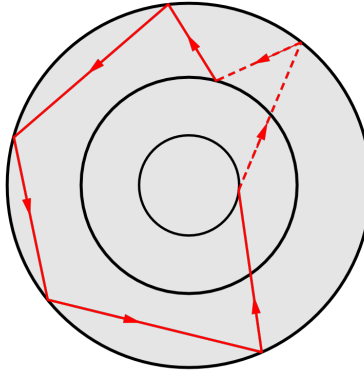


Figure 2.6: A two strings attached to two giant gravitons state. To distinguish the two strings, one of them has been indicated with dashed lines. Both giants are submaximal and so are moving on circles with a radius $|z| < 1$. One of the strings has only two boundary magnons. The second string has two boundary magnons and three bulk magnons. Notice that each open string has a non-vanishing central charge. It is only for the full state that the central charge vanishes. See [1] for closely related observations.

This is again in complete agreement with (A.12) after we set $\theta = \frac{2\pi k}{J}$ and recall that $r = \sqrt{1 - \frac{n}{N}}$. This is a convincing check of the boundary terms in the dilatation operator and of our large N asymptotic eigenstates. In the description of maximal giant gravitons, the boundary magnon always stretches from the center of the disk to a point on the circumference of the circle $|z| = 1$. Consequently, for the maximal giant the boundary magnon subtends an angle of zero and it never has a non-zero momentum. For submaximal giants we see that the boundary magnons do in general carry non-zero momentum. This is completely expected: in the case of a maximal giant graviton, the boundary magnons are locked in the first and last position of the open string lattice. As we move away from the maximal giant graviton, the coefficients of the boundary terms which allow the boundary magnons to hop in the lattice, increase from zero, allowing the boundary magnons to move and hence, to carry a non-zero momentum. In the Appendix B we have checked that the two loop answer in the field theory agrees with the $O(\lambda^2)$ term of (2.23).

Notice that the vector sum of the directed lines segments vanishes. This is nothing but -1 the statement that our operator vanishes unless $q_M^{-1} = q_1 q_2 \cdots q_{M-1}$. This condition ensures that although each magnon transforms in a representation of $SU(2|2)$ with non-zero central charges, the complete state enjoys an $SU(2|2)$ symmetry that has no central extension. It is for this reason that the central charges must sum to zero and hence that the vector sum of the red segments must vanish. This is achieved in an interesting way for certain multi-string states: each open string can transform under an $SU(2|2)$ that has a non-zero central charge and it is only for the full state of all open strings plus giants that the central charge vanishes. An example of this for a two string state is given in Figure 2.6.

To conclude this section, we will consider an example involving a dual giant graviton. In this case, the giant graviton orbits on a circle [4; 5]

$$r = \sqrt{1 + \frac{n}{N}} > 1 \quad (2.28)$$

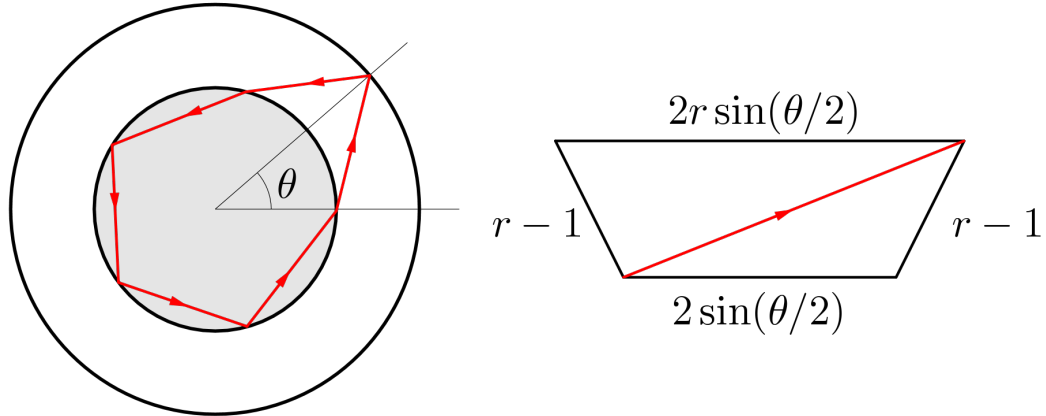


Figure 2.7: A boundary magnon subtending an angle θ has a length of $\sqrt{(r-1)^2 + 4r \sin^2 \frac{\theta}{2}}$.

The length of the line segment corresponding to the boundary magnon is again given by the length of the diagonal of an isosceles trapezium, as shown in

Figure 2.7. Consequently

$$\begin{aligned} E &= 1 + \lambda((1-r)^2 + 4r \sin^2 \frac{\theta}{2}) + O(\lambda^2) \\ &= 1 + \lambda(1 + r^2 - r(e^{i\theta} + e^{-i\theta})) + O(\lambda^2) \end{aligned} \quad (2.29)$$

which is in perfect agreement with (2.19) after we set $\theta = \frac{2\pi k}{J}$ and $r = \sqrt{1 + \frac{n}{N}}$.

2.7 From asymptotic states to exact eigenstates

The states we have written down above are asymptotic states in the sense that we have implicitly assumed that all of the magnons are well separated. In this case the excitations can be treated individually and the symmetry algebra acts as a tensor product representation. However, the magnons can come close together and even swap positions. When they swap positions, we get different asymptotic states that must be combined to obtain the exact eigenstate. The asymptotic states must be combined in a way that is compatible with the algebra, as explained in [12]. This requirement ultimately implies a unique way to complete the asymptotic states to obtain the exact eigenstate.

When two bulk magnons swap positions, the corresponding asymptotic states are combined using the two particle S –matrix. The relevant two particle S –matrix has been determined in [12; 13]. It is also possible for a bulk magnon to reflect/scatter off a boundary magnon. For maximal giant gravitons [21], the reflection from the boundary preserves the fact that the boundary magnon has zero momentum and it reverses the sign of the momentum of the bulk magnon. In this section we would like to investigate the scattering of a bulk magnon off a boundary magnon for a non-maximal giant graviton.

We must require that the total central charge k of the state vanishes. Thus, after the scattering the directed line segments must still sum to zero. Further the central charge C of the state must remain unchanged. Taken together, these conditions uniquely fix the momentum of both bulk and boundary magnon after the scattering.

In Figure 2.8 the process of scattering a bulk magnon off the boundary magnon is shown. After the scattering the magnons that have a different momentum, corresponding to line

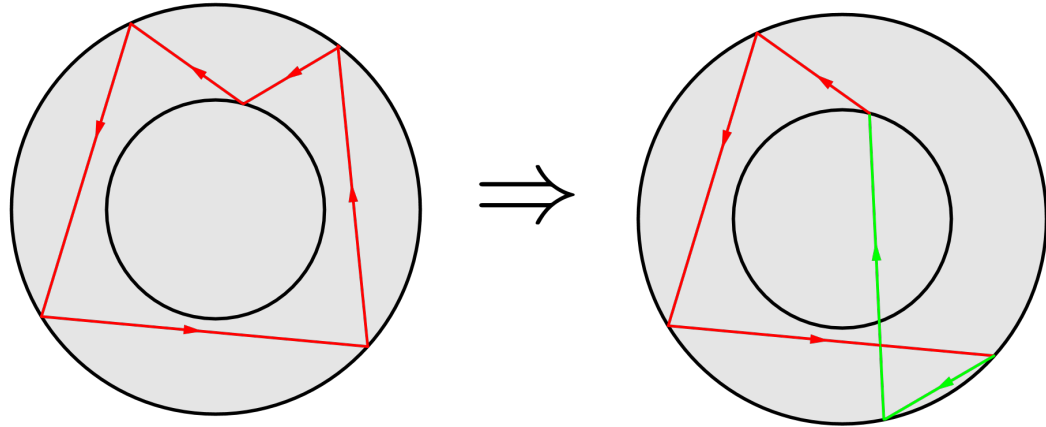


Figure 2.8: A bulk magnon scatters with a boundary magnon. In the process the direction of the momentum of the bulk magnon is reversed.

segments that have changed and these are shown in green. In this case the giant graviton is close enough to a maximal giant that the momentum of the boundary magnon is reversed, so this is a reflection-like scattering. Before and after the scattering the line segments line up to form a closed circuit, so that the central charge k of the state before and after scattering is zero. To analyze the constraint arising from fixing the central charge C , we parametrize the problem as shown in figure 9. There is a single parameter which is fixed by requiring

$$\begin{aligned} & \sqrt{1 + 8\lambda \sin^2 \frac{\varphi_2}{2}} + \sqrt{1 + 8\lambda \left([1+r]^2 + 4r^2 \sin^2 \frac{\varphi_1}{2} \right)} \\ &= \sqrt{1 + 8\lambda \sin^2 \frac{\theta}{2}} + \sqrt{1 + 8\lambda \left([1+r]^2 + 4r^2 \sin^2 \left(\frac{\varphi_1 + \varphi_2 + \theta}{2} \right) \right)} \end{aligned} \quad (2.30)$$

which is the condition that the state has the correct central charge C . In the above formula we have

$$r = \sqrt{1 - \frac{b_0}{N}} \quad (2.31)$$

The equation (2.30) has two solutions, one of which is negative $\theta = -\varphi_2$ and describes the state before the scattering. We need to choose the solution for which $\theta \neq -\varphi$. Notice that for $b_0 = N$ this condition implies that $\theta = \varphi_2$ which is indeed the correct answer [21]. In this case, the bulk magnon reflects off the boundary with a reverse in the direction of its momentum but no change in its

magnitude. The momentum of the bulk magnon remains zero. When $b_0 = 0$ the momenta of the two magnons is exchanged which is again the correct answer [12; 13]. When $0 < b_0 < N$ we find the solution to (2.30) for the momentum of the bulk magnon interpolates between reflection like scattering (when the momentum of the magnon is reversed) and magnon like scattering (when the momenta of the two magnons are exchanged). In this case though, in general, the magnitude of the momenta of the bulk and the boundary magnons are not preserved by the scattering - the scattering is inelastic. Finally, the scattering of a bulk magnon from a boundary magnon attached to a dual giant graviton is always magnon like scattering. i.e. neither of the momenta change direction.

The fact that the scattering between boundary and bulk magnons is not elastic has far reaching consequences. First, the system will not be integrable. In the case of purely elastic scattering for all magnon scatterings, the number of asymptotic states that must be combined to construct the exact energy eigenstate is roughly $(M - 1)!$ for M magnons.

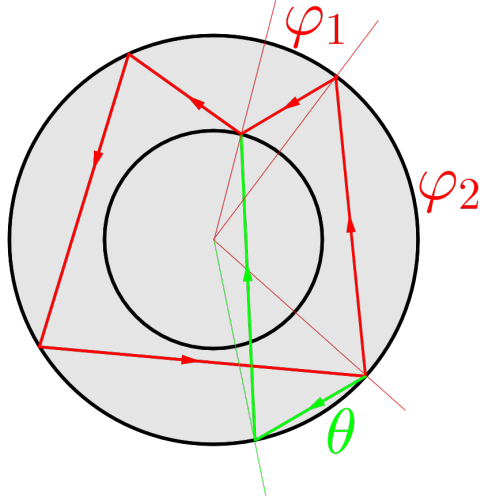


Figure 2.9: A bulk magnon scatters with a boundary magnon. In the process the direction of the momentum of the bulk magnon is reversed. Before the scattering the boundary magnon subtends an angle φ_1 and the bulk magnon subtends an angle φ_2 . After the scattering the boundary magnon subtends an angle $\varphi_1 + \varphi_2 + \theta$ and the bulk magnon subtends an angle $-\theta$.

This is the number of ways of arranging the magnons (distinguished by their momentum) up to cyclicity. There are M magnon momenta appearing and these momenta are the same for all the asymptotic states. The exact eigenstates can then be constructed using a coordinate space Bethe ansatz. For the case of inelastic scattering, the momenta appearing depend on the specific asymptotic state one considers and there are many more than $(M - 1)!$ asymptotic states that must be combined to construct the exact eigenstate. In this case constructing the exact eigenstates from the asymptotic states appears to be a formidable problem.

2.8 S -matrix and boundary reflection matrix

We have a good understanding of the symmetries of the theory and the representations under which the states transform. Following Beisert [12; 13], this is all that is needed to obtain the magnon scattering matrix. In this section we will carry out this analysis.

Each magnon transforms under a centrally extended representation of the $\mathfrak{su}(2|2)$ algebra

$$\{Q_a^\alpha, Q_b^\beta\} = \epsilon^{\alpha\beta} \epsilon_{ab} \frac{k_i}{2}, \quad \{S_\alpha^a, S_\beta^b\} = \epsilon_{\alpha\beta} \epsilon^{ab} \frac{k_i^*}{2}, \quad (2.32)$$

$$\{S_\alpha^a, Q_b^\beta\} = \delta_b^a L_\alpha^\beta + \delta_\alpha^\beta R^a{}_b + \delta_b^a \delta_\alpha^\beta C_i \quad (2.33)$$

There are also the usual commutators for the bosonic $\mathfrak{su}(2)$ generators. There are three central charges k_i , k_i^* , C_i for each $SU(2|2)$ factor. Following [21] we set the central charges of the two copies to be equal. It is useful to review how the bosonic part of the $SU(2|2)^2$ symmetry acts in the gauge theory. $\mathcal{N} = 4$ super Yang-Mills theory has 6 hermitian adjoint scalars ϕ^i that transform as a vector of $SO(6)$. We have combined them into the complex fields as follows

$$\begin{aligned} X &= \phi^1 + i\phi^2, & \bar{X} &= \phi^1 - i\phi^2, \\ Y &= \phi^3 + i\phi^4, & \bar{X} &= \phi^3 - i\phi^4, \\ X &= \phi^4 + i\phi^6, & \bar{X} &= \phi^5 - i\phi^6. \end{aligned} \quad (2.34)$$

The bosonic subgroup of $SU(2|2)^2$ is $SU(2) \times SU(2) = SO(4)$ that rotates $\phi^1, \phi^2, \phi^3, \phi^4$ as a vector. In terms of complex fields, Y, X and \bar{Y}, \bar{X} transform under the different $SU(2|2)$ groups. Z, \bar{Z} do not transform. To specify the representation that each magnon transforms in, following [12; 13] we specify parameters a_k, b_k, c_k, d_k for each magnon, where

$$Q_a^\alpha |\phi^b\rangle = a + k\delta_a^b |\psi^\alpha\rangle, \quad Q_a^\alpha |\psi^\beta\rangle = b_k \epsilon^{\alpha\beta} \epsilon_{ab} |\phi^b\rangle,$$

$$S_\alpha^a |\phi^b\rangle = c_k \epsilon_{\alpha\beta} \epsilon^{ab} |\psi^\beta\rangle, \quad S_\alpha^a |\psi^\beta\rangle = d_k \delta_\alpha^\beta |\phi^a\rangle,$$

for the k th magnon. We are using the non-local notation of [13]. Using the representation introduced above

$$Q_1^1 Q_2^2 |\phi^2\rangle = a_k Q_1^1 |\psi^2\rangle = b_k a_k \epsilon^{12} \epsilon_{12} |\phi^2\rangle, \quad Q_2^2 Q_1^1 |\phi^2\rangle = 0, \quad (2.35)$$

so that $k_k = 2a_k b_k$. An identical argument using the S_α^a supercharges gives $k_k = 2c_k d_k$. Consider next a state with a total of K magnons. If we are to obtain a representation without central extension, we must require that the central charges vanish

$$\begin{aligned} \frac{k}{2} &= \sum_{k=1}^K \frac{k_k}{2} = \sum_{k=1}^K a_k b_k = 0, \\ \frac{k^*}{2} &= \sum_{k=1}^K \frac{k_k^*}{2} = \sum_{k=1}^K c_k d_k = 0. \end{aligned} \quad (2.36)$$

To obtain a formula for the central charge C consider

$$Q_a^\alpha S_\beta^b |\phi^c\rangle = c_k Q_a^\alpha \epsilon^{bc} \epsilon_{\beta\gamma} |\psi^\gamma\rangle = c_k b_k \epsilon^{bc} \epsilon_{\beta\gamma} \epsilon^{\alpha\gamma} \epsilon_{ad} |\phi^d\rangle. \quad (2.37)$$

Now set $a = b$ and $=$ and sum over both indices to obtain

$$Q_a^\alpha S_\alpha^a |\phi^c\rangle = 2b_k c_k |\phi^c\rangle \quad (2.38)$$

Very similar manipulations show that

$$S_\alpha^a Q_a^\alpha |\phi^c\rangle = 2a_k d_k |\phi^c\rangle \quad (2.39)$$

so that we learn the value of the central charge C_k

$$\{Q_a^\alpha, S_\alpha^a\} |\phi^c\rangle = 4C |\phi^c\rangle = 2(a_k d_k + b_k c_k) |\phi^c\rangle, \quad \Rightarrow \quad C_k = \frac{1}{2}(a_k d_k + b_k c_k). \quad (2.40)$$

Using

$$\{S_2^1, Q_1^1\} = L_2^1 \quad L_2^1 |\psi^2\rangle = |\psi^1\rangle \quad (2.41)$$

we easily find

$$\{S_2^1, Q_1^1\} |\psi^2\rangle = (a_k d_k - b_k c_k) |\psi^1\rangle \quad \Rightarrow \quad a_k d_k - b_k c_k = 1. \quad (2.42)$$

This is also the condition to get an atypical representation of $\mathfrak{su}(2|2)$ [13].

Following [12], a useful parametrization for the parameters of the representation is given by

$$a_k = \sqrt{g} \eta_k, \quad b_k = \frac{\sqrt{g}}{\eta_k} f_k \left(1 - \frac{x_k^+}{x_k^-} \right), \quad (2.43)$$

$$c_k = \frac{\sqrt{g} i \eta_k}{f_k x_k^+}, \quad d_k = \frac{\sqrt{g} x_k^+}{i \eta_k} \left(1 - \frac{x_k^-}{x_k^+} \right). \quad (2.44)$$

The parameters x_k^\pm are set by the momentum p_k of the magnon

$$e^{i \frac{2\pi p_k}{J}} = \frac{x_k^+}{x_k^-}. \quad (2.45)$$

The parameter f_k is a pure phase, given by the product $\prod_j e^{i p_j}$, where j runs over all magnons to the left of the magnon considered. To ensure unitarity $|\eta_k|^2 = i(x_k^- - x_k^+)$. The condition $a_k d_k - b_k c_k = 1$ to get an atypical representation implies that

$$x_k^+ + \frac{1}{x_k^+} - x_k^- - \frac{1}{x_k^-} = \frac{i}{g}. \quad (2.46)$$

This equation will be very useful in verifying some of the S -matrix formulas given below. A useful parametrization for the parameters specifying the representation for a boundary magnon is given by

$$a_k = \sqrt{g} \eta_k, \quad b_k = \frac{\sqrt{g}}{\eta_k} f_k \left(1 - r \frac{x_k^+}{x_k^-} \right), \quad (2.47)$$

$$c_k = \frac{\sqrt{g} i \eta_k}{f_k x_k^+}, \quad d_k = \frac{\sqrt{g} x_k^+}{i \eta_k} \left(1 - r \frac{x_k^-}{x_k^+} \right). \quad (2.48)$$

where $r = \sqrt{1 - \frac{n}{N}}$ is the radius of the path on which the giant graviton of momentum n orbits² and the parameters x_k^\pm are again set by the momentum

²For an open string attached to a dual giant graviton, we would have $r = \sqrt{1 + \frac{n}{N}}$ where n is the momentum of the dual giant graviton.

carried by the boundary magnon according to (2.45). For the boundary magnon, f_k is again a phase as described above and now $|\eta_k|^2 = i(rx_k^- - x_k^+)$. For a maximal giant graviton $r = 0$ and the boundary magnon carries no momentum and $|\eta_k|^2 = ix_k^+$. For the boundary magnon, the condition $a_k d_k - b_k c_k = 1$ to get an atypical representation implies that

$$x_l^+ + \frac{1}{x_k^+} - rx_k^- - \frac{r}{x_k^-} = \frac{i}{g}. \quad (2.49)$$

This equation will again be useful below. Equation (2.49) interpolates between (2.46) for $r = 1$, which is the correct condition for a bulk magnon and the condition obtained for $r = 0$

$$x_k^+ + \frac{1}{x_k^+} = \frac{i}{g} \quad (2.50)$$

which was used in [21] for the boundary magnon attached to a maximal giant graviton.

Following [12; 13] one can check that the above parametrization obeys (2.36). Finally,

$$\begin{aligned} a_k b_k c_k d_k &= g^2 (e^{-p_k} - 1)(e^{ip_k} - 1) = 4g^2 \sin^2 \frac{p_k}{2} \\ &= \frac{1}{4} [(a_k d_k + b_k c_k)^2 - (a_k d_k - b_k c_k)^2] = \frac{1}{4} [(2C_k)^2 - 1] \end{aligned} \quad (2.51)$$

so that

$$C_k = \pm \sqrt{\frac{1}{4} + 4g^2 \sin^2 \frac{p_k}{2}} \quad (2.52)$$

The components of an energy eigenstate in different asymptotic regions are related by the bulk-bulk and boundary-bulk magnon scattering matrices S and R . S and R must commute with the $\mathfrak{su}(2|2)$ group. The labels of the representations of individual magnons can change under the scattering but they must do so in a way that preserves the central charges of the total state. In the picture of the energy eigenstates provided by the LLM plane, the central charges are given by the directed line segments (which are vectors and hence can also be viewed as complex numbers), one for each magnon. The fact that these line segments close into polygons is the statement that the central charges k and k^* of our total state vanishes. The sum of the lengths squared of these line segments determines the central charge C . By scattering these segments can

rearrange themselves as long as the sums $\sum_i \sqrt{1 + 2\lambda l_i^2}$ with l_i the length of segment i is preserved and so long as they still form a closed polygon

Implementing the consequences of invariance under $SU(2|2)^2$ is exactly parallel to the analysis of [12; 13; 21]. For the S –matrix describing the scattering of two bulk magnons, the reader is referred to [12; 13]. When considering the equations for the reflection/scattering matrix describing the reflection/scattering of a bulk magnon from a boundary magnon, we need to pay attention to the fact that the central charges of the representation are no longer swapped between the two magnons. Rather, the central charges after the reflection are determined by solving (2.30). Denote the central charge of the boundary magnon before the reflection by p_B . Denote the central charge of the bulk magnon before the reflection by p_b . Denote the central charge of the boundary magnon after the reflection by k_B . Denote the central charge of the bulk magnon after the reflection by k_b . Denote the reflection/scattering matrix by \mathcal{R} . Since the S –matrix has to commute with the bosonic $\mathfrak{su}(2)$ generators Schurs Lemma implies that it must be proportional to the identity in each given irreducible representation of $\mathfrak{su}(2)$. This immediately implies that

$$\mathcal{R}|\phi_{p_B}^a \phi_{p_b}^b\rangle = A_{12}^R |\phi_{k_B}^{\{a} \phi_{k_b}^{b\}}\rangle + B_{12}^R |\phi_{k_B}^{[a} \phi_{k_b}^{b]}\rangle + \frac{1}{2} C_{12}^R \epsilon^{ab} \epsilon_{\alpha\beta} |\psi_{k_B}^\alpha \psi_{k_b}^\beta\rangle \quad (2.53)$$

$$\mathcal{R}|\psi_{p_B}^a \psi_{p_b}^b\rangle = D_{12}^R |\psi_{k_B}^{\{a} \psi_{k_b}^{b\}}\rangle + E_{12}^R |\psi_{k_B}^{[a} \psi_{k_b}^{b]}\rangle + \frac{1}{2} F_{12}^R \epsilon^{ab} \epsilon_{\alpha\beta} |\phi_{k_B}^\alpha \phi_{k_b}^\beta\rangle \quad (2.54)$$

$$\mathcal{R}|\phi_{p_B}^a \psi_{p_b}^\beta\rangle = G_{12}^R |\psi_{k_B}^\beta \phi_{k_b}^{b\}}\rangle + H_{12}^R |\phi_{k_B}^a \psi_{k_b}^\beta\rangle \quad (2.55)$$

$$\mathcal{R}|\psi_{p_B}^\alpha \phi_{p_b}^b\rangle = K_{12}^R |\psi_{k_B}^\alpha \phi_{k_b}^{b\}}\rangle + L_{12}^R |\phi_{k_B}^a \psi_{k_b}^\alpha\rangle \quad (2.56)$$

The analysis now proceeds as in [12; 13]. Demanding the S –matrix commutes

with the supercharges implies

$$\begin{aligned}
 A_{12}^R &= S_{12}^0 \frac{\eta_1 \eta_2 x_1' x_1^+ (x_1^- - x_2^+) \left((x_2^+ - rx_2^-)(rx_2' - x_2') x_2^+ + (x_2^- - rx_2^+)(x_2' - rx_2') x_2' \right)}{\eta_1' \eta_2' x_2' x_2^+ (x_1^- - x_1^+) (x_1^+ - x_1') \left(x_1^+ (rx_2^+ - x_2^-) + x_2^- (rx_2^- - x_2^+) \right)}, \\
 B_{12}^R &= A_{12}^R \left[1 + \frac{2x_2' (x_1' - x_1^+)}{x_1' (x_1^- - x_2^+) (x_1' - x_2' - rx_1' x_2')} \frac{B_1}{B_2} \right] \\
 B_1 &= x_2^- x_1' \left[(x_1^- - x_1^+) (2x_1^- - x_1') (x_2^+ x_1' - x_1^+ x_2^+) \right. \\
 &\quad \left. - x_1' x_1^- (x_2^+ - rx_2^-) (x_1^- - x_2^+) \right] \frac{rx_2' - x_2'}{rx_2' - x_2'} \\
 &\quad + [x_1' x_1^+ (x_1^- - x_2^+) (x_2^- - rx_2^+) + x_2^+ x_2^- (x_1^- - x_2^+) (x_1' - x_1^+)] x_1' x_2', \\
 B_2 &= (rx_2^- - x_2^+) \left[x_1^+ x_2' x_1' - \frac{rx_2^+ - x_2^-}{rx_2^- - x_2^+} - x_1' x_1^- x_2^- \frac{rx_2' - x_2'}{rx_2' - x_2'} \right], \\
 C_{12}^R &= S_{12}^0 \frac{2\eta_2 \eta_1 C_1}{fx_2^+ (x_1^+ - x_1') (x_1^+ (rx_2^+ - x_2^-) + x_2^- (rx_2^- - x_2^+)) (x_1' - x_2' - rx_1' x_2')}, \\
 C_1 &= x_1' \frac{x_1^- - x_2^+}{x_1^- - x_1^+} \left(x_1' x_1^- x_2^- (x_2^+ - rx_2^- (rx_2' - x_2')) + x_1^+ x_1' x_2^- (x_2^- - rx_2^+ (x_2' - rx_2')) \right) \\
 &\quad + x_2^- x_2^+ (x_1^+ - x_1') \left(x_1^- (rx_1' x_2' + x_1' x_2' - 2x_1' x_2') + x_1' x_2^- (rx_2^- - x_1' + x_1' - x_2') \right) \\
 D_{12}^R &= -S_{12}^0 \\
 E_{12}^R &= -S_{12}^0 \left[1 - 2x_1^+ x_2' \frac{\frac{x_1'}{x_1^-} (x_1' - x_1^+ + x_2' - rx_2') - (x_1' - x_1^+) - \frac{x_1' x_2^-}{x_1^+ x_2'} \frac{x_2^+ - rx_2^-}{x_2^- - rx_2^+} (x_2' - rx_2')} {[x_1^+ + x_2^- \frac{x_2^+ - rx_2^-}{x_2^- - rx_2^+}] [rx_1' x_2' - x_1' x_2']} \right] \\
 F_{12}^R &= S_{12}^0 \frac{2x_1^+ x_1' f(x_1' - x_1') (x_2' - rx_2') (x_2^- - rx_2^+)}{\eta_1' \eta_2' x_1^- x_1' [x_1^+ (x_2^- - rx_2^+) + x_2^- (x_2^+ - rx_2^-)] [x_1' x_2' - rx_1' x_2']} \\
 &\quad \times \left[x_1^- - x_1' + \frac{rx_2^- - x^+ 2}{x_2^- - rx_2^+} \frac{x_2^- x_1^-}{x_1^+} + \frac{x_2' - rx_2^-}{x_2' - rx_2'} \frac{x_1' x_2'}{x_1'} \right] \\
 G_{12}^R &= S_{12}^0 \frac{\eta_1 x_1^+ \left[x_2^+ (rx_2^- - x_2^+) (rx_2' - x_2') + x_2^+ (rx_2^+ - x_2^-) (x_2' - rx_2') \right]}{\eta_2' x_2' (x_1^- - x_1^+) \left[x_1^+ (x_2^- - rx_2^+) + x_2^- (x_2^+ - rx_2^-) \right]} \\
 H_{12}^R &= S_{12}^0 \frac{\eta_1 (x_1' - x_1^+) \left[x_1^- x_2^- (rx_2^- - x_2') + x_1^+ x_1' (rx_2^+ - x_2^-) \right]}{\eta_1' x_1' (x_1^- - x_1^+) \left[x_1^+ (x_2^- - rx_2^+) + x_2^- (x_2^+ - rx_2^-) \right]} \\
 K_{12}^R &= S_{12}^0 \frac{\eta_2 x_2^- \left[x_1^- x_1' (rx_2' - x_2') + x_1' x_2^- (rx_2' - x_2') \right]}{\eta_2' x_1' x_2' \left[x_1^+ (x_2^- - rx_2^+) + x_2^- (x_2^+ - rx_2^-) \right]} \\
 L_{12}^R &= S_{12}^0 \frac{\eta_2 x_2^- (x_1^- - x_1') (x_1' - x_1^+)}{\eta_1' x_1' (x_1^- - x_1^+) \left[x_1^+ (x_2^- - rx_2^+) + x_2^- (x_2^+ - rx_2^-) \right]} \tag{2.57}
 \end{aligned}$$

where

$$\frac{x_1^+}{x_1^-} = e^{ip_b} \quad \frac{x_2^+}{x_2^-} = e^{ip_B} \quad (2.58)$$

$$\frac{x_{1'}^+}{x_{1'}^-} = e^{ik_b} \quad \frac{x_{2'}^+}{x_{2'}^-} = e^{ik_B} \quad (2.59)$$

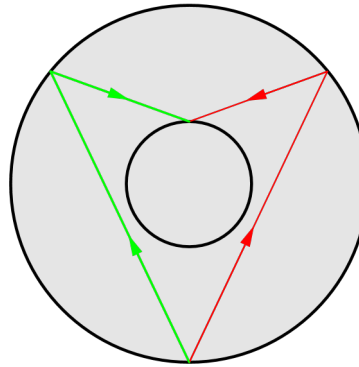


Figure 2.10: A bulk magnon scatters with a boundary magnon. The sum of the momenta of the two magnons is π . Here we only show two of the magnons; we indicate them in red before the scattering and in green after the scattering. In the process the direction of the momentum both magnons is reversed.

Thus, the S -matrix is determined up to an overall phase. Here we have simply chosen $D_{12}^R = -S_{12}^0$ which specifies the overall phase. This overall phase is constrained by crossing symmetry [87]. It is simple to verify that this R matrix is unitary for any value of r and any momenta, and further that it reproduces the bulk S -matrix for $r = 1$ and the reflection matrix for scattering from a maximal giant graviton for $r = 0$. In performing this check we compared to the expressions in [88]. To provide a further check of these expressions, we have considered the case that the boundary and the bulk magnons have momenta that sum to π , as shown in figure 2.10. In this situation it is very simple to compute the final momenta of the two magnons - the final momenta are minus the initial momenta. In Appendix E we have computed the value of $\frac{1}{2} \left(1 + \frac{B_{12}^R}{A_{12}^R} \right)$ at one loop. We find this agrees perfectly with the answer obtained from (2.57). To

perform this check, one needs to express x^\pm in terms of p by solving $x^+ = x^- e^{ip}$ and (2.49) for the boundary magnon or (2.46) for the bulk magnon. Doing this we find

$$x^- = e^{i\frac{p}{2}} \left(\frac{1}{2g \sin \frac{p}{2}} + 2g \sin \frac{p}{2} \right) + O(g^2) \quad (2.60)$$

for a bulk magnon and

$$x^- = -\frac{i}{g(r - e^{ip})} + i g e^{-ip} (r - e^{ip}) \frac{r e^{ip} - 1}{r + e^{ip}} + O(g^2) \quad (2.61)$$

for a boundary magnon. Inserting these expansions into (2.57) and keeping only the leading order (which is g^0) at small g , we reproduce (E.13) for any allowed value of r .

It is a simple matter to verify that the boundary Yang-Baxter equation is not satisfied by this reflection matrix, indicating that the system is not integrable. This conclusion follows immediately upon verifying that changing the order in which the bulk magnons scatter with the boundary magnon leads to final states in which the magnons have different momenta. Consequently, the integrability is lost precisely because the scattering of the boundary and bulk magnons, for boundary magnons attached to a non-maximal giant graviton, is inelastic.

2.9 Links to the Double Coset Ansatz and Open Spring Theory

There is an interesting limiting case that we can consider, obtained by taking each open string word to simply be a single Y , i.e. each open string is a single magnon. In this case one must use the correlators computed in [10; 11] as opposed to the correlators computed in [7]. The case with distinguishable open strings is much simpler since when the correlators are computed, only contractions between corresponding open strings contribute; when the open strings are identical, it is possible to contract any two of them. In this case one must consider operators that treat these “open strings” symmetrically, leading to the operators constructed in [10]. In a specific limit, the action of the dilatation operator factors into an action on the Z s and an action on the Y s [15; 16]. The action on the Y s can be diagonalized by Fourier transforming to a double coset

which describes how the magnons are attached to the giant gravitons [16; 20]. For an operator labeled by a Young diagram R with p long rows or columns, the action on the Z s then reduces to the motion of p particles along the real line with their coordinates given by the lengths of the Young diagram R , interacting through quadratic pair-wise interaction potentials [17]. For interesting related work see [89]. Our goal in this section is to explain the string theory interpretation of these results.

The conclusion of [16; 20] is that eigenstates of the dilatation operator given by operators corresponding to Young diagrams R that have p long rows or columns can be labeled by a graph with p vertices and directed edges. The number of directed edges matches the number of magnons Y used to construct the operator. These graphs have a natural interpretation in terms of the Gauss Law expected from the worldvolume theory of the giant graviton branes [63]. Since the giant graviton has a compact world volume, the Gauss Law implies the total charge on the giant's world volume vanishes. Each string end point is charged, so this is a constraint on the possible open string configurations: the number of strings emanating from the giant must equal the number of strings terminating on the giant. Thus, the graphs labeling the operators are simply enumerating the states consistent with the Gauss Law. To stress this connection we use the language “Gauss graphs” for the labels, we refer to the vertices of the graph as branes since each one is a giant graviton brane and we identify the directed edges as strings since each is a magnon. The action of the dilatation operator is nicely summarized by the Gauss graph labeling the operator. Count the number n_{ij} of strings (of either orientation) stretching between branes i and j in the Gauss graph. The action of the dilatation operator on the Gauss graph operator is then given by

$$DO_{R,r}(\sigma) = -\frac{g_{YM}^2}{8\pi^2} \sum_{i < j} n_{ij}(\sigma) \Delta_{ij} O_{R,r}(\sigma). \quad (2.62)$$

The operator Δ_{ij} is defined in Appendix C. For a proof of this, see [16; 20]. To obtain anomalous dimensions one needs to solve an eigenproblem on the R, r labels, which has been accomplished in [17] in complete generality.

For three open strings stretched between three giant gravitons we have to

solve the following eigenvalue problem

$$\begin{aligned}
& \frac{g_{YM}^2}{8\pi^2} \left[(2N - c_1 - c_2 + 3)O(c_1, c_2, c_3) - \sqrt{(N - c_1 + 1)(N - c_2 + 1)}O(c_1 + 1, c_2 - 1, c_3) \right. \\
& \quad \left. - \sqrt{(N - c_1)(N - c_2 + 2)}O(c_1 - 1, c_2 + 1, c_3) \right] \\
& \frac{g_{YM}^2}{8\pi^2} \left[(2N - c_2 - c_3 + 5)O(c_1, c_2, c_3) - \sqrt{(N - c_2 + 1)(N - c_3 + 1)}O(c_1, c_2 - 1, c_3 + 1) \right. \\
& \quad \left. - \sqrt{(N - c_2 + 2)(N - c_3 + 2)}O(c_1, c_2 + 1, c_3 - 1) \right] \\
& \frac{g_{YM}^2}{8\pi^2} \left[(2N - c_1 - c_3 + 4)O(c_1, c_2, c_3) - \sqrt{(N - c_3 + 2)(N - c_1 + 1)}O(c_1 + 1, c_2, c_3 - 1) \right. \\
& \quad \left. - \sqrt{(N - c_3 + 3)(N - c_1)}O(c_1 - 1, c_2, c_3 + 1) \right] \\
& = \gamma O(c_1, c_2, c_3) \tag{2.63}
\end{aligned}$$

where c_1 , c_2 and c_3 are the lengths of the columns = momenta of the three giant gravitons and γ is the anomalous dimension. At large N , approximating for example $O(c_1, c_2, c_3) = O(c_1 + 1, c_2, c_3 - 1)$ which amounts to ignoring back reaction on the giant gravitons, we have

$$\begin{aligned}
& \frac{g_{YM}^2 N}{8\pi^2} \left[\sqrt{1 - \frac{c_1}{N}} - \sqrt{1 - \frac{c_2}{N}} \right]^2 O(c_1, c_2, c_3) + \frac{g_{YM}^2 N}{8\pi^2} \left[\sqrt{1 - \frac{c_2}{N}} - \sqrt{1 - \frac{c_3}{N}} \right]^2 O(c_1, c_2, c_3) \\
& \frac{g_{YM}^2 N}{8\pi^2} \left[\sqrt{1 - \frac{c_3}{N}} - \sqrt{1 - \frac{c_1}{N}} \right]^2 O(c_1, c_2, c_3) = \gamma O(c_1, c_2, c_3). \tag{2.64}
\end{aligned}$$

The Gauss graph associated with this operator has a string stretching between the brane of momentum c_1 and the brane of momentum c_3 , a string stretching between the brane of momentum c_1 and the brane of momentum c_2 and a string stretching between the brane of momentum c_2 and the brane of momentum c_3 .

On the string theory side, since our magnons don't carry any momentum, we have three giants moving in the plane with magnons stretched radially between them. Identifying the central charges, we find they are radial vectors with length equal to the distance between the giants. With these central charges we can write down the energy

$$E = \sqrt{1 + 2\lambda(r_1 - r_2)^2} + \sqrt{1 + 2\lambda(r_1 - r_3)^2} + \sqrt{1 + 2\lambda(r_3 - r_2)^2}. \tag{2.65}$$

Using the usual translation between the momentum of the giant graviton and the radius of the circle it moves on

$$r_i = \sqrt{1 - \frac{c_i}{N}} \quad i = 1, 2, 3 \tag{2.66}$$

we find that the order λ term in the expansion of (2.65) precisely matches the gauge theory result (2.64).

If we don't ignore back reaction on the giant graviton, we find that (2.63) leads to a harmonic oscillator eigenvalue problem. In this case, we are keeping track of the Z s slipping past a magnon, from one giant onto the next. In this way, one of the giants will grow and one will shrink thereby changing the radius of their orbits and hence the length of the magnon stretched between them. In this process we would expect the energy to vary continuously, which is exactly what we see at large N . A specific harmonic oscillator state (see [17] for details) corresponds to two giant gravitons executing a periodic motion. In one period, the giants first come towards each other and then move away from each other again. Exciting these oscillators to any finite level, we find an energy that is of order the 't Hooft coupling divided by N . These very small energies translate into motions with a huge period.

There is an important point worth noting. The harmonic oscillator problem that arises from (2.63) is obtained by expanding (2.63) assuming that $c_1 - c_2$ is order \sqrt{N} and c_1, c_2 are of order N . The oscillator Hamiltonian then arises as a consequence of (and depends sensitively on) the order 1 shifts in the coefficients of the terms in (2.63). Thus to really trust the oscillator Hamiltonian we find we must be sure that (2.63) is accurate enough that we can expand it and the order 1 term we obtain is accurate. This is indeed the case, as we discuss in Appendix D.

2.10 Summary of chapter

To summarize this chapter we have used the description of the action of the dilatation operator derived using an approach which relies heavily on group representation theory techniques, to study the anomalous dimensions of operators with a bare dimension that grows as N , as the large N limit is taken. For these operators, even just to capture the leading large N limit, we are forced to sum much more than just the planar diagrams and this is precisely what the representation theoretic approach manages to do. We have demonstrated an exact agreement with results coming from the dual gravity description, which

is convincing evidence in support of this approach. It gives definite correct results in a systematic large N expansion, demonstrating that the representation theoretic methods provide a useful language and calculational framework with which to tackle the kinds of large N but non-planar limits we have studied in this chapter. Of course, we have mainly investigated the leading large N limit and the computation of $\frac{1}{N}$ corrections is an interesting problem that we hope to return to in the future.

The progress that was made in understanding the planar limit of $\mathcal{N} = 4$ super Yang-Mills theory is impressive (see [47] for a comprehensive review). Of course, much of the progress is thanks to integrability. There are however results that do not rely on integrability, only on the symmetries of the theory. In our study we clearly have a genuine extension of methods (giant magnons, the $SU(2|2)$ scattering matrix) that worked in the planar limit, into the large N but non-planar setting. Further, even though integrability does not persist, it is present when the radius r of the circle on which the graviton moves is $r = 0$ (maximal giant graviton) or $r = 1$ (point-like giant graviton). If we perturb about these two values of r , we are departing from integrability in a controlled way and hence we might still be able to exploit integrability. For more general values of r , we have managed to find asymptotic eigenstates in which the magnons are well separated and we expect these to be very good approximate eigenstates. Indeed, anomalous dimensions computed using these asymptotic eigenstates exactly agree with the dual string theory energies. Without the power of integrability it does not seem to be easy to patch together asymptotic states to obtain exact eigenstates.

We have a clearer understanding of the non-planar integrability discovered in [64; 14; 15; 16; 20; 17]. The magnons in these systems remain separated and hence free, so they are actually non-interacting. One of the giants would need to lose all of its momentum before any two magnons would scatter. It is satisfying that the gauge theory methods based on group representation theory are powerful enough to detect this integrability directly in the field theory. The results we have found here give the all loops prediction for the anomalous dimensions of these operators. In the limit when we consider a very large number of fields there would seem to be many more circumstances in which one could construct

operators that are ultimately dual to free systems. This is an interesting avenue that deserves careful study, since these simple free systems may provide convenient starting points, to which interactions may be added systematically.

A possible instability associated to open strings attached to giants has been pointed out in [80]. In this case it seems that the spectrum of the spin chain becomes continuous, the ground state is no longer BPS and supersymmetry is broken. The transition that removes the BPS state is simply that the gap from the ground state to the continuum closes. Of course, the spectrum of energies is discrete but this is only evident at subleading orders in $1/N$ when one accounts for the back reaction of the giant graviton-branes. The question of whether these BPS states with given quantum numbers exist or not has been linked to a walls of stability type description [90] in [1]. It would be interesting to see if these issues can be understood using the methods of this chapter.

Chapter 3

Interacting double coset magnons

3.1 Outline of chapter

In this chapter we consider the anomalous dimensions of restricted Schur polynomials constructed using $n \sim O(N)$ complex adjoint scalars Z and m complex adjoint scalars Y . We fix $m \ll n$ so that our operators are almost half BPS. At leading order in $\frac{m}{n}$ this system corresponds to a dilute gas of m free magnons. Adding the first correction of order $\frac{m}{n}$ to the anomalous dimension, which arises at two loops, we find nonzero magnon interactions. The form of this new operator mixing is studied in detail [91] for a system of two giant gravitons with four strings attached. The work discussed in this chapter was reported in Phys. Rev. D 93, 0650057 (2016).

3.2 Chapter introduction

The original instance of the AdS/CFT correspondence [92] provides a definition for a class of quantum type IIB string theories: those that are embedded in spacetimes which are asymptotically $\text{AdS}_5 \times S^5$ with background five form flux. The definition for this class of string theories is in terms of the highly

symmetric superconformal four dimensional $\mathcal{N} = 4$ super Yang-Mills theory with gauge group $U(N)$. The correspondence claims a one-to-one and onto mapping between states of the quantum gravity and quantum operators of the gauge theory. Consequently, the mapping will identify all the objects known to string theory, perturbative and nonperturbative, with operators in $\mathcal{N} = 4$ super Yang-Mills theory. Apart from the perturbative spectrum of closed strings, there are D-branes and their open string excitations, as well as other spacetime geometries, living in the gauge theory. An interesting class of D-branes are the giant graviton branes [4; 5; 6]. We now have a good idea of how to describe the operators that correspond to certain examples of these branes. The examples we have in mind are almost $\frac{1}{2}$ -Bogomol'nyi-Prasad-Sommerfield (BPS) giant gravitons. The dual operators are built from two complex scalar fields Z and Y of the $\mathcal{N} = 4$ super Yang-Mills theory. We need to use order N fields, so that these operators have a large dimension in the large N limit. For operators with such a large classical dimension the usual large N techniques, i.e. an expansion organized by genus of contributing ribbon graphs, is not possible [51]. New techniques to study the large N limit have been developed. For the free theory, bases of operators that diagonalize the two point function to all orders in $1/N$ have been identified [3; 52; 53; 54; 55; 56; 57; 61; 7; 10; 93]. Techniques to study the anomalous dimension of these operators have also been developed, first for descriptions in which the giant graviton plus open string system is treated using words in the gauge theory to represent the open string [63; 8; 9; 76; 79; 80; 82] and second for descriptions which treat all fields in the operator democratically [15; 16; 20; 17]. Our operators are built using $n \sim O(N)$ Z s and m Y s with $n \gg m$, which implies that we are close to the $\frac{1}{2}$ -BPS giant graviton and that we have a new small parameter $\frac{m}{n}$ in the game. The condition that $n \gg m$ is crucial for our approximations which is not too surprising: a systematically small deformation of a BPS operator will be simpler than the generic operator. Part of the motivation for this chapter is to consider the first order correction in a systematic $\frac{m}{n}$ expansion. In both the open string description and in the more democratic description, there is a close connection [94] between the dynamics of the Y fields and the LLM plane [50] description of giant magnon dynamics in the dual string theory [21; 48; 22]. In this study we are interested in the anomalous

dimensions of gauge theory operators corresponding to restricted Schur polynomials that treat the fields democratically. This corresponds to a dilute gas of magnons. The spectrum of anomalous dimensions has been computed to all loops at large N and to leading order in the small parameter $\frac{m}{n}$ [94; 19]. This all loop answer is possible thanks to supersymmetry [12]. The result agrees with explicit one loop computations in [16; 20], two loop computations in [18] and even three loop computations performed in [95] using a collective coordinate [71; 72; 74; 1] approach. The result has an interesting structure which is worth understanding to appreciate the results we report here. The operators we study are labeled by irreducible representations of the symmetric group S_n , that is, by Young diagrams with n boxes. To specify the Young diagram we can write a list of row lengths. The row lengths must sum to n , so that the Young diagram is determined by some partition of n . Denoting the Young diagram by r the notation “ $r \vdash n$ ” says “ r is a partition of n ”. The operator we are interested in is defined by

$$\chi_{R,(r,s)\alpha\beta}(Z, Y) = \frac{1}{n!m!} \sum_{\sigma \in S_{n+m}} \chi_{R,(r,s)\alpha\beta}(\sigma) \text{Tr}(\sigma Z^{\otimes n} \otimes Y^{\otimes m}). \quad (3.1)$$

The labels $R \vdash n+m$, $r \vdash n$, $s \vdash m$ label irreducible representations of S_{n+m} , S_n and S_m respectively. (r, s) labels a representation of the subgroup $S_n \times S_m$. The above polynomial is only nonzero if (r, s) arises from R after restricting to the $S_n \times S_m$ subgroup. Since it may arise more than once, we need multiplicity labels (denoted α and β above) to keep track of the copy we are considering. One way to ensure that (r, s) arises after restricting to the subgroup is to realize r by removing m boxes from Young diagram R . These removed boxes are then reassembled to give s . Use m_i to count the number of boxes that must be removed from row i of R to get r . Assemble the m_i to produce the vector \vec{m} . The vector \vec{m} is conserved to leading order in $\frac{m}{n}$. In this thesis we will study the first subleading corrections in $\frac{m}{n}$ to the anomalous dimension. This explores the first contributions which induce magnon interactions for the dilute magnon gas. If we are ever to understand the non- perturbative sectors of string theory using the gauge theory/ gravity correspondence, it seems that we must move beyond small deformations of $\frac{1}{2}$ -BPS operators. One way to do this is to construct a good understanding of this system, beyond the leading

order in $\frac{m}{n}$. This is a key motivation for this chapter. There are already corrections of order $\frac{m}{n}$ to the one loop anomalous dimension. These corrections do not lead to new operator mixing they only correct the anomalous dimension. The first nontrivial corrections appear at two loops. Consequently, in Sec. 3.3 we review the structure of the two loop dilatation operator. It is useful to rewrite the action of the two loop dilatation operator in a basis, the Gauss graph basis, that diagonalizes the leading order. In this way it will become apparent that the subleading correction induces new operator mixing. In the process of transforming to the Gauss graph basis we encounter new types of traces that have not been computed before. In Appendix I we develop techniques powerful enough to evaluate the most general trace we could encounter, which is much more general than the traces that appear at two loops. These results will be useful in further studies of the dynamics of Gauss graph operators. To illustrate our results, in Sec. 3.4 we consider a state of two giant gravitons with four strings attached. Our results show a number of interesting features. Operators labeled by different Gauss graphs start to mix implying that we do indeed have an interacting system of magnons. As a consequence of these interactions, the vector \vec{m} is no longer conserved and operators with different \vec{m} labels mix. Finally, at the leading order in $\frac{m}{n}$ and at large N , the all loop dilatation operator factorizes into an action on the Y s times an action on the Z s. Although this factorization was only exhibited at one loop in [16] and at two loops in [18], the arguments of [19] as well as the form of the all loop anomalous dimension [12] implies that this factorization holds to all loops; see [94] for further discussion. The subleading term that we have evaluated does not factorize into an action on the Y s times an action on the Z s. This proves that the action of the dilatation operator only factorizes into an action on the Y s times an action on the Z s at the leading order in a systematic $\frac{m}{n}$ expansion. In Sec. 3.5 we discuss these results and suggest a number of interesting directions in which the present study can be extended.

3.3 The two loop dilatation operator

The complete two loop dilatation operator in the $\mathfrak{su}(2)$ sector is given by [85]

$$D_4 = D_4^{(1)} + D_4^{(2)} + D_4^{(3)} \quad (3.2)$$

where

$$\begin{aligned} D_4^{(1)} &= -2g^2 : \text{Tr} \left(\left[[Y, Z], \frac{\partial}{\partial Z} \right] \left[\left[\frac{\partial}{\partial Y}, \frac{\partial}{\partial Z} \right], Z \right] \right) : \\ D_4^{(2)} &= -2g^2 : \text{Tr} \left(\left[[Y, Z], \frac{\partial}{\partial Y} \right] \left[\left[\frac{\partial}{\partial Y}, \frac{\partial}{\partial Z} \right], Y \right] \right) : \\ D_4^{(3)} &= -2g^2 : \text{Tr} \left([[Y, Z], T^a] \left[\left[\frac{\partial}{\partial Y}, \frac{\partial}{\partial Z} \right], T^a \right] \right) : \end{aligned} \quad (3.3)$$

and

$$g = \frac{g_{YM}^2}{16\pi^2}. \quad (3.4)$$

The sum over a in $D_4^{(3)}$ is easily performed with the help of the identity

$$\text{Tr}(T^a A T^a B) = \text{Tr}(A) \text{Tr}(B). \quad (3.5)$$

which follows from the completeness of the $T^a \in \mathfrak{u}(N)$. The size of these three terms is easily estimated as follows: $D_4^{(1)}$ has two derivatives with respect to Z which act on n Z fields and one with respect to Y which acts on m Y fields. The size of this term is thus $\sim n^2 m$. Similarly, we estimate that $D^{(2)} \sim nm^2$ and $D^{(3)} \sim Nnm \sim n^2 m$. Thus, the leading order comes from $D_4^{(1)}$ and $D_4^{(3)}$, while the first correction to the leading term comes from $D_4^{(2)}$. In Sec. 3.3.1 we will review the results for the action of $D_4^{(1)}$ and $D_4^{(3)}$. In the process we will introduce the basis of operators, the Gauss graph operators, that diagonalizes the action of the leading dilatation operator. Following this, we study the action of $D_4^{(2)}$ in Sec. 3.3.2. To transform this action to the Gauss graph basis requires that we develop new techniques to evaluate certain traces that appear. These techniques are developed in Appendix I and the action of $D_4^{(2)}$ in the Gauss graph basis is discussed in Sec. 3.3.2.

3.3.1 Leading contribution

Acting on a restricted Schur polynomial, the action of $D_4^{(1)}$ is

$$D_4^{(1)} \chi_{R,(r,s)\alpha\beta} = g^2 \sum (L_{T,(t,u)\mu\nu;R,(r,s)\gamma\delta}^{(a)} + L_{T,(t,u)\mu\nu;R,(r,s)\gamma\delta}^{(b)}) \chi_{T,(t,u)\gamma\delta} \quad (3.6)$$

where

$$\begin{aligned}
 L_{T,(t,u)\mu\nu;R,(r,s)\gamma\delta}^{(a)} = & \sum_{R''T''} \frac{d_T n(n-1)m}{d_t d_u d_{R''}(n+m)(n+m-1)} c_{R,R'} c_{R',R''} [\text{Tr}(I_{T''R''}(2, m+2, m+1) \\
 & \times P_{R,(r,s)\alpha\beta}[(1, m+2) - (1, m+1)](2, m+2) I_{R''T''}(2, m+2) \\
 & \times P_{T,(t,u)\delta\gamma}(2, m+2)[(m+1, 2, 1) - (2, m+1, 1)]) \\
 & + \text{Tr}(I_{T''R''}(2, m+2)[(1, m+1) - (m+2, m+1)]P_{R,(r,s)\alpha\beta}(1, m+2, 2) I_{R''T''} \\
 & \times ((1, m+1)(2, m+2)P_{T,(t,u)\delta\gamma}(2, m+2)(2, m+1) \\
 & - (m+1, 2, m+2)P_{T,(t,u)\delta\gamma}(2, m+2)(2, 1)))] \quad (3.7)
 \end{aligned}$$

and

$$\begin{aligned}
 L_{T,(t,u)\mu\nu;R,(r,s)\gamma\delta}^{(b)} = & \sum_{R'T'} \frac{d_T n(n-1)m}{d_t d_u d_{R'}(n+m)} c_{R,R'} [\text{Tr}(I_{T'R'}[(1, m+2, m+1)P_{R,(r,s)\alpha\beta} \\
 & - (m+2, m+1)P_{R,(r,s)\alpha\beta}(1, m+1)]I_{R'T'} \\
 & \times [(1, m+1)P_{T,(t,u)\delta\gamma} - P_{T,(t,u)\delta\gamma}(1, m+1)]) \\
 & + \text{Tr}(I_{T'R'}[(1, m+1, m+2)P_{R,(r,s)\alpha\beta} - (m+2, m+1)P_{R,(r,s)\alpha\beta}(1, m+2)] \\
 & \times I_{R'T'}[(1, m+1)P_{T,(t,u)\delta\gamma} - P_{T,(t,u)\delta\gamma}(1, m+1)])] \quad (3.8)
 \end{aligned}$$

In the above expression the traces run over the direct sum of the carrier spaces $R \oplus T$. The Young diagrams R and T both label irreducible representations of S_{n+m} . Primes denote Young diagrams obtained by dropping boxes, with one box dropped for each prime. Thus, for example, T'' is an irreducible representation of S_{n+m-2} , obtained by dropping two boxes from T . The factors $I_{T'R'}$ and $I_{T''R''}$ are intertwining maps mapping from the carrier space T' to R' and from T'' to R'' respectively. $c_{RR'}$ is the factor of the box that must be dropped from R to get R' . We use a little letter to denote dimensions of irreducible representations of the symmetric group so that, for example, d_R is the dimension of the symmetric group representation labeled by Young diagram R . Finally, $P_{R,(r,s)\alpha\beta}$ denotes the intertwining maps which correctly restrict the trace in R to the subspace relevant for the restricted character, that is $\chi_{R,(r,s)\alpha\beta(\sigma)} = \text{Tr}(P_{R,(r,s)\alpha\beta}\Gamma^{(R)}(\sigma))$. The above result is exact in the sense that all orders in $1/N$ are included. The traces appearing in the above expression run over the direct sum of carrier spaces $R \oplus T$. To exploit the simplifications of the large N limit, we now employ the distant corners approximation.

In this approximation, the traces over $R \oplus T$ are reduced to a trace over the tensor product of the direct sum of the carrier spaces $r \oplus t$ and $V_p^{\otimes m}$ where R has a total of p rows and V_p is a p -dimensional vector space. The trace over $r \oplus t$ is rather straightforward. The bulk of the work then entails tracing over $V_p^{\otimes m}$. From now on we will work with normalized restricted Schur polynomials $O_{R,(r,s)\alpha\beta}$ which are a scaled version of the $\chi_{R,(r,s)\alpha\beta}$

$$O_{O_{R,(r,s)\alpha\beta}}(Z, Y) = \sqrt{\frac{\text{hooks}_r \text{hooks}_s}{f_R \text{hooks}_R}} \chi_{O_{R,(r,s)\alpha\beta}}(Z, Y). \quad (3.9)$$

To denote the length of a given row of a Young diagram, we will indicate the Young diagram label with a subscript which identifies the row. Thus r_1 is the length of the first row of r and T_2 is the length of the second row in T . After tracing over $r \oplus t$, we have

$$\begin{aligned} D_4^{(1)} O_{R,(r,s)\alpha\beta}(Z, Y) &= -2g^2 \sum_{i < j} \frac{m}{\sqrt{d_u d_s}} \left(\text{Tr}_{V_p^{\otimes m}} (E_{ii}^{(1)} P_{R,(r,s)\alpha\beta} E_{jj}^{(1)} P_{T,(t,u)\delta\gamma}) \right. \\ &\quad \left. + \text{Tr}_{V_p^{\otimes m}} (E_{ii}^{(1)} P_{R,(r,s)\alpha\beta} E_{jj}^{(1)} P_{T,(t,u)\delta\gamma}) \right) \Delta_{ij} O_{T,(t,u)\delta\gamma}(Z, Y) \end{aligned} \quad (3.10)$$

where

$$\begin{aligned} \Delta_{ij} O_{T,(t,u)\gamma\delta}(Z, Y) &\equiv \left[\sqrt{(N + R_2)(N + R_2 - 1)(N + R_1 - 1)(N + R_1 - 2)} \delta_{T_{jj}^{\prime\prime}, R_{ii}^{\prime\prime}} \delta_{t_{jj}', r_{ii}'} \right. \\ &\quad + \sqrt{(N + R_2 - 2)(N + R_2 - 3)(N + R_1)(N + R_1 + 1)} \delta_{T_{ii}^{\prime\prime}, T_{jj}^{\prime\prime}} \delta_{t_{ii}', r_{jj}'} \\ &\quad - (2N - 3) \left(\sqrt{(N + R_1 - 1)(N + R_2 - 1)} \delta_{T_j', R_i'} \delta_{t_j', r_i'} \right. \\ &\quad \left. + \sqrt{(N + R_2 - 2)(N + R_1)} \delta_{T_i', R_j'} \delta_{t_i', r_j'} \right) \\ &\quad \left. + [2(N + R_1 - 1)(N + R_2 - 2) - (n - 1)(2N + n - 3)] \delta_{T,R} \delta_{t,r} O_{T,(t,u)\gamma\delta}(Z, Y) \right] \end{aligned} \quad (3.11)$$

and of course $n = r_1 + r_2$. The delta functions which appear are 1 if the Young diagram labels have the same shape and 0 otherwise. In the above formula, the matrices $E_{ij}^{(A)}$ which appear are a basis for the representation of $\mathfrak{u}(p)$ on $V_p^{\otimes m}$. Concretely, E_{ij} is a matrix with every entry equal to zero except for the entry in the i th row and j th column, which is equal to 1. In terms of E_{ij} we can write

$$E_{ij}^{(A)} = \mathbb{1} \otimes \mathbb{1} \otimes \cdots \otimes E_{ij} \otimes \cdots \otimes \mathbb{1} \quad (3.12)$$

where E_{ij} appears in the A th factor of the tensor product and 1 is the p dimensional unit matrix. To obtain the result (3.10) we have used

$$\sqrt{\frac{\text{hooks}_T \text{hooks}_r}{\text{hooks}_R \text{hooks}_s}} = 1 \left(1 + O\left(\frac{m}{n}\right) \right) \quad (3.13)$$

and we have only kept the leading order. The action of $D_4^{(1)}$ is a product of two factors: an action on Young diagrams R, r and an independent action on Young diagram s . To evaluate this second action explicitly, we need to trace over $V_p^{\otimes m}$. This is most easily achieved by moving to the basis of Gauss graph operators. Each Gauss graph operator is labeled by an element of the double coset $H \backslash S_m / H$ where $H = S_{m_1} \times S_{m_2} \cdots \times S_{m_p}$. The relation between the Gauss graph operator $[O_{R,r}(\sigma)]$ and the normalized restricted Schur polynomial is

$$O_{R,r}(\sigma) = \frac{|H|}{\sqrt{m!}} \sum_{j,k} \sum_{s \vdash m} \sum_{\mu_1, \mu_2} \sqrt{d_s} \Gamma_{ij}^{(s)}(\sigma) B_{j\mu_1}^{s \rightarrow 1_H} B_{k\mu_2}^{s \rightarrow 1_H} O_{R,(r,s)\mu_1\mu_2}. \quad (3.14)$$

This transformation can be understood as a Fourier transform applied to the double coset. The branching coefficients $B_{j\mu_1}^{s \rightarrow 1_H}$ give a resolution of the projector from the irreducible representation s of S_m to the trivial representation of H

$$\frac{1}{|H|} \sum_{\sigma \in H} \Gamma_{ij}^{(s)}(\sigma) = \sum_{\mu} B_{j\mu}^{s \rightarrow 1_H} B_{k\mu}^{s \rightarrow 1_H} \quad (3.15)$$

In terms of the Gauss graph operator, we find

$$D_4^{(1)} O_{R,r}(\sigma) = -2g^2 \sum_{i < j} n_{ij}(\sigma) \Delta_{ij} O_{R,r}(\sigma). \quad (3.16)$$

The numbers $n_{ij}(\sigma)$ can be read off of the element of the double coset element σ . For more details see Appendix H

After using (3.5), the action of $D_4^{(3)}$ reduces to the action of the one loop dilatation operator. Consequently, we will not discuss this term further.

3.3.2 Subleading contribution

There are a number of different sources for the subleading contribution. Firstly, the leading two loop terms computed above receive corrections-see equation (3.3). These corrections do not lead to additional mixing. They only imply a

correction to the anomalous dimension. Similarly, even the one loop anomalous dimension receives an $\frac{m}{n}$ correction [also from using the approximation given in (3.3)], without any additional operator mixing. The first correction that implies new operator mixing comes from the leading contribution to $D_4^{(2)}$ and it will be the focus of this subsection. This term has not been considered before.

Acting on a normalized restricted Schur polynomial, we find

$$D_4 O_{R,(r,s)\alpha\beta}(Z, Y) = \sum_{T,(t,u)\mu\nu} \left(M_{T,(t,u)\mu\nu;R,(r,s)\alpha\beta}^{(a)} - M_{T,(t,u)\mu\nu;R,(r,s)\alpha\beta}^{(b)} \right. \\ \left. - M_{T,(t,u)\mu\nu;R,(r,s)\alpha\beta}^{(c)} + M_{T,(t,u)\mu\nu;R,(r,s)\alpha\beta}^{(d)} \right) O_{T,(t,u)\mu\nu}(Z, Y), \quad (3.17)$$

where

$$M_{T,(t,u)\mu\nu;R,(r,s)\alpha\beta}^{(a)} = \sum_{R'R''} \delta_{R''T''} \frac{d_T m(m-1) n c_{RR'} c_{R'R''}}{d_{R''} d_t d_u (m+n)(m+n-1)} \sqrt{\frac{f_T \text{hooks}_T \text{hooks}_r \text{hooks}_s}{f_R \text{hooks}_R \text{hooks}_t \text{hooks}_u}} \\ \times \text{Tr} \left(I_{T''R''} \Gamma_R((2, m+1)) [\Gamma_R((1, m+1)), P_{R,(r,s)\alpha\beta}] \right. \\ \left. \times I_{R''T'} \Gamma_T((1, m+1)) [\Gamma_T((2, m+1)), P_{T,(t,u)\mu\nu}] \right), \\ M_{T,(t,u)\mu\nu;R,(r,s)\alpha\beta}^{(b)} = \sum_{R'} \delta_{R'T'} \frac{d_T m(m-1) n c_{RR'}}{d_{R'} d_t d_u (m+n)} \sqrt{\frac{f_T \text{hooks}_T \text{hooks}_r \text{hooks}_s}{f_R \text{hooks}_R \text{hooks}_t \text{hooks}_u}} \\ \times \text{Tr} \left(I_{T'R'} \Gamma_R((2, m+1)) [\Gamma_R((1, m+1)), P_{R,(r,s)\alpha\beta}] \right. \\ \left. \times I_{R'T'} [\Gamma_T((1, m+1)), P_{T,(t,u)\mu\nu}] \right), \\ M_{T,(t,u)\mu\nu;R,(r,s)\alpha\beta}^{(c)} = \sum_{R'} \delta_{R'T'} \frac{d_T m(m-1) n c_{RR'}}{d_{R'} d_t d_u (m+n)} \sqrt{\frac{f_T \text{hooks}_T \text{hooks}_r \text{hooks}_s}{f_R \text{hooks}_R \text{hooks}_t \text{hooks}_u}} \\ \times \text{Tr} \left(I_{T'R'} [\Gamma_R((1, m+1)), P_{R,(r,s)\alpha\beta}] \Gamma_R((2, m+1)) \right. \\ \left. \times I_{R'T'} [\Gamma_T((1, m+1)), P_{T,(t,u)\mu\nu}] \right),$$

and

$$M_{T,(t,u)\mu\nu;R,(r,s)\alpha\beta}^{(d)} = \sum_{R'R''} \delta_{R''T''} \frac{d_T m(m-1) n c_{RR'} c_{R'R''}}{d_{R''} d_t d_u (m+n)(m+n-1)} \sqrt{\frac{f_T \text{hooks}_T \text{hooks}_r \text{hooks}_s}{f_R \text{hooks}_R \text{hooks}_t \text{hooks}_u}} \\ \times \text{Tr} \left(I_{T''R''} [\Gamma_R((1, m+1)), P_{R,(r,s)\alpha\beta}] \Gamma_R((2, m+1)) \right. \\ \left. \times I_{R''T''} [\Gamma_T((1, m+1)), P_{T,(t,u)\mu\nu}] \Gamma_T((2, m+1)) \right).$$

The traces appearing above again run over the direct sum of carrier spaces $R \oplus T$ and the action given above is again correct to all orders in $1/N$. To

take advantage of the simplifications of the large N limit, we again employ the distant corners approximation, which again leads to an expression that has a single trace over $V_p^{\otimes m}$ remaining

$$\begin{aligned}
 M_{T,(t,u)\mu\nu;R,(r,s)\alpha\beta}^{(a)} &= \sum_{R'R''} \delta_{R''T''} \frac{d_T m(m-1) n C_{RR'} C_{R'R''}}{d_{R''} d_t d_u (m+n)(m+n-1)} \sqrt{\frac{f_T \text{hooks}_T \text{hooks}_r \text{hooks}_s}{f_R \text{hooks}_R \text{hooks}_t \text{hooks}_u}} d_{r'_i} \delta_{r'_i t'_i} \\
 &\quad \times \left[\text{Tr}_{V_p^{\otimes m}} \left(E_{kj}^{(1)} E_{ll}^{(2)} p_{s\alpha\beta} E_{ii}^{(1)} E_{jk}^{(2)} p_{u\mu\nu} \right) - \text{Tr}_{V_p^{\otimes m}} \left(E_{kj}^{(1)} p_{s\alpha\beta} E_{ii}^{(1)} E_{jk}^{(2)} p_{u\mu\nu} \delta_{kl} \right) \right. \\
 &\quad \left. - \text{Tr}_{V_p^{\otimes m}} \left(E_{ki}^{(1)} E_{ll}^{(2)} p_{s\alpha\beta} E_{ik}^{(2)} p_{u\mu\nu} \delta_{ij} \right) + \text{Tr}_{V_p^{\otimes m}} \left(E_{ki}^{(1)} p_{s\alpha\beta} E_{ik}^{(2)} p_{u\mu\nu} \delta_{ij} \delta_{kl} \right) \right], \\
 M_{T,(t,u)\mu\nu;R,(r,s)\alpha\beta}^{(b)} &= \sum_{R'} \delta_{R'T'} \frac{d_T m(m-1) n c_{RR'}}{d_{R'} d_t d_u (m+n)} \sqrt{\frac{f_T \text{hooks}_T \text{hooks}_r \text{hooks}_s}{f_R \text{hooks}_R \text{hooks}_t \text{hooks}_u}} d_{r'_i} \delta_{r'_i t'_k} \\
 &\quad \times \left[\text{Tr}_{V_p^{\otimes m}} \left(E_{ka}^{(1)} E_{ak}^{(2)} p_{s\alpha\beta} E_{ii}^{(1)} p_{u\mu\nu} \right) - \text{Tr}_{V_p^{\otimes m}} \left(E_{ba}^{(1)} E_{ab}^{(2)} p_{s\alpha\beta} E_{ii}^{(1)} p_{u\mu\nu} \delta_{ik} \right) \right. \\
 &\quad \left. - \text{Tr}_{V_p^{\otimes m}} \left(p_{u\mu\nu} E_{ki}^{(1)} E_{ik}^{(2)} p_{s\alpha\beta} \right) + \text{Tr}_{V_p^{\otimes m}} \left(E_{bi}^{(1)} E_{ib}^{(2)} p_{s\alpha\beta} E_{kk}^{(1)} p_{u\mu\nu} \right) \right], \\
 M_{T,(t,u)\mu\nu;R,(r,s)\alpha\beta}^{(c)} &= \sum_{R'} \delta_{R'T'} \frac{d_T m(m-1) n c_{RR'}}{d_{R'} d_t d_u (m+n)} \sqrt{\frac{f_T \text{hooks}_T \text{hooks}_r \text{hooks}_s}{f_R \text{hooks}_R \text{hooks}_t \text{hooks}_u}} d_{r'_i} \delta_{r'_i t'_k} \\
 &\quad \times \left[\text{Tr}_{V_p^{\otimes m}} \left(E_{kk}^{(1)} p_{s\alpha\beta} E_{ic}^{(1)} E_{ci}^{(2)} p_{u\mu\nu} \right) - \text{Tr}_{V_p^{\otimes m}} \left(p_{s\alpha\beta} E_{ik}^{(1)} E_{ki}^{(2)} p_{u\mu\nu} \right) \right. \\
 &\quad \left. - \text{Tr}_{V_p^{\otimes m}} \left(E_{ii}^{(1)} p_{s\alpha\beta} E_{ab}^{(1)} E_{ba}^{(2)} p_{u\mu\nu} \delta_{ik} \right) + \text{Tr}_{V_p^{\otimes m}} \left(E_{ii}^{(1)} p_{s\alpha\beta} E_{ck}^{(1)} E_{kc}^{(2)} p_{u\mu\nu} \right) \right],
 \end{aligned}$$

and

$$\begin{aligned}
 M_{4T,(t,u)\mu\nu;R,(r,s)\alpha\beta}^{(d)} &= \sum_{R'R''} \delta_{R''T''} \frac{d_T m(m-1) n c_{RR'} C_{R'R''}}{d_{R''} d_t d_u (m+n)(m+n-1)} \sqrt{\frac{f_T \text{hooks}_T \text{hooks}_r \text{hooks}_s}{f_R \text{hooks}_R \text{hooks}_t \text{hooks}_u}} d_{r'_i} \delta_{r'_i t'_k} \\
 &\quad \times \left[\text{Tr}_{V_p^{\otimes m}} \left(E_{ka}^{(1)} E_{ai}^{(2)} p_{s\alpha\beta} E_{ib}^{(1)} E_{bk}^{(2)} p_{u\mu\nu} \delta_{ij} \delta_{kl} \right) - \text{Tr}_{V_p^{\otimes m}} \left(E_{la}^{(1)} E_{ai}^{(2)} p_{s\alpha\beta} E_{ik}^{(1)} E_{kl}^{(2)} p_{u\mu\nu} \delta_{ij} \right) \right. \\
 &\quad \left. - \text{Tr}_{V_p^{\otimes m}} \left(E_{ki}^{(1)} E_{ij}^{(2)} p_{s\alpha\beta} E_{jb}^{(1)} E_{bk}^{(2)} p_{u\mu\nu} \delta_{lk} \right) + \text{Tr}_{V_p^{\otimes m}} \left(E_{li}^{(1)} E_{ij}^{(2)} p_{s\alpha\beta} E_{jk}^{(1)} E_{kl}^{(2)} p_{u\mu\nu} \right) \right].
 \end{aligned}$$

To compute the remaining trace over $V_p^{\otimes m}$ we will again move to the Gauss graph basis. This requires computing traces that have not been considered in previous works. Schematically, these traces are of the form

$$\text{Tr}(A p_{s\mu\nu} B p_{u\gamma\delta}) \tag{3.18}$$

where A and B can be any product of the $E_{ab}^{(A)}$ s. The details of how to compute these traces in general are given in Appendix I. To summarize the key ideas, consider an intertwining map $p_{s\mu\nu}$ built on the state $|\bar{v}_1, \bar{m}_1\rangle$ with symmetry

group H_1 and the map $p_{t\gamma\delta}$ built on the state $|\bar{v}_2, \vec{m}_2\rangle$ with symmetry group H_2 . The transformation to Gauss graph basis is given by

$$\begin{aligned} T &= \sum_{s\mu\nu lm} \sum_{u\gamma\delta np} \text{Tr}(Ap_{s\mu\nu}Bp_{u\gamma\delta}) B_{m\mu}^{s \rightarrow 1_H} B_{l\nu}^{s \rightarrow 1_H} \Gamma_{ml}^{(s)}(\sigma_1) B_{p\gamma}^{s \rightarrow 1_H} B_{n\delta}^{s \rightarrow 1_H} \Gamma_{pn}^{(u)}(\sigma_2) \\ &= \frac{1}{|H_1||H_2|} \sum_{\psi_i \in S_m} \langle v_2 | \sigma_2^{-1} (\psi_2^{-1} A \psi_2) \psi_1 | v_1 \rangle \langle v_2 | (\psi_2^{-1} B^T \psi_2) \psi_1 \sigma_1 | v_1 \rangle \end{aligned} \quad (3.19)$$

The final sum over ψ_1 and ψ_2 then gives

$$T = \frac{(m-2)!}{|H_1||H_2|} |O(\sigma_1)|^2 n_{ab}(\sigma_2) n_{cd}(\sigma_2) \delta_{AB}([\sigma_1], [\sigma_2]) \quad (3.20)$$

The indices a, b, c, d are read from A and B as explained in Appendix I and

$$|O(\sigma_1)|^2 = \prod_{i,j=1}^p n_{ij}(\sigma_1)! = \langle O_{R,r}(\sigma_1)^\dagger O_{R,r}(\sigma_1) \rangle. \quad (3.21)$$

The delta function $\delta_{AB}([\sigma_1], [\sigma_2])$ is defined using A and B . This is also explained in Appendix I. Using these results, we find

$$D_4^{(2)} O_{R,r}(\sigma_1) = \sum_{T,t,\sigma_2} \left(M_{T,t;R,r}^{1,\sigma_1,\sigma_2} - M_{T,t;R,r}^{2,\sigma_1,\sigma_2} - M_{T,t;R,r}^{3,\sigma_1,\sigma_2} + M_{T,t;R,r}^{4,\sigma_1,\sigma_2} \right) O_{T,t}(\sigma_2), \quad (3.22)$$

where

$$\begin{aligned} M_{T,t;R,r}^{1,\sigma_1,\sigma_2} &= \sum_{R',R''} \delta_{R''T''} \delta_{r'_i t'_i} \sqrt{\frac{C_{RR'} C_{R'R''} C_{TT'} C_{T'T''}}{l_{R_j} l_{T_k}}} |O_{R,r}(\sigma_1)|^2 \delta_{AB}([\sigma_1], [\sigma_2]) \\ &\times \left[n_{ik}(\sigma_2) n_{kl}(\sigma_2) - \delta_{kl} \sum_{a=1}^p n_{ik}(\sigma_2) n_{ka}(\sigma_2) \right. \\ &\quad \left. - \delta_{ij} \sum_{b=1}^p n_{bk}(\sigma_2) n_{kl}(\sigma_2) + \delta_{ij} \delta_{kl} \sum_{a,b=1}^p n_{bk}(\sigma_2) n_{ka}(\sigma_2) \right]. \end{aligned}$$

Similarly

$$\begin{aligned}
 M_{T,t;R,r}^{2,\sigma_1,\sigma_2} &= \sum_{R'} \delta_{R'T'} \delta_{r'_i t'_k} \sqrt{C_{RR'} C_{TT'}} |O_{R,r}(\sigma_1)|^2 \delta_{AB}([\sigma_1], [\sigma_2]) \\
 &\times \left[\sum_{a,b=1}^p n_{ik}(\sigma_2) n_{ba}(\sigma_2) - \delta_{ik} \sum_{a,b,c=1}^p n_{ib}(\sigma_2) n_{ca}(\sigma_2) \right. \\
 &\quad \left. - \sum_{a,b=1}^p n_{ak}(\sigma_2) n_{bi}(\sigma_2) + \sum_{a,b=1}^p n_{kb}(\sigma_2) n_{ai}(\sigma_2) \right], \\
 M_{T,t;R,r}^{3,\sigma_1,\sigma_2} &= \sum_{R'} \delta_{R'T'} \delta_{r'_i t'_k} \sqrt{C_{RR'} C_{TT'}} |O_{R,r}(\sigma_1)|^2 \delta_{AB}([\sigma_1], [\sigma_2]) \\
 &\times \left[\sum_{a,b=1}^p n_{bk}(\sigma_2) n_{ia}(\sigma_2) - \sum_{a,b=1}^p n_{ka}(\sigma_2) n_{ib}(\sigma_2) \right. \\
 &\quad \left. - \delta_{ik} \sum_{a,b,c=1}^p n_{bi}(\sigma_2) n_{ac}(\sigma_2) + \sum_{a,b=1}^p n_{ki}(\sigma_2) n_{ba}(\sigma_2) \right], \\
 \end{aligned} \tag{3.23}$$

$$\begin{aligned}
 M_{T,t;R,r}^{4,\sigma_1,\sigma_2} &= \sum_{R',R''} \delta_{R''T''} \delta_{r'_i t'_k} \sqrt{\frac{C_{RR'} C_{R'R''} C_{TT'} C_{T'T''}}{l_{R_j} l_{T_l}}} |O_{R,r}(\sigma_1)|^2 \delta_{AB}([\sigma_1], [\sigma_2]) \\
 &\times \left[\delta_{ij} \delta_{kl} \sum_{a,b=1}^p n_{bl}(\sigma_2) n_{la}(\sigma_2) - \delta_{ij} \sum_{a=1}^p n_{kl}(\sigma_2) n_{la}(\sigma_2) \right. \\
 &\quad \left. - \delta_{kl} \sum_{b=1}^p n_{bl}(\sigma_2) n_{li}(\sigma_2) + n_{kl}(\sigma_2) n_{li}(\sigma_2) \right], \\
 \end{aligned} \tag{3.24}$$

Notice that both $M_{T,t;R,r}^{1,\sigma_1,\sigma_2}$ and $M_{T,t;R,r}^{4,\sigma_1,\sigma_2}$ depend on the length of the rows of the Young diagrams R and T that participate. Since these lengths determine the angular momentum of the giants, they determine the radius to which the giants will expand. This is the first dependence of the anomalous dimensions on the geometry of the giant graviton.

3.4 Example: A 2 giant graviton boundstate with 4 strings attached

In this section we will consider the simplest nontrivial system that exhibits the general structure of the subleading operator mixing problem. This problem

is a system of two giant gravitons with four strings attached. As we have explained, there are $\frac{m}{n}$ corrections to the anomalous dimension from the one loop contribution as well as from $D_4^{(1)}$ and $D_4^{(3)}$ at two loops. These corrections do not induce extra operator mixing, so that the Gauss graph operators continue to have a good anomalous dimension. The only extra operator mixing comes from the subleading contribution $D_4^{(2)}$, and this is what we aim to explore.

Each element of the Gauss graph basis is labeled by two Young diagrams R, r as well as a Gauss graph. We will number the states according to their Gauss graph labeling as shown below

$$\begin{aligned} |1, R, r\rangle &= \left| \begin{array}{c} \bullet \\ \bullet \\ \bullet \end{array} \begin{array}{c} \bullet \\ \bullet \end{array}, R, r \right\rangle, & |2, R, r\rangle &= \left| \begin{array}{c} \bullet \\ \bullet \\ \bullet \end{array} \begin{array}{c} \bullet \\ \bullet \end{array}, R, r \right\rangle, & |3, R, r\rangle &= \left| \begin{array}{c} \bullet \\ \bullet \end{array} \begin{array}{c} \bullet \\ \bullet \end{array}, R, r \right\rangle, \\ |4, R, r\rangle &= \left| \begin{array}{c} \bullet \\ \bullet \\ \bullet \end{array} \begin{array}{c} \bullet \\ \bullet \end{array}, R, r \right\rangle, & |5, R, r\rangle &= \left| \begin{array}{c} \bullet \\ \bullet \end{array} \begin{array}{c} \bullet \\ \bullet \end{array}, R, r \right\rangle, & |6, R, r\rangle &= \left| \begin{array}{c} \bullet \\ \bullet \end{array} \begin{array}{c} \bullet \\ \bullet \end{array}, R, r \right\rangle, \\ |7, R, r\rangle &= \left| \begin{array}{c} \bullet \\ \bullet \end{array} \begin{array}{c} \bullet \\ \bullet \end{array}, R, r \right\rangle, & |8, R, r\rangle &= \left| \begin{array}{c} \bullet \\ \bullet \end{array} \begin{array}{c} \bullet \\ \bullet \end{array}, R, r \right\rangle, & |9, R, r\rangle &= \left| \begin{array}{c} \bullet \\ \bullet \end{array} \begin{array}{c} \bullet \\ \bullet \end{array}, R, r \right\rangle. \end{aligned}$$

The states $|i\rangle$ for $i = 5, 6, 7, 8, 9$ are BPS at the leading order in $\frac{m}{n}$. The subleading corrections to the anomalous dimension coming from one loop, as well as from $D_4^{(1)}$ and $D_4^{(3)}$ at two loops is a multiplicative order $\frac{m}{n}$ correction and vanishes because the leading order anomalous dimension vanishes. Evaluating the subleading order contribution coming from $D_4^{(2)}$, we find

$$D_4^{(2)}|i, R, r\rangle = 0 \quad i = 5, 6, 7, 8, 9 \quad (3.25)$$

so that the states that are BPS at the leading order do not receive a subleading correction. This is not peculiar to the example we consider and is to be expected generally, since for the BPS states we have $n_{ab}(\sigma_2) = 0$ for $a \neq b$. The state $|4, R, r\rangle$ also does not mix with other states. However, for this state we have a

nontrivial correction to the eigenvalue since

$$\begin{aligned}
 D_4|4, R, r\rangle = & \sum_{T,t} 64 \left[\delta_{RT} \left(\frac{\delta_{r'_1 t'_1}}{l_{R_2}} + \frac{\delta_{r'_2 t'_2}}{l_{R_1}} \right) \delta_{R''_{12} T''_{12}} (N + l_{R_1} - 1)(N + l_{R_2} - 2) \right. \\
 & + \delta_{RT} \frac{\delta_{r'_1 t'_1}}{l_{R_1}} \delta_{R''_{11} T''_{11}} (N + l_{R_1} - 1)(N + l_{R_1} - 2) + \delta_{RT} \frac{\delta_{r'_2 t'_2}}{l_{R_2}} \delta_{R''_{22} T''_{22}} (N + l_{R_2} - 2)(N + l_{R_2} - 3) \\
 & - \delta_{RT} \delta_{r'_1 t'_1} \delta_{R'_1 T'_1} (N + l_{R_1} - 1) - \delta_{RT} \delta_{r'_2 t'_2} \delta_{R'_2 T'_2} (N + l_{R_2} - 2) \\
 & - \delta_{R_{21}^+ T} \frac{\delta_{r'_1 t'_2}}{\sqrt{l_{R_1}(l_{R_1} - 1)}} \delta_{R''_{11} T''_{12}} (N + l_{R_1} - 2) \sqrt{(N + l_{R_1} - 1)(N + l_{R_2} - 1)} \\
 & - \delta_{R_{12}^+ T} \frac{\delta_{r'_2 t'_1}}{\sqrt{l_{R_1}(l_{R_1} + 1)}} \delta_{R''_{12} T''_{11}} (N + l_{R_1} - 1) \sqrt{(N + l_{R_1})(N + l_{R_2} - 2)} \\
 & - \delta_{R_{21}^+ T} \frac{\delta_{r'_2 t'_1}}{\sqrt{l_{R_2}(l_{R_2} - 1)}} \delta_{R''_{22} T''_{12}} (N + l_{R_2} - 3) \sqrt{(N + l_{R_1})(N + l_{R_2} - 2)} \\
 & - \delta_{R_{21}^+ T} \frac{\delta_{r'_1 t'_2}}{\sqrt{l_{R_2}(l_{R_2} + 1)}} \delta_{R''_{12} T''_{22}} (N + l_{R_2} - 2) \sqrt{(N + l_{R_1} - 1)(N + l_{R_2} - 1)} \\
 & + \delta_{R_{21}^+ T} \delta_{r'_1 t'_2} \delta_{R'_1 T'_2} \sqrt{(N + l_{R_1} - 1)(N + l_{R_2} - 1)} \\
 & \left. + \delta_{R_{12}^+ T} \delta_{r'_2 t'_1} \delta_{R'_2 T'_1} \sqrt{(N + l_{R_1})(N + l_{R_2} - 2)} \right] |4, T, t\rangle \quad (3.26)
 \end{aligned}$$

The remaining states $|i\rangle$ with $i = 1, 2, 3$ mix under the action of $D_4^{(2)}$. Using a matrix notation

$$D_4^{(2)}|i, R, r\rangle = \sum_{T,t} (D_4^{(2)})_{ij} |j, T, t\rangle \quad i, j = 1, 2, 3 \quad (3.27)$$

the action of $D_4^{(2)}$ in this subspace is given by

$$D_4^{(2)} = A \begin{bmatrix} 8 & 0 & 0 \\ 0 & 4 & 0 \\ 0 & 0 & 8 \end{bmatrix} + B \begin{bmatrix} 0 & 1 & 0 \\ 1 & 0 & 1 \\ 0 & 1 & 0 \end{bmatrix} + C \begin{bmatrix} 0 & 1 & 0 \\ 0 & 0 & 1 \\ 0 & 0 & 0 \end{bmatrix} + C^\dagger \begin{bmatrix} 0 & 0 & 0 \\ 1 & 0 & 0 \\ 0 & 1 & 0 \end{bmatrix}$$

where the coefficients A , B and C are quoted in Appendix I. The coefficients A , B and C are operators that have a nontrivial action of the R, r labels of the Gauss graph operators. It is straightforward to check that the matrix coefficients of these operators do not commute and hence they are not simultaneously diagonalizable. This implies that the action of the dilatation operator no longer factorizes into commuting actions on the Z and Y fields. It is this failure of factorization that we were referring to when we talked about the general structure of the mixing problem.

3.5 Summary of chapter

Our results have a number of interesting features that deserve comment. In the $\frac{m}{n} = 0$ limit, the action of the dilatation operator factorizes into an action on the Z fields and an action on the Y fields. The subleading correction has spoiled this factorization of the dilatation operator. This is rather natural: in the limit $\frac{m}{n} = 0$ we consider a giant graviton built with an infinite number ($n = \infty$) of Z fields, so that the backreaction of the magnons on the giant graviton can be neglected. Without backreaction, we expect the dynamics of the giant is completely decoupled from the dynamics of the magnons and this is the root of the factorized action of the dilatation operator. By adding the first correction, we are saying that n is large but not infinite. In this situation, although backreaction is small, it is not zero. The magnons will now provide a small perturbation to the dynamics of the giant; the action of the dilatation operator will no longer factorize into an action on the giant (i.e. on the Z s) times an action on the magnons (i.e. on the Y s).

The subleading correction spoiled the factorization of the dilatation operator by introducing further operator mixing. Another interesting results of our analysis is that the subleading corrections did not induce extra mixing for the BPS operators. Indeed, after accounting for the complete $\frac{m}{n}$ correction to two loops, we found our BPS operators remain uncorrected and continue to have a vanishing anomalous dimension. Although our computation is performed in a specific example, we argued that we expect this conclusion to be general since for the BPS operators we have $n_{ab}(\sigma) = 0$ for $a \neq b$. Looking at the result (3.22), it is clear that vanishing $n_{ab}(\sigma)$ implies a vanishing action of $D_4^{(2)}$.

The form of the action of the dilatation operator implies that when the correction to the anomalous dimension is nonzero it will depend on the length of the rows of the Young diagrams labeling the operator. Since these lengths determine the angular momentum of the giants, they determine the radius to which the giants will expand. This implies that the anomalous dimensions start to depend on the geometry of the giant graviton.

The dynamics of open strings on the worldvolume of a giant graviton is expected to give rise to a Yang-Mills theory at low energy. The lightest mode of

the open strings attached to the giant becomes the gauge boson of the theory. This suggests that within $kalN = 4$ super Yang-Mills theory, we should see classes of operators whose dynamics is captured by a new emergent gauge theory. The acronym emergent is particularly apt in this case because this new Yang-Mills theory will be local on a space that is distinct from the space of the original spacetime of the $kalN = 4$ super Yang-Mills theory. The gauge symmetry which determines the interactions of the theory is a local symmetry with respect to this new space and the time of the original spacetime. The space of the emergent Yang-Mills theory is the worldvolume of the giant graviton, which itself is built from the Z s. So this space and an associated local gauge invariance is to emerge from the dynamics of the Z matrices in the large N limit. For the operators dual to giant gravitons studied in this thesis, it is natural to think that the magnons themselves will become the gauge bosons. Indeed, the allowed state space of the magnons is parametrized by a double coset. The structure of this double coset is determined by the expected Gauss law of the emergent gauge theory. To really understand the mechanism behind this emergence it is important that we get a good handle on how the magnons interact. It is by studying these interactions that we may hope to recognize the Yang- Mills theory that must emerge. In this thesis we have computed the first of these interactions and we have developed tools that allow us to study these interactions in general.

Chapter 4

Conclusions

In this thesis, we used the duality between the type IIB superstring theory and the $U(N)$, $\mathcal{N} = 4$ SYM theory in a large N but non-planar limit. On the gauge theory side of the correspondence, we computed all loop anomalous dimensions in the restricted Schur polynomial basis. These restricted Schur polynomials are dual to a system of excited strings suspended between giant gravitons. The excitations of the strings are identified as magnon particles. The anomalous dimensions compute the energy spectrum of the magnon particles. The energies of the magnons computed in the string theory are in complete agreement with the anomalous dimensions computed in the SYM. This result is a consequence of the $SU(2|2)^2$ symmetry.

Another interesting result is the complete determination, up to an overall phase, of the reflection/scattering matrix between a boundary magnon and a bulk magnon. Recall that a boundary magnon is a magnon stretched from an end point of a string to a giant graviton. Again, we have used the constraints following from the $SU(2|2)^2$ symmetry to determine the S –matrix. As a consequence of the boundary conditions on the open spin chain, the system is not integrable. This result is developed in the Chapter 2 of this dissertation.

Apart from the above results we have also derived in Chapter 3 the two-loop subleading contribution to the magnon energies. The corrections induce a mixing of the double coset operators. The action of the leading higher-loop dilatation operator is decoupled in terms of two separate actions on the Z ’s and

Y 's. The subleading contribution we have considered spoils this factorization.

We have given the complete formula for the interaction of Gauss graphs at subleading order and at two loops.

There are many sectors other than the $\mathfrak{su}(2)$ sector of $\mathcal{N} = 4$ SYM. Among these sectors, one can for instance study the $\mathfrak{su}(3)$ sector, which was already initiated in the previous years. Other sectors that can be considered are $\mathfrak{su}(2|3)$, $\mathfrak{sl}(2)$ and $\mathfrak{psu}(2,2|4)$. In fact, especially for the case of the $\mathfrak{sl}(2)$ and $\mathfrak{su}(2|3)$ sectors, a basis of operators was constructed in terms of restricted Schur polynomials that take into account fermions. Another interesting problem is to study the overall phase of the S –matrix using crossing symmetry.

Appendices

Appendix A

Large N eigenstates

In section 2.5 we explained that at any finite loop order (γ) the change in length $\Delta L = \gamma$ of the open string word lattice is finite while the total length L of the lattice is N . This implies that at large N the ratio $\frac{\Delta L}{L} \rightarrow 0$ and we can treat the lattice length as fixed. This observation is most easily used by first introducing “simple states” that have a definite number of Z s, in the lattice associated to each open string. This is accomplished by relaxing the identification of the open string word with the lattice. The dilatation operators action now allows magnons to move off the open string, mixing simple states with states that are not simple. However, by modifying these simple states we can build states that are closed under the action of the dilatation operator. Our simple states are defined by taking a “Fourier transform” of the states (2.10). The simplest system to consider is that of a single giant, with a single string attached, excited by only two magnons (i.e. only boundary magnons - no bulk magnons). The string word is composed using J Z fields and the complete operator using $J + n$ Z s. Introduce the phases

$$q_a = e^{\frac{i2\pi k_a}{J}} \tag{A.1}$$

with $k_a = 0, 1, \dots, J - 1$. As a consequence of the fact that the lattice is a discrete structure, momenta are quantized with the momentum spacing set by the inverse of the total lattice size. This explains the choice of phases in (A.1).

The simple states we consider are thus given by

$$\begin{aligned}
 |q_1, q_2\rangle = & \sum_{m_1=0}^{J-1} \sum_{m_2=0}^{m_1} q_1^{m_1} q_2^{m_2} |1^{n+m_1-m_2+1}, 1^{n+m_1-m_2}, 1^{n+m_1-m_2}; \{J-m_1+m_2\}\rangle \\
 & + \sum_{m_2=0}^{J-1} \sum_{m_1=0}^{m_2} q_1^{m_1} q_2^{m_2} |1^{n+J+m_1-m_2+1}, 1^{n+J+m_1-m_2}, 1^{n+J+m_1-m_2}; \{m_2-m_1\}\rangle
 \end{aligned} \tag{A.2}$$

This Fourier transform is a transform on the lattice describing the open string worldsheet. The two magnons sit at positions m_1 and m_2 on this lattice. If $m_2 > m_1$, there are $m_2 - m_1$ Zs between the magnons. If $m_1 > m_2$, there are $J + m_2 - m_1$ Zs between the magnons. The Zs before the first magnon of the string and after the last magnon of the string, are mixed up with the Zs of the giant - they do not sit on the open string word. All of the terms in (A.2) are states with different positions for the two magnons, but each is a giant that contains precisely n Zs with an open string attached, and the open string contains precisely J Zs. We cant distinguish where the string begins and where the string begins and where the giant ends: the open string and giant morph smoothly into each other. This is in contrast to the case of a maximal giant graviton, where the magnons mark the endpoints of the open string¹. If this interpretation is consistent we must recover the expected inner product on the lattice and we do: Consider a giant with momentum n . An open string with a lattice of J sites is attached to the giant. The string is excited by M magnons, at positions $n_1, \dots, n_M - 1$ and n_M , with $n_{j+1} > n_j$. The corresponding normalized states, denoted by $|n; J; n_1, n_2, \dots, n_k\rangle$ will obey²

$$\langle n; J; n_1, n_2, \dots, n_M | n, J, n_1, n_2, \dots, n_M \rangle = \delta_{m_2 n_2} \dots \delta_{m_k n_k} \tag{A.3}$$

$$n_{k+1} > n_k, m_{k+1} > m_k$$

¹For the maximal giant graviton, the boundary magnons are not able to hop and so sit forever at the end of the open string. For a non-maximal giant graviton the boundary magnons can hop. Even if they are initially placed at the string endpoint, they will soon explore the bulk of the string.

²As a consequence of the fact that it is not possible to distinguish where the open string begins and where the giant ends, there is no delta function setting the positions of the first magnons to be equal to each other - we have put this constraint in by hand in (A.3).

This is the statement that, up to the ambiguity of where the open string starts, the magnons must occupy the same sites for a non-zero overlap. It is clear that $(G(X) \equiv 1^{x+1}, 1^x, 1^x \text{ and again, } n_{j+1} > n_j, m_{j+1} > m_j)$

$$\begin{aligned} \langle G(n + J + m_1 - m_2); \{m_2, \dots, m_M\} | G(n + J + n_1 - n_2); \{n_2, \dots, n_M\} \rangle \\ = \delta_{m_2 n_2} \cdots \delta_{m_k n_k} \end{aligned}$$

reproducing the lattice inner product. The simple states are an orthogonal set of states. To check this, compute the coefficient c_a of the state $|1^{n+a+1}, 1^{n+a}, 1^{n+a}; J - a\rangle$. Looking at the two terms in (A.2) we find the following two contributions

$$\begin{aligned} c_a &= \sum_{m_1=a}^{J-1} q_1^{m_1} q_2^{m_1-a} + \sum_{m_1=0}^{a-1} q_1^{m_1} q_2^{m_1-a} \\ &= \begin{cases} J q_2^{-a} & \text{if } k_1 + k_2 = 0 \\ 0 & \text{if } k_1 + k_2 \neq 0 \end{cases} \end{aligned} \quad (\text{A.4})$$

Thus, $q_1 = q_2^{-1}$ to get a non-zero result. We will see that this zero lattice momentum constraint maps into the constraint that the $\mathfrak{su}(2|2)$ central charges of the complete magnon state must vanish. Our simple states are then given by setting $q_2 = q_1^{-1}$ and are labeled by a single parameter q_1 ; denote the simple states using a subscript s as $|q_1\rangle_s$. The asymptotic large N eigenstates are a small modification of these simple states. When we apply the dilatation operator to the simple states nothing prevents the boundary magnons from “hopping past the endpoints of the open string”, so the simple states are not closed under the action of the dilatation operator. We need to relax the sharp cut off on the magnon movement, by allowing the sums that appear in (A.2) above to be unrestricted. We accomplish this by introducing a “cut off” function, shown in Figure 2.2. In terms of this cut off function $f(\cdot)$ our eigenstates are

$$\begin{aligned} |\psi(q_1)\rangle &= \sum_{m_2=0}^{n+J} \sum_{m_1=0}^{m_2} f(m_2) q^{m_1-m_2} |1^{n+J+m_1-m_2+1}, 1^{n+J+m_1-m_2}, 1^{n+J+m_1-m_2}; \{m_2 - m_1\}\rangle \\ &+ \sum_{m_1=0}^{m_2+J} \sum_{m_2=0}^n f(m_1) f(J - m_1 + m_2) \\ &\times q^{m_1-m_2} |1^{n+m_1-m_2+1}, 1^{n+m_1-m_2}, 1^{n+m_1-m_2}; \{J + m_2 - m_1\}\rangle \end{aligned} \quad (\text{A.5})$$

The dilatation operator can not arrange that the number of Z s between two magnons becomes negative. Thus, any bounds on sums in the definition of our simple states enforcing this are respected. On the other hand, the dilatation operator allows boundary magnons to hop arbitrarily far beyond the open string endpoint. Bounds in the sums for simple states enforcing this are not respected. Replace these bounds enforced as the upper limit of a sum, by bounds enforced by the cut off function. From figure 2.2 we see that the cut off function is defined using a parameter δJ . We require that $\frac{\delta J}{J} \rightarrow 0$ as $N \rightarrow \infty$, so that at large N the difference between these eigenstates and the simple states $|q_1\rangle_s$ vanishes, as demonstrated in Appendix C. We also want to ensure that

$$f(i) = f(i+1) + \epsilon \quad \forall i \quad (\text{A.6})$$

with $\epsilon \rightarrow 0$ as $N \rightarrow \infty$. (A.6) is needed to ensure that we do indeed obtain an eigenstate. It is straight forward to choose a function $f(x)$ with the required properties. We could for example choose δJ to be of order $N^{\frac{1}{4}}$. Our large N answers are not sensitive to the details of the cut off function $f(x)$. When $1/N$ corrections to the eigenstates are computed $f(x)$ may be more constrained and we may need to reconsider the precise form of the cut off function and how we implement the bounds.

It is now straight forward to verify that, at large N , we have

$$\begin{aligned} D|\psi(q_1)\rangle &= 2\frac{g_{YM}^2}{8\pi^2} \left(1 + \left[1 - \frac{n}{N} \right] - \sqrt{1 - \frac{n}{N}}(q_1 + q_1^{-1}) \right) \\ &= 2g^2 \left(1 + \left[1 - \frac{n}{N} \right] - \sqrt{1 - \frac{n}{N}}(q_1 + q_1^{-1}) \right) \end{aligned} \quad (\text{A.7})$$

For the dual giant graviton of momentum n

$$\begin{aligned} D|\psi(q_1)\rangle &= 2\frac{g_{YM}^2}{8\pi^2} \left(1 + \left[1 + \frac{n}{N} \right] - \sqrt{1 + \frac{n}{N}}(q_1 + q_1^{-1}) \right) \\ &= 2g^2 \left(1 + \left[1 + \frac{n}{N} \right] - \sqrt{1 + \frac{n}{N}}(q_1 + q_1^{-1}) \right) \end{aligned} \quad (\text{A.8})$$

The generalization to include more magnons is straight forward. We will simply consider increasingly complicated examples and for each simply quote the final results. The discussion is most easily carried out using the occupation

notation. For example, the simple states corresponding to three magnons are

$$\begin{aligned}
 |q_1, q_2, q_3\rangle &= \sum_{n_3=0}^{J-1} \sum_{n_2=0}^{n_3} \sum_{n_1=0}^{n_2} q_1^{n_1} q_2^{n_2} q_3^{n_3} |G(n+J+n_1-n_3); \{(n_2-n_1), (n_3-n_2)\}\rangle \\
 &+ \sum_{n_1=0}^{J-1} \sum_{n_3=0}^{n_1} \sum_{n_2=0}^{n_3} q_1^{n_1} q_2^{n_2} q_3^{n_3} |G(n+n_1-n_3); \{(J+n_2-n_1), (n_3-n_2)\}\rangle \\
 &+ \sum_{n_2=0}^{J-1} \sum_{n_1=0}^{n_2} \sum_{n_3=0}^{n_1} q_1^{n_1} q_2^{n_2} q_3^{n_3} |G(n+n_1-n_3); \{(n_2-n_1), (J+n_3-n_2)\}\rangle
 \end{aligned} \tag{A.9}$$

where we have again lumped together the Young diagram labels $G(x) = R, R_1^1, R_2^1 = 1^{x+1}, 1^x, 1^x$. The coefficient of the ket $|G(n+J-a-b); \{(a), (b)\}\rangle$ is given by the sum

$$\sum_{n_1=0}^{J-1} (q_1 q_2 q_3)^{n_1} q_2^a q_3^{a+b} \tag{A.10}$$

which vanishes if $k_1 + k_2 + k_3 \neq 0$. Consequently we can set $q_3 = q_1^{-1} q_2^{-1}$.

Including the cut off function, our energy eigenstates are given by

$$\begin{aligned}
 |\psi(q_1, q_2)\rangle &= \sum_{n_3=0}^{\infty} \sum_{n_2=0}^{n_3} \sum_{n_1=0}^{n_2} q_1^{n_1-n_3} q_2^{n_2-n_3} f(n_3) |G(n+J+n_1-n_3); \{(n_2-n_1), (n_3-n_2)\}\rangle \\
 &+ \sum_{n_1=0}^{J+n_2} \sum_{n_3=0}^{\infty} \sum_{n_2=0}^{n_3} q_1^{n_1-n_3} q_2^{n_2-n_3} f(n_1) f(J+n_3-n_1) |G(n+n_1-n_3); \{(J+n_2-n_1), (n_3-n_2)\}\rangle \\
 &+ \sum_{n_2=0}^{J+n_3} \sum_{n_1=0}^{n_2} \sum_{n_3=0}^{\infty} q_1^{n_1-n_3} q_2^{n_2-n_3} f(n_2) f(J+n_3-n_1) |G(n+n_1-n_3); \{(n_2-n_1), (J+n_3-n_2)\}\rangle
 \end{aligned}$$

It is a simple matter to see that

$$D|\psi(q_1, q_2)\rangle = (E_1 + E_2 + E_3)|\psi(q_1, q_2)\rangle \tag{A.11}$$

where

$$\begin{aligned}
 E_1 &= 2g^2 \left(1 + \left[1 - \frac{n}{N} \right] - \sqrt{1 - \frac{n}{N}} (q_1 + q_1^{-1}) \right) \\
 E_2 &= g^2 (2 - q_2 - q_2^{-1}) \\
 E_3 &= 2g^2 \left(1 + \left[1 - \frac{n}{N} \right] - \sqrt{1 - \frac{n}{N}} (q_3 + q_3^{-1}) \right)
 \end{aligned} \tag{A.12}$$

Now consider the extension to states containing many magnons: For an M magnon state, consider all M cyclic orderings of the “magnon positions”

$$\begin{aligned}
 n_1 &\leq n_2 \leq n_3 \leq \cdots \leq n_{M-2} \leq n_{M-1} \leq n_M \leq J-1 \\
 n_M &\leq n_1 \leq n_2 \leq n_3 \leq \cdots \leq n_{M-2} \leq n_{M-1} \leq J-1 \\
 n_{M-1} &\leq n_M \leq n_1 \leq n_2 \leq n_3 \leq \cdots \leq n_{M-2} \leq J-1 \\
 &\vdots \quad \vdots \quad \vdots \\
 n_2 &\leq n_3 \leq \cdots \leq n_{M-2} \leq n_{M-1} \leq n_M \leq n_1 \leq J-1
 \end{aligned} \tag{A.13}$$

Construct the differences $\{n_2 - n_1, n_3 - n_2, n_4 - n_3, \dots, n_M - n_{M-1}, n_1 - n_M\}$. Every difference except for one is positive. Add J to the difference that is negative, i.e. the resulting differences are $\{\Delta_2, \Delta_3, \Delta_4, \dots, \Delta_M, \Delta_1\}$ with

$$\Delta_i = \begin{cases} n_i - n_{i-1} & \text{if } n_i \geq n_{i-1} \\ J + n_i - n_{i-1} & \text{if } n_i \leq n_{i-1} \end{cases} \tag{A.14}$$

For each ordering in (A.13) we have a term in the simple state. This term is obtained by summing over all values of $\{n_1, n_2, \dots, n_M\}$ consistent with the ordering considered, of the following summand

$$q_1^{n_1} q_2^{n_2} \cdots q_M^{n_M} |1^{n_1+\Delta_1+1}, 1^{n_2+\Delta_2}, 1^{n_3+\Delta_3}, \dots, 1^{n_M+\Delta_M}; \{(\Delta_2), (\Delta_3), \dots, (\Delta_M)\}\rangle \tag{A.15}$$

Repeating the argument we outlined above, this term vanishes unless $q_M^{-1} = q_1 q_2 \cdots q_{M-1}$ so that the summand can be replaced by

$$q_1^{n_1-n_M} q_2^{n_2-n_M} \cdots q_{M-1}^{n_{M-1}-n_M} |1^{n_1+\Delta_1+1}, 1^{n_2+\Delta_2}, 1^{n_3+\Delta_3}, \dots, 1^{n_{M-1}+\Delta_{M-1}}; \{(\Delta_2), (\Delta_3), \dots, (\Delta_M)\}\rangle \tag{A.16}$$

Finally, consider the extension to many string states and an arbitrary system of giant graviton branes. Each open string word is constructed as explained above. We add extra columns (one for each giant graviton) and rows (one for each dual giant graviton) to R . The labels R_1^k and R_2^k specify how the open strings are connected to the giant and dual giant gravitons. When describing twisted string states, the strings describe a closed loop, “punctuated by” the giant gravitons on which they end. As an example, consider a two giant graviton state, with a pair of strings stretching between the giant gravitons. The two

strings carry a total momentum of J . Notice that we are using the two strings to define a single lattice of J sites. One might have thought that the two strings would each define an independent lattice. To understand why we use the two strings to define a single lattice, recall that we are identifying the zero lattice momentum constraint with the constraint that the $\mathfrak{su}(2|2)$ central charges of the complete magnon state must vanish. There is a single $\mathfrak{su}(2|2)$ constraint on the two string state, not one constraint for each string. We interpret this as implying there is a single zero lattice momentum constraint for the two strings, and hence there is a single lattice for the two strings. This provides a straight forward way to satisfy the $\mathfrak{su}(2|2)$ central charge constraints. The first giant graviton has a momentum of b_0 and the second a momentum of b_1 . The first string is excited by M magnons with locations $\{n_1, n_2, \dots, n_{M-1}, n_M\}$ and the second by \tilde{M} magnons with locations $\{\tilde{n}_1, \tilde{n}_2, \dots, \tilde{n}_{\tilde{M}-1}, \tilde{n}_{\tilde{M}}\}$ where we have switched to the lattice notation. We need to consider the $M + \tilde{M}$ orderings of the $\{n_i\}$ and $\{\tilde{n}_i\}$. Given a specific pair of orderings, we can again form the differences

$$\begin{aligned} \Delta_i &= \begin{cases} n_1 - \tilde{n}_M & \text{if } n_1 \geq \tilde{n}_M \\ J + n_1 - \tilde{n}_M & \text{if } n_1 \leq \tilde{n}_M \end{cases} \\ \Delta_i &= \begin{cases} n_i - n_{i-1} & \text{if } n_i \geq n_{i-1} \\ J + n_i - n_{i-1} & \text{if } n_i \leq n_{i-1} \end{cases} \quad i = 2, 3, \dots, M \\ \Delta_{M+1} &= \begin{cases} \tilde{n}_1 - n_M & \text{if } n_M \geq \tilde{n}_1 \\ J + \tilde{n}_1 - n_M & \text{if } n_M \leq \tilde{n}_1 \end{cases} \\ \Delta_{M+i} &= \begin{cases} \tilde{n}_i - \tilde{n}_{i-1} & \text{if } \tilde{n}_i \geq \tilde{n}_{i-1} \\ J + \tilde{n}_i - \tilde{n}_{i-1} & \text{if } \tilde{n}_i \leq \tilde{n}_{i-1} \end{cases} \quad i = 2, 3, \dots, \tilde{M} \end{aligned} \quad (\text{A.17})$$

For each ordering we again have a term in the simple state, obtained by summing over all values of $\{n_1, n_2, \dots, n_{M-1}, n_M, \tilde{n}_1, \tilde{n}_2, \dots, \tilde{n}_{\tilde{M}-1}, \tilde{n}_{\tilde{M}}\}$ consistent with

the ordering considered, of the following summand

$$q_1^{n_1} q_2^{n_2} \cdots q_M^{n_M} \tilde{q}_1^{\tilde{n}_1} \tilde{q}_2^{\tilde{n}_2} \cdots \tilde{q}_{\tilde{M}}^{\tilde{n}_{\tilde{M}}} \\ \times \left| G(\Delta_1, \Delta_{M+1}); \{(\Delta_2), (\Delta_3), \cdots, (\Delta_M)\}, \{(\Delta_{M+2}), (\Delta_{M+3}), \cdots, (\Delta_{M+\tilde{M}})\} \right\rangle \quad (\text{A.18})$$

where

In the first Young diagram above there are $b_1 + y + 1$ rows with 2 boxes in each row and $b_0 + x - b_1 - y - 1$ rows with 1 box in each row. Repeating the argument we outlined above, this term vanishes unless $\tilde{q}_M^{-1} = q_1 \cdots q_M \tilde{q}_1 \cdots \tilde{q}_{M-1}$ so that the summand can be replaced by

$$q_1^{n_1-\tilde{n}_{\tilde{M}}} q_2^{n_2-\tilde{n}_{\tilde{M}}-\tilde{n}_{\tilde{M}}} \cdots q_M^{n_M-\tilde{n}_{\tilde{M}}} \tilde{q}_2^{\tilde{n}_2-\tilde{n}_{\tilde{M}}} \cdots \tilde{q}_{\tilde{M}}^{\tilde{n}_{\tilde{M}}-\tilde{n}_{\tilde{M}}} \\ \times \left| G(\Delta_1, \Delta_{M+1}); \{(\Delta_2), (\Delta_3), \cdots, (\Delta_M)\}, \{(\Delta_{M+2}), (\Delta_{M+3}), \cdots, (\Delta_{M+\tilde{M}})\} \right\rangle \quad (\text{A.20})$$

Appendix B

Two loop computation of boundary magnon energy

The dilatation operator, in the $\mathfrak{su}(2)$ sector, can be expanded as [84; 85]

$$D = \sum_{k=0}^{\infty} \left(\frac{g_{YM}^2}{16\pi^2} \right)^k D_{2k} = \sum_{k=0}^{\infty} g^{2k} D_{2k}, \quad (\text{B.1})$$

where the tree level, one loop and two loop contributions are

$$D_0 = \text{Tr} \left(Z \frac{\partial}{\partial Z} \right) + \text{Tr} \left(Y \frac{\partial}{\partial Y} \right), \quad (\text{B.2})$$

$$D_2 = -2 : \text{Tr} \left([Z, Y] \left[\frac{\partial}{\partial Z}, \frac{\partial}{\partial Y} \right] \right) :, \quad (\text{B.3})$$

$$D_4 = D_4^{(a)} + D_4^{(b)} + D_4^{(c)}, \quad (\text{B.4})$$

$$\begin{aligned} D_4^{(a)} &= -2 : \text{Tr} \left(\left[[Y, Z], \frac{\partial}{\partial Z} \right] \left[\left[\frac{\partial}{\partial Y}, \frac{\partial}{\partial Z} \right], Z \right] \right) : \\ D_4^{(b)} &= -2 : \text{Tr} \left(\left[[Y, Z], \frac{\partial}{\partial Y} \right] \left[\left[\frac{\partial}{\partial Y}, \frac{\partial}{\partial Z} \right], Y \right] \right) : \\ D_4^{(c)} &= -2 : \text{Tr} \left([[Y, Z], T^a] \left[\left[\frac{\partial}{\partial Y}, \frac{\partial}{\partial Z} \right], T^a \right] \right) : \end{aligned} \quad (\text{B.5})$$

The boundary magnon energy we computed above came from D_2 . By computing the contribution from D_4 we can compare to the second term in the expansion of the string energies. Since we are using the planar approximation when contracting fields in the open string words, in the limit of well separated

magnons, the action of D_4 can again be written as a sum of terms, one for each magnon. Thus, if we compute the action of D_4 on a state $|1^{n+1}, 1^n, 1^n; \{n_1, n_2\}\rangle$ with a single string and a single bulk magnon, its a trivial step to obtain the action of D_4 on the most general state.

A convenient way to summarize the result is to quote the action of D_4 on a state for which the magnons have momenta q_1, q_2, q_3 . Of course, we will have to choose the q_i so that the total central charge vanishes as explained in Chapter 2. Thus we could replace $q_3 \rightarrow (q_1 q_2)^{-1}$ in the formulas below. We will write the answer for a general giant graviton system with strings attached. For the boundary terms, each boundary magnon corresponds to an end point of the string and each end point is associated with a specific box in the Young diagram. Denote the factor of the box corresponding to the first magnon by c_F and the factor of the box associated to the last magnon by c_L . A straight forward but somewhat lengthy computation, using the methods developed in [8; 9] gives

$$\begin{aligned}
 (D_4)_{\text{first magnon}} |\psi(q_1, q_2, q_3)\rangle &= -\frac{g^4}{2} \left[\left(1 + \frac{c_F}{N}\right)^2 - \left(1 + \frac{c_F}{N}\right) \sqrt{\frac{c_F}{N}} (q_1 + q_1^{-1}) \right. \\
 &\quad \left. + \frac{c_F}{N} (q_1^2 + 2 + q_1^{-2}) \right] |\psi(q_1, q_2, q_3)\rangle \\
 &= -\frac{g^4}{2} \left[1 + \frac{c_F}{N} - \sqrt{\frac{c_F}{N}} (q_1 + q_1^{-1}) \right]^2 |\psi(q_1, q_2, q_3)\rangle \\
 &= -\frac{1}{2} \left[g^2 \left(1 + \frac{c_F}{N} - \sqrt{\frac{c_F}{N}} (q_1 + q_1^{-1}) \right) \right]^2 |\psi(q_1, q_2, q_3)\rangle
 \end{aligned} \tag{B.6}$$

in perfect agreement with (2.23). The term $D_4^{(b)}$ does not make a contribution to the action on distant magnons, since we sum only the planar open string word contractions. The remaining terms $D_4^{(a)}, D_4^{(c)}$ both make a contribution to the action on distant magnons. For completeness note that

$$(D_4)_{\text{first magnon}} |\psi(q_1, q_2, q_3)\rangle = -\frac{1}{2} [g^2 (2 - (q_1 + q_1^{-1}))]^2 |\psi(q_1, q_2, q_3)\rangle \tag{B.7}$$

Appendix C

The difference between simple states and eigenstates vanishes at large N

In this section we want to quantify the claim made in section 2.5 that the difference between our simple states and our exact eigenstates vanishes in the large N limit. We will do this by computing the difference between the simple states and eigenstates and observing this difference has a norm that goes to zero in the large N limit.

For simplicity, we will consider a two magnon state. The generalization to many magnon states is straight forward. Our simple states have the form

$$\begin{aligned} |q\rangle = \mathcal{N} \left(\sum_{m_1=0}^{J-1} \sum_{m_2=0}^{m_1} q^{m_1-m_2} |1^{n+m_1-m_2+1}, 1^{n+m_1-m_2}, 1^{n+m_1-m_2}; \{J-m_1+m_2\}\rangle \right. \\ \left. + \sum_{m_2=0}^{J-1} \sum_{m_1=0}^{m_2} q^{m_1-m_2} |1^{n+J+m_1-m_2+1}, 1^{n+J+m_1-m_2}, 1^{n+J+m_1-m_2}; \{m_2-m_1\}\rangle \right) \end{aligned} \quad (\text{C.1})$$

Requiring that $\langle q|q \rangle = 1$ we find

$$\mathcal{N} = \frac{1}{J\sqrt{J+1}} \quad (C.2)$$

With this normalization we find that the simple states are orthogonal

$$\langle q_a|q_a \rangle = \delta_{k_a k_b} + O\left(\frac{1}{J}\right) \quad \text{where} \quad q_a = e^{i\frac{2\pi k_a}{J}}, q_b = e^{i\frac{2\pi k_b}{J}}. \quad (C.3)$$

This is perfectly consistent with the fact that in the planar limit the lattice states, given by $|1^{n+m_1-m_2+1}, 1^{n+m_1-m_2}, 1^{n+m_1-m_2}; \{J-m_1+m_2\}\rangle$ are orthogonal and our simple states are simply a Fourier transform of these.

Our eigenstates have the form (we will see in a few moments that the normalization in the next equation below is the same as the normalization in (C.2))

$$\begin{aligned} |q\rangle &= \mathcal{N} \left(\sum_{m_2=0}^{\infty} \sum_{m_1=0}^{m_2} f(m_2) q^{m_1-m_2} |1^{n+J+m_1-m_2+1}, 1^{n+J+m_1-m_2}, 1^{n+J+m_1-m_2}; \{m_2-m_1\}\rangle \right. \\ &+ \left. \sum_{m_1=0}^{J+m_2} \sum_{m_2=0}^{\infty} f(m_1) f(J-m_1+m_2) q^{m_1-m_2} |1^{n+m_1-m_2+1}, 1^{n+m_1-m_2}, 1^{n+m_1-m_2}; \{J-m_1+m_2\}\rangle \right) \\ &\equiv |q\rangle + |\delta q\rangle \end{aligned} \quad (C.4)$$

where

$$\begin{aligned} |\delta q\rangle &= \mathcal{N} \left(\sum_{m_2=J}^{n+J+1} \sum_{m_1=0}^{m_2} f(m_2) q^{m_1-m_2} |1^{n+J+m_1-m_2+1}, 1^{n+J+m_1-m_2}, 1^{n+J+m_1-m_2}; \{m_2-m_1\}\rangle \right. \\ &+ \left. \sum_{m_1=J}^{J+m_2} \sum_{m_2=0}^{n+m_1} f(m_1) f(J-m_1+m_2) q^{m_1-m_2} |1^{n+m_1-m_2+1}, 1^{n+m_1-m_2}, 1^{n+m_1-m_2}; \{J-m_1+m_2\}\rangle \right) \\ &+ \sum_{m_1=0}^{J-1} \sum_{m_2=m_1+1}^{m_1+n} f(J-m_1+m_2) q^{m_1-m_2} |1^{n+m_1-m_2+1}, 1^{n+m_1-m_2}, 1^{n+m_1-m_2}; \{J-m_1+m_2\}\rangle \\ &= \mathcal{N} \left(\sum_{m_2=J}^{J+\delta J} \sum_{m_1=0}^{m_2} f(m_2) q^{m_1-m_2} |1^{n+J+m_1-m_2+1}, 1^{n+J+m_1-m_2}, 1^{n+J+m_1-m_2}; \{m_2-m_1\}\rangle \right. \\ &+ \left. \sum_{m_1=J}^{l_-} \sum_{m_2=0}^{J+\delta J} f(m_1) f(J-m_1+m_2) q^{m_1-m_2} |1^{n+m_1-m_2+1}, 1^{n+m_1-m_2}, 1^{n+m_1-m_2}; \{J-m_1+m_2\}\rangle \right) \\ &+ \sum_{m_1=0}^{J-1} \sum_{m_2=m_1+1}^{m_1+\delta J} f(J-m_1+m_2) q^{m_1-m_2} |1^{n+m_1-m_2+1}, 1^{n+m_1-m_2}, 1^{n+m_1-m_2}; \{J-m_1+m_2\}\rangle \end{aligned}$$

APPENDIX C. THE DIFFERENCE BETWEEN SIMPLE STATES AND EIGENSTATES VANISHES AT LARGE N

and l_- is the smallest of $J + m_2$ and $J + \delta J$. It is rather simple to see that $|\delta q\rangle$ is given by a sum of $O(J)$ terms and that each term has a coefficient of order δJ . Consequently, up to an overall constant factor $c_{\delta q}$ which is independent of J , we can bound the norm of $|\delta q\rangle$ as

$$\langle \delta q | \delta q \rangle \leq c_{\delta q} J(\delta J) \mathcal{N}^2 = c_{\delta q} \frac{(\delta J)^2}{J(J+1)} \quad (\text{C.5})$$

which goes to zero in the large J limit, proving our assertion that the difference between the simple states and the large N eigenstates vanishes in the large N limit.

Appendix D

Review of dilatation operator action

The studies [64; 14] have computed the dilatation operator action without invoking the distant corners approximation. The only approximation made in these studies is that correlators of operators with p long rows/columns with operators that have p long rows/columns and some short rows/columns, vanishes in the large N limit. These results are useful since they provide data against which the distant corners approximation could be compared. Further, we have demonstrated that the action of the dilatation operator reduces to a set of decoupled harmonic oscillators in [15; 16; 20; 17]. However, to obtain this result we needed to expand one of the factors in the dilatation operator to subleading order. The agreement of the resulting spectrum¹ is strong evidence that the distant corners approximation is valid. It is worth discussing these details and explaining why we do indeed obtain the correct large N limit. This point is not made explicitly in [15; 16; 20; 17].

$$DO_{R,(r,s)}(Z, Y) = \sum_{T,(t,u)} N_{R,(r,s);T,(t,u)} O_{T,(t,u)}(Z, Y)$$

¹One can also compare the states that have a definite scaling dimension. The states obtained in the distant corners approximation are in perfect agreement with the states obtained in [64; 14] by a numerical diagonalization of the dilatation operator.

is given by

$$N_{R,(r,s);T,(t,u)} = -g_{YM}^2 \sum_{R'} \frac{c_{RR'd_T nm}}{d_{R'} d_t d_u (n+m)} \sqrt{\frac{f_T \text{hooks}_T \text{hooks}_r \text{hooks}_s}{f_R \text{hooks}_R \text{hooks}_t \text{hooks}_u}} \times \\ \times \text{Tr} \left([\Gamma_R((n, n+1)), P_{R \rightarrow (r,s)}] I_{R'T'} [\Gamma_T((n, n+1)), P_{T \rightarrow (t,u)}] I_{T'R'} \right)$$

The above formula is exact. After using the distant corners approximation to simplify the trace and prefactor, this becomes

$$DO_{R,(r,s)\mu_1\mu_2} = -g_{YM}^2 \sum_{u\nu_1\nu_2} \sum_{i < j} \delta_{\vec{m},\vec{n}} M_{s\mu_1\mu_2;u\nu_1\nu_2}^{(ij)} \Delta_{ij} O_{R,(r,s)\nu_1\nu_2} \quad (\text{D.1})$$

Notice that we have a factorized action: the Δ_{ij} (explained below) acts only on the Young diagrams R, r and

$$M_{s\mu_1\mu_2;u\nu_1\nu_2}^{(ij)} = \frac{m}{\sqrt{d_s d_u}} \left(\langle \vec{m}, s, \mu_2; a | E_{ii}^{(1)} \vec{m}, u, \nu_2; b \rangle \langle \vec{m}, s, \mu_1; b | E_{jj}^{(1)} \vec{m}, u, \nu_1; a \rangle \right. \\ \left. + \langle \vec{m}, s, \mu_2; a | E_{ii}^{(1)} \vec{m}, u, \nu_2; b \rangle \langle \vec{m}, s, \mu_1; b | E_{jj}^{(1)} \vec{m}, u, \nu_1; a \rangle \right) \quad (\text{D.2})$$

where a and b are summed, acts only on the s, μ_1, μ_2 labels of the restricted Schur polynomial. a labels states in the irreducible representation s and b labels states in the irreducible representation t . To spell out the action of operator Δ_{ij} it is useful to split it up into three terms

$$\Delta_{ij} = \Delta_{ij}^+ + \Delta_{ij}^0 + \Delta_{ij}^- \quad (\text{D.3})$$

Denote the row lengths of r by r_i and the row lengths of R by R_i . Introduce the Young diagram r_{ij}^+ obtained from r by removing a box from row j and adding it to row i . Similarly r_{ij}^- is obtained by removing a box from row i and adding it to row j . In terms of these Young diagrams we have

$$\Delta_{ij}^0 O_{R,(r,s)\mu_1\mu_2} = -(2N + R_i + R_j - i - j) O_{R,(r,s)\mu_1\mu_2}, \quad (\text{D.4})$$

$$\Delta_{ij}^+ O_{R,(r,s)\mu_1\mu_2} = \sqrt{(N + R_i - i)(N + R_j - j + 1)} O_{R_{ij}^+, (r_{ij}^+, s)\mu_1\mu_2}, \quad (\text{D.5})$$

$$\Delta_{ij}^- O_{R,(r,s)\mu_1\mu_2} = \sqrt{(N + R_i - i + 1)(N + R_j - j)} O_{R_{ij}^-, (r_{ij}^-, s)\mu_1\mu_2}. \quad (\text{D.6})$$

As a matrix Δ_{ij} has matrix elements

$$\Delta_{ij}^{R,r;T,t} = \sqrt{(N + R_i - i)(N + R_j - j + 1)} \delta_{T,R_{ij}^+} \delta_{t,r_{ij}^+} \\ + \sqrt{(N + R_i - i + 1)(N + R_j - j)} \delta_{T,R_{ij}^-} \delta_{t,r_{ij}^-} - (2N + R_i + R_j - i - j) \delta_{R,T} \delta_{t,r}. \quad (\text{D.7})$$

In terms of these matrix elements we can write (D.1) as

$$DO_{R,(r,s)\mu_1\mu_2} = -g_{YM}^2 \sum_{u\nu_1\nu_2} \sum_{i < j} \delta_{\vec{m},\vec{n}} M_{s\mu_1\mu_2;u\nu_1\nu_2}^{(ij)} \Delta_{ij}^{R,r;T,t} O_{R,(r,s)\nu_1\nu_2} \quad (\text{D.8})$$

Although the distant corners approximation has been used to extract the large N value of $M_{s\mu_1\mu_2;u\nu_1\nu_2}^{(ij)}$ the action of $\Delta_{ij}^{R,r;T,t}$ is computed exactly. In particular, the coefficients appearing in (D.7) are simply the factors associated with the boxes that are added or removed by $\Delta_{ij}^{R,r;T,t}$, and hence in developing a systematic large N expansion for $\Delta_{ij}^{R,r;T,t}$ we can trust the shifts of numbers of order N by numbers of order 1.

The limit in which the dilatation operator reduces to sets of decoupled oscillators corresponds to the limit in which the difference between the row (or column) lengths of Young diagram R are fixed to be $O(\sqrt{N})$ while the row lengths themselves are order N . The continuum variables are then

$$x_i = \frac{R_{i+1} - R_i}{\sqrt{R_1}}, \quad i = 1, 2, \dots, p-1 \quad (\text{D.9})$$

when R has p rows (or columns) and the shortest row (or column) is R_1 . In this case, the leading and subleading (order N and order \sqrt{N}) contribution to $\Delta_{ij} O_{R,(r,s)\mu_1\mu_2}$ vanish, leaving a contribution of order 1. This contribution is sensitive to the exact form of the coefficients appearing in (D.7), and it is with these shifts that we reproduce the numerical results of [64; 14].

Appendix E

One loop computation of bulk/boundary magnon scattering

In this appendix we will compute the scattering of a bulk and boundary magnon, to one loop, using the asymptotic Bethe ansatz. See [96] where studies of this type were first suggested and [97] for related systems. We can introduce a wave function $\psi(l_1, l_2, \dots)$ as follows

$$O = \sum_{l_1, l_2, \dots} \psi(l_1, l_2, \dots) O(R, R_1^k, R_2^k; \{l_1, l_2, \dots\}) \quad (\text{E.1})$$

We assume that the boundary magnon (at l_1) and the next magnon along the open string (at l_2) are very well separated from the remaining magnons. These magnons are both assumed to be Y impurities. To obtain the scattering we want, we only need to focus on these two magnons. The time independent Schrödinger equation following from our one loop dilatation operator is

$$\begin{aligned} E\psi(l_1, l_2) = & \left(3 + \frac{c}{N}\right) \psi(l_1, l_2) - \sqrt{\frac{c}{N}} (\psi(l_1 - 1, l_2) + \psi(l_1 + 1, l_2)) \\ & - (\psi(l_1, l_2 - 1) + \psi(l_1, l_2 + 1)) \end{aligned} \quad (\text{E.2})$$

where c is the factor of the box that the endpoint associated to the magnon at l_1 belongs to. The equation (E.2) is valid whenever the two magnons are not adjacent in the open string word, i.e. when $l_2 > l_1 + 1$.¹ In the situation that the magnons are adjacent, we find

$$E\psi(l_1, l_1+1) = \left(1 + \frac{c}{N}\right)\psi(l_1, l_1+1) - \sqrt{\frac{c}{N}}\psi(l_1-1, l_2) - \psi(l_1+1, l_1+2) \quad (\text{E.3})$$

We make the following Bethe ansatz for the wave function

$$\psi(l_1, l_2) = e^{ip_1 l_1 + ip_2 l_2} + R_{12}e^{ip'_1 l_1 + ip'_2 l_2} \quad (\text{E.4})$$

It is straight forward to see that this ansatz obeys (E.2) as long as

$$E = 3 + \frac{c}{N} - \sqrt{\frac{c}{N}}(e^{ip_1} + e^{-ip_1}) - (e^{ip_2} + e^{-ip_2}) \quad (\text{E.5})$$

and

$$\sqrt{\frac{c}{N}}(e^{ip_1} + e^{-ip_1}) + e^{ip_2} + e^{-ip_2} = \sqrt{\frac{c}{N}}(e^{ip'_1} + e^{-ip'_1}) + e^{ip'_2} + e^{-ip'_2} \quad (\text{E.6})$$

Note that (E.5) is indeed the correct one loop anomalous dimension and (E.6) can be obtained by equating the $O(\lambda)$ terms on both sides of (2.30), as it should be. From (E.3) we can solve for the reflection coefficient R . The result is

$$R_{12} = \frac{2e^{ip_2} - \sqrt{\frac{c}{N}}e^{ip_1+ip_2} - 1}{2e^{ip'_2} - \sqrt{\frac{c}{N}}e^{ip'_1+ip'_2} - 1} \quad (\text{E.7})$$

Two simple checks of this result are

1. We see that $R_{12}R_{21} = 1$.
2. If we set $c = N$ we recover the S-matrix of [96].

We will now move beyond the $\mathfrak{su}(2)$ sector by considering a state with a single Y impurity and a single X impurity. The operator with a Y impurity at l_1 and an X impurity at l_2 is denoted $O(R, R_1^k, R_2^k, \{l_1, l_2, \dots\})_{YX}$ and the operator with an X impurity at l_1 and a Y impurity at l_2 is denoted

¹Notice that we are associating a lattice site to every field in the spin chain and not just to the Z s.

$O(R, R_1^k, R_2^k; \{l_1, l_2, \dots\})_{XY}$. We now introduce a pair of wave functions as follows

$$O = \sum_{l_1, l_2, \dots} \left[\psi_{YX}(l_1, l_2, \dots) O(R, R_1^k, R_2^k; \{l_1, l_2, \dots\})_{YX} + \psi_{XY}(l_1, l_2, \dots) O(R, R_1^k, R_2^k; \{l_1, l_2, \dots\})_{XY} \right]. \quad (\text{E.8})$$

From the one loop dilatation operator we find the time independent Schrödinger equation (E.2) for each wave function, when the impurities are not adjacent. When the impurities are adjacent, we find the following two time independent Schrödinger equations

$$E\psi_{YX}(l_1, l_1 + 1) = \left(2 + \frac{c}{N}\right) \psi_{YX}(l_1, l_1 + 1) - \sqrt{\frac{c}{N}} \psi_{YX}(l_1 - 1, l_1 + 1) - \psi_{XY}(l_1, l_1 + 1) - \psi_{YX}(l_1, l_1 + 2) \quad (\text{E.9})$$

$$E\psi_{XY}(l_1, l_1 + 1) = \left(2 + \frac{c}{N}\right) \psi_{XY}(l_1, l_1 + 1) - \sqrt{\frac{c}{N}} \psi_{XY}(l_1 - 1, l_1 + 1) - \psi_{YX}(l_1, l_1 + 1) - \psi_{XY}(l_1, l_1 + 2) \quad (\text{E.10})$$

Making the following Bethe ansatz for the wave function

$$\begin{aligned} \psi_{YX}(l_1, l_1 + 1) &= e^{ip_1 l_1 + ip_2 l_2} + A e^{ip'_1 l_1 + ip'_2 l_2} \\ \psi_{XY}(l_1, l_1 + 1) &= B e^{ip'_1 l_1 + ip'_2 l_2} \end{aligned} \quad (\text{E.11})$$

we find that the two equations of the form (E.2) imply that both $\psi_{XY}(l_1, l_2)$ and $\psi_{YX}(l_1, l_1 + 1)$ have the same energy, which is given in (E.5). The equations (E.9) and (E.10) imply that

$$\begin{aligned} A &= \frac{e^{ip'_2} + e^{ip_2} - 1 - \sqrt{\frac{c}{N}} e^{ip'_1 + ip'_2}}{1 + \sqrt{\frac{c}{N}} e^{ip'_1 + ip'_2} - 2 e^{ip'_2}} \\ B &= \frac{e^{ip_2} - e^{ip'_2}}{1 + \sqrt{\frac{c}{N}} e^{ip'_1 + ip'_2} - 2 e^{ip'_2}}. \end{aligned} \quad (\text{E.12})$$

It is straight forward but a bit tedious to check that $|A|^2 + |B|^2 = 1$ which is a consequence of unitarity. To perform this check it is necessary to use the conservation of momentum $p_1 + p_2 = p'_1 + p'_2$, as well as the constraint (E.6).

We now finally obtain

$$\frac{A}{R_{12}} = \frac{e^{ip'_2} + e^{ip_2} - 1 - \sqrt{\frac{c}{N}} e^{ip'_1 + ip'_2}}{2 e^{ip_2} - \sqrt{\frac{c}{N}} e^{ip_1 + ip_2} - 1}. \quad (\text{E.13})$$

This should be equal to

$$\frac{1}{2} \left(1 + \frac{B_{12}^R}{A_{12}^R} \right) \quad (\text{E.14})$$

where A_{12}^R and B_{12}^R are the S-matrix elements computed in section 2.8, describing the scattering between a bulk and a boundary magnon. This allows us to perform a non-trivial check of the S -matrix elements we computed.

Appendix F

Another check of the S –matrix

F.1 Numerical one-loop perturbative check of the reflection S –matrix

In this section we perform numerical checks of the analytic expression for the S –matrix between a boundary and a bulk magnon, for various values of $r \in [0, 1]$. Toward this end, recall the following elements the S –matrix

$$A_{12}^R = S_0 \frac{\eta_1 \eta_2 x_1'^+ x_1^+ (x_1^- - x_2^+) \left((x_2^+ - rx_2^-)(rx_2'^+ - x_2'^-) x_2^+ + (x_2^- - rx_2^+)(x_2'^+ - rx_2'^+) x_2'^+ \right)}{\eta_1' \eta_2' x_2'^+ x_2^+ (x_1^- - x_1^+) (x_1^+ - x_1'^+) \left(x_1^+ (rx_2^+ - x_2^-) + x_2^- (rx_2^- - x_2^+) \right)}, \quad (\text{F.1})$$

and

$$B_{12}^R = A_{12}^R \left[1 + \frac{2x_2'^- (x_1'^- - x_1'^+)}{x_1'^+ (x_1^- - x_2^+) (x_1'^- - rx_1'^+ x_2'^+)} \frac{B_1}{B_2} \right] \quad (\text{F.2})$$

where

$$\begin{aligned} B_1 &= x_2^- x_1'^+ \left[(x_1^- - x_1^+) (2x_1^- - x_1'^-) (x_2^+ x_1'^+ - x_1^+ x_2^+) \right. \\ &\quad \left. - x_1'^+ x_1^- (x_2^+ - rx_2^-) (x_1^- - x_2^+) \right] \frac{rx_2'^+ - x_2'^-}{rx_2'^- - x_2'^+} \\ &\quad + \left[x_1'^+ x_1^+ (x_1^- - rx_2^+) (x_2^- - rx_2^+) + x_2^+ x_2^- (x_1^- - x_1^+) (x_1'^+ - x_1^+) \right] x_1'^- x_2'^-, \\ B_2 &= (rx_2^- - x_2^+) \left[x_1^+ x_2'^- x_1'^- \frac{rx_2^+ - x_2^-}{rx_2^- - x_2^+} - x_1'^+ x_1^- x_2^- \frac{rx_2'^+ - x_2'^-}{rx_2'^- - x_2'^+} \right], \end{aligned}$$

and the initial and final boundary momenta of the boundary magnon are coded in x_2^\pm and $x_2'^\pm$. For the bulk magnon x_1^\pm and $x_1'^\pm$ capture the initial and final momenta. We denote by $\frac{1}{2} \left(1 + \frac{B_{12}^R}{A_{12}^R}\right) \Big|_{1\text{-loop}}$ the one loop piece of (E.14). To evaluate this one loop piece we need a relation between the initial and final momenta which can be obtained by solving the conservation of energy and momentum conditions

$$\begin{cases} p_1 + p_2 = p'_1 + p'_2, \\ e^{ip_1} + e^{-ip_1} + r(e^{ip_2} + e^{-ip_2}) = e^{ip'_1} + e^{-ip'_1} + r(e^{ip'_2} + e^{-ip'_2}) \end{cases} \quad (\text{F.3})$$

The solutions to (F.3) are used in the one loop correct expressions for x^\pm ;

1.

$$x^+ = x^- e^{ip} \quad (\text{F.4})$$

2. For a bulk magnon

$$x^- = e^{-i\frac{p}{2}} \left(\frac{1}{2g \sin(\frac{p}{2})} + 2g \sin(\frac{p}{2}) \right) + O(g^2). \quad (\text{F.5})$$

3. For a boundary magnon

$$x^- = -\frac{i}{g(r - e^{ip})} + i g e^{-ip} (r - e^{ip}) \frac{r e^{ip} - 1}{r + e^{ip}} + O(g^2). \quad (\text{F.6})$$

We use (F.4), (F.5) and (F.6) to numerically evaluate $\frac{1}{2} \left(1 + \frac{B_{12}^R}{A_{12}^R}\right) \Big|_{1\text{-loop}}$.

The expression (E.13) becomes

$$\frac{A}{R_{12}} = \frac{e^{ip'_1} + e^{ip_1} - 1 - r e^{ip'_1 + ip'_2}}{2 e^{ip_1} - r e^{ip_1 + ip_2} - 1} \quad (\text{F.7})$$

We now are ready to compare (F.7) and $\frac{1}{2} \left(1 + \frac{B_{12}^R}{A_{12}^R}\right) \Big|_{1\text{-loop}}$.

F.2 Setting up the numerical test

F.2.1 Solutions for $p_2 = 0$

As a warm up example set the initial boundary magnon momentum

$$p_2 = 0$$

and consider a bulk magnon with initial momentum p_1 treated as an independent variable. In this case one can solve the one loop conservation of energy and momentum, and (F.3) becomes

$$\begin{cases} p'_1 + p'_2 = p_1 \\ r \cos(p_1 - p'_1) + \cos(p'_1) = r + \cos(p_1) \end{cases} \quad (\text{F.8})$$

The non-trivial analytic solutions to (F.8) in terms of p_1 are

$$p'_1 = 2 \operatorname{atan} \left(\frac{r-1}{r+1} \tan \left(\frac{p_1}{2} \right) \right) \quad (\text{F.9})$$

$$p'_2 = p_1 - p'_1 \quad (\text{F.10})$$

F.2.2 General solutions for $p_2 \neq 0$

Now consider the case $p_2 \neq 0$. Recall the energy momentum conditions

$$\begin{cases} p'_1 + p'_2 = p_1 + p_2 \\ r \cos(p'_2) + \cos(p'_1) = r \cos(p_2) + \cos(p_1) \end{cases} \quad (\text{F.11})$$

If we fix p_2 constant and non-zero and treat p_1 as an independent variable, we can solve (F.11) analytically. We find

$$\begin{aligned} p'_1 = 2 \operatorname{atan} & \left[\frac{1}{2} \left(\frac{2r \tan(\frac{p_1}{2}) \cos(p_2) + r \sin(p_2) - r \tan^2(\frac{p_1}{2}) \sin(p_2)}{1 + r \cos(p_2) - r \tan(\frac{p_1}{2}) \sin(p_2)} \right) \right. \\ & \left. \pm \left(\frac{1}{4} \left[\frac{2r \tan(\frac{p_1}{2}) \cos(p_2) + r \sin(p_2) - r \tan^2(\frac{p_1}{2}) \sin(p_2)}{1 + r \cos(p_2) - r \tan(\frac{p_1}{2}) \sin(p_2)} \right]^2 \right. \right. \\ & \left. \left. + \frac{\tan^2(\frac{p_1}{2})(1 - r \cos(p_2)) - r \tan(\frac{p_1}{2}) \sin(p_2)}{1 + r \cos(p_2) - r \tan(\frac{p_1}{2}) \sin(p_2)} \right)^{\frac{1}{2}} \right] \end{aligned} \quad (\text{F.12})$$

Given $0 \leq r \leq 1$ and $p_2 \neq 0$, one finds the solutions

$$\begin{aligned} p'_1 = 2 \operatorname{atan} & \left[\frac{1}{2} \left(\frac{2r \tan(\frac{p_1}{2}) \cos(p_2) + r \sin(p_2) - r \tan^2(\frac{p_1}{2}) \sin(p_2)}{1 + r \cos(p_2) - r \tan(\frac{p_1}{2}) \sin(p_2)} \right) \right. \\ & \left. - \left(\frac{1}{4} \left[\frac{2r \tan(\frac{p_1}{2}) \cos(p_2) + r \sin(p_2) - r \tan^2(\frac{p_1}{2}) \sin(p_2)}{1 + r \cos(p_2) - r \tan(\frac{p_1}{2}) \sin(p_2)} \right]^2 \right. \right. \\ & \left. \left. + \frac{\tan^2(\frac{p_1}{2})(1 - r \cos(p_2)) - r \tan(\frac{p_1}{2}) \sin(p_2)}{1 + r \cos(p_2) - r \tan(\frac{p_1}{2}) \sin(p_2)} \right)^{\frac{1}{2}} \right] \end{aligned} \quad (\text{F.13})$$

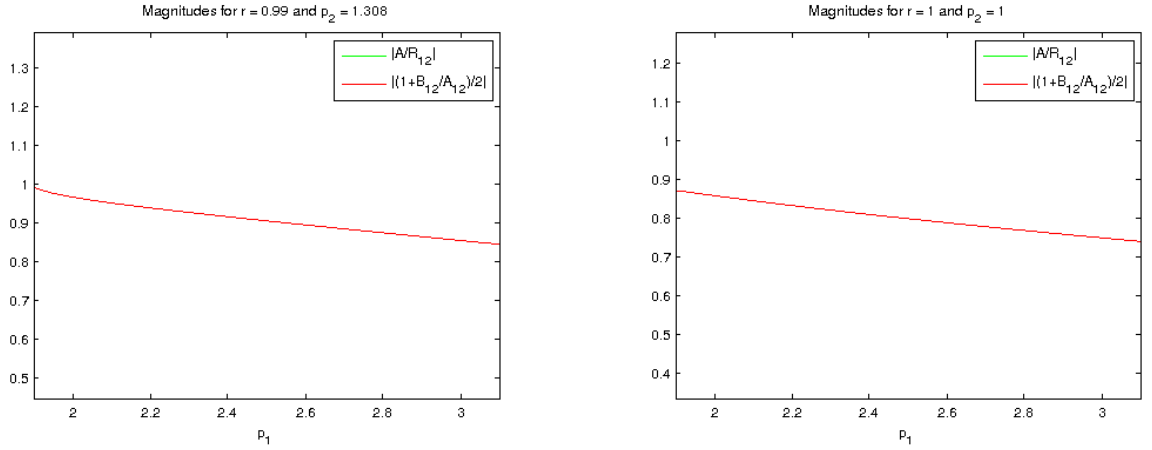
$$p'_2 = p_1 + p_2 - p'_1. \quad (\text{F.14})$$

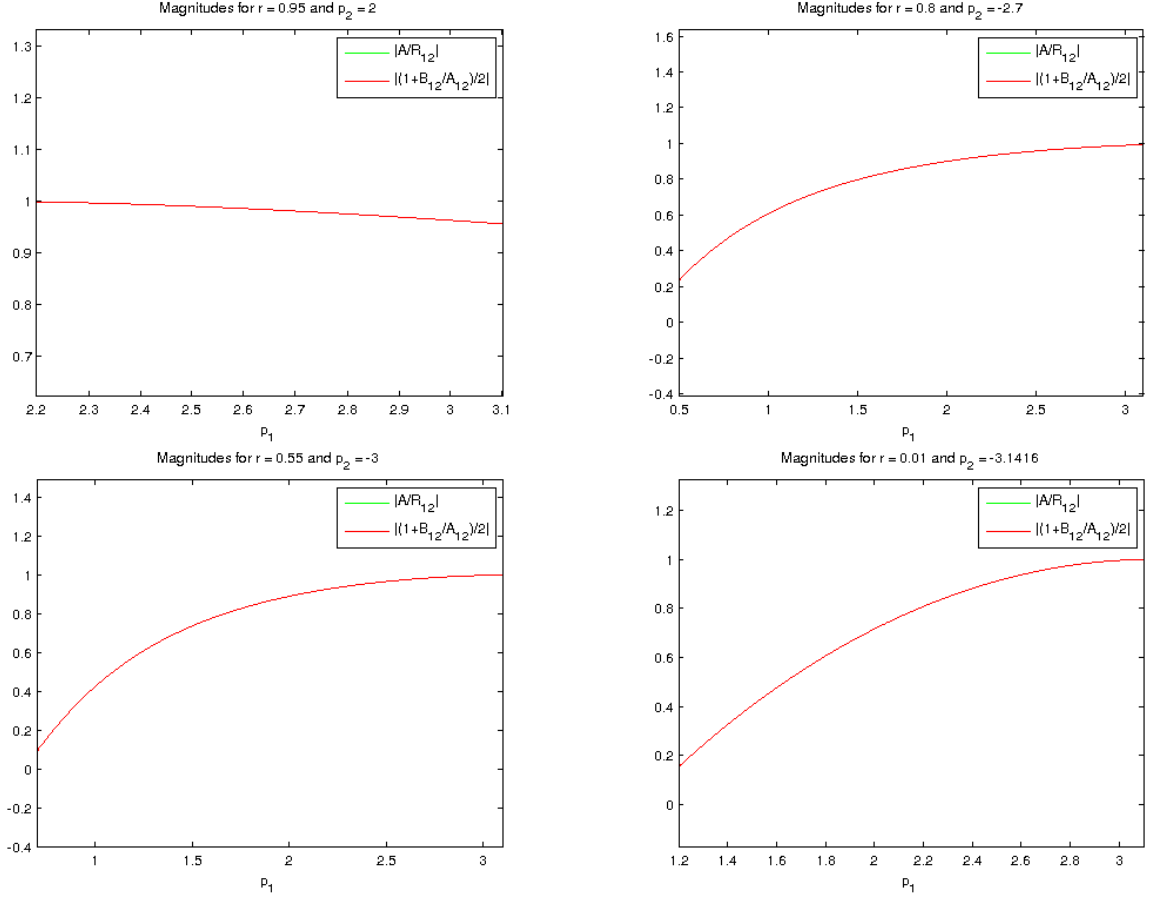
Setting $p_2 = 0$, one quickly checks that (F.13) and (F.14) reduce to (F.9) and (F.10).

Now, use (F.13) and (F.14) to compare the two sets of complex numbers $\frac{A}{R_{12}}$ and $\frac{1}{2} \left(1 + \frac{B_{12}^R}{A_{12}^R}\right) \Big|_{1\text{-loop}}$.

F.2.3 Numerical plots for the magnitudes

The following numerical plots compare the magnitudes $\frac{1}{2} \left|1 + \frac{B_{12}}{A_{12}}\right|$ and $\left|\frac{A}{R_{12}}\right|$ for the set of values $\{r = 0.01, p_2 = -3.1416\}$, $\{r = 0.55, p_2 = -3\}$, $\{r = 0.8, p_2 = -2.7\}$, $\{r = 0.95, p_2 = 2\}$, $\{r = 0.99, p_2 = 1.308\}$ and $\{r = 1, p_2 = 1\}$. The range of the initial momentum of the bulk magnon p_1 is shown on the horizontal axis of the plots.

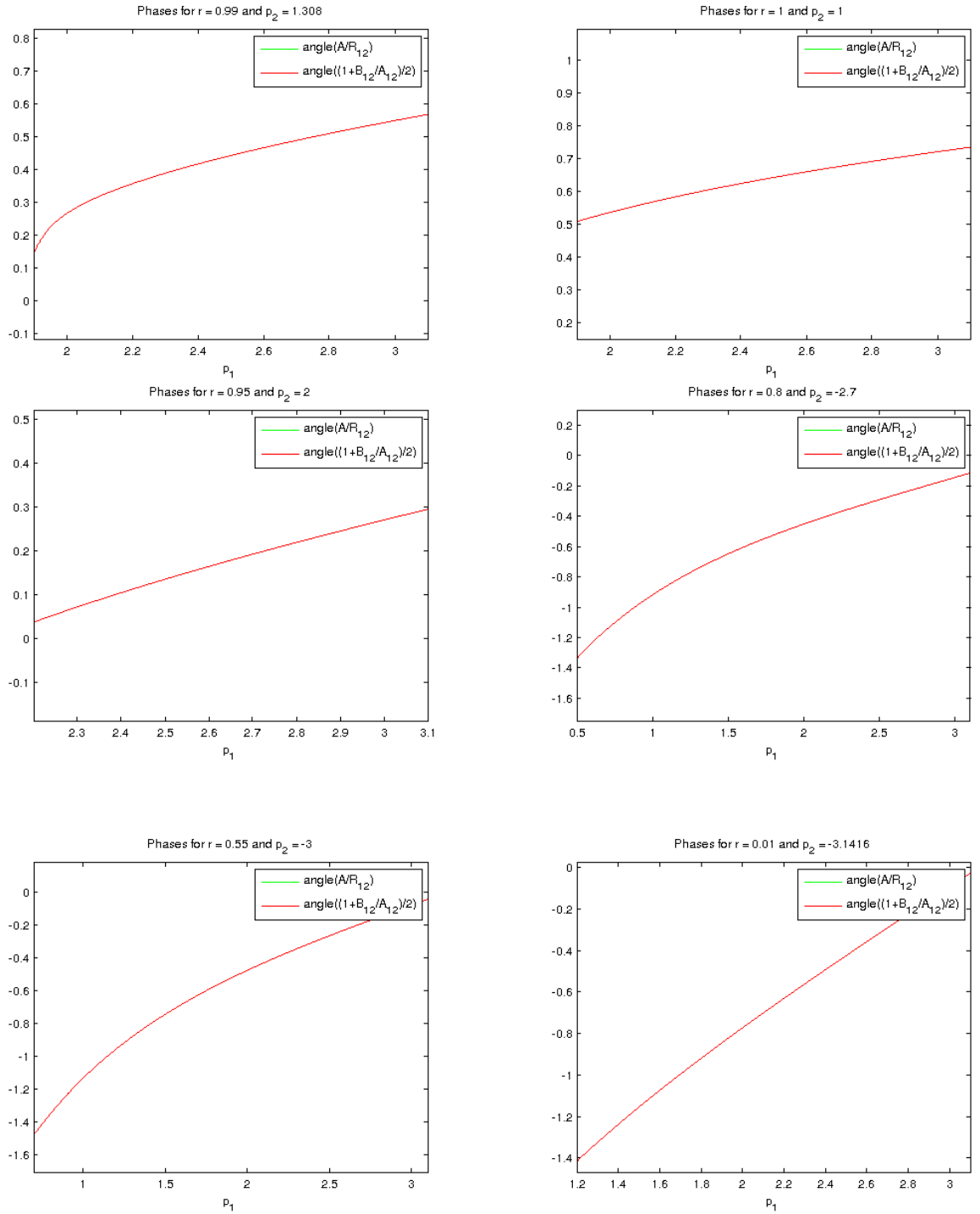




F.2.4 Numerical plots for the phase differences

Similarly, the following numerical plots compare the phases of $\frac{1}{2} \left(1 + \frac{B_{12}}{A_{12}} \right)$ and $\left(\frac{A}{R_{12}} \right)$ for the set of values where $\{r = 0.01, p_2 = -3.1416\}$, $\{r = 0.55, p_2 = -3\}$, $\{r = 0.8, p_2 = -2.7\}$, $\{r = 0.95, p_2 = 2\}$, $\{r = 0.99, p_2 = 1.308\}$ and $\{r = 1, p_2 = 1\}$. The range of the initial momentum of the bulk magnons p_1 appear on the horizontal axis.

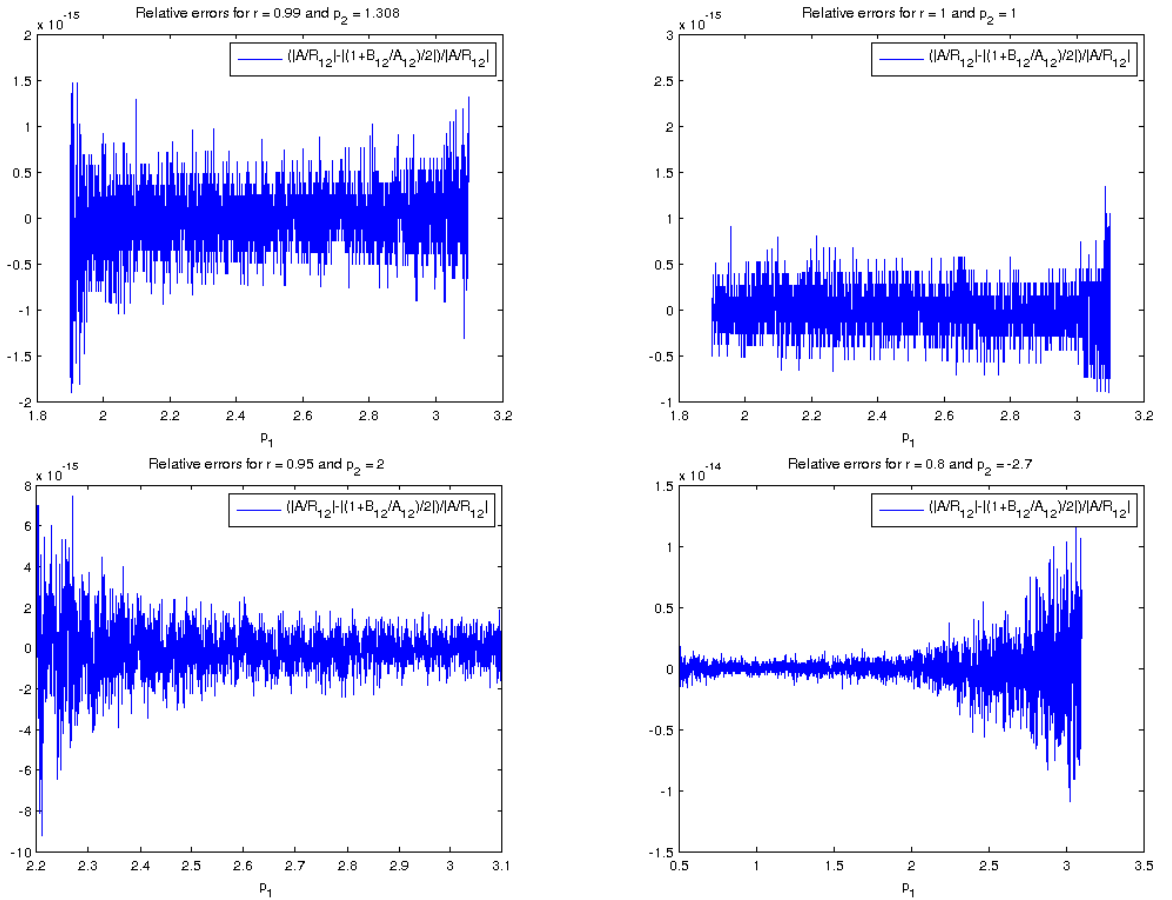
APPENDIX F. ANOTHER CHECK OF THE S -MATRIX



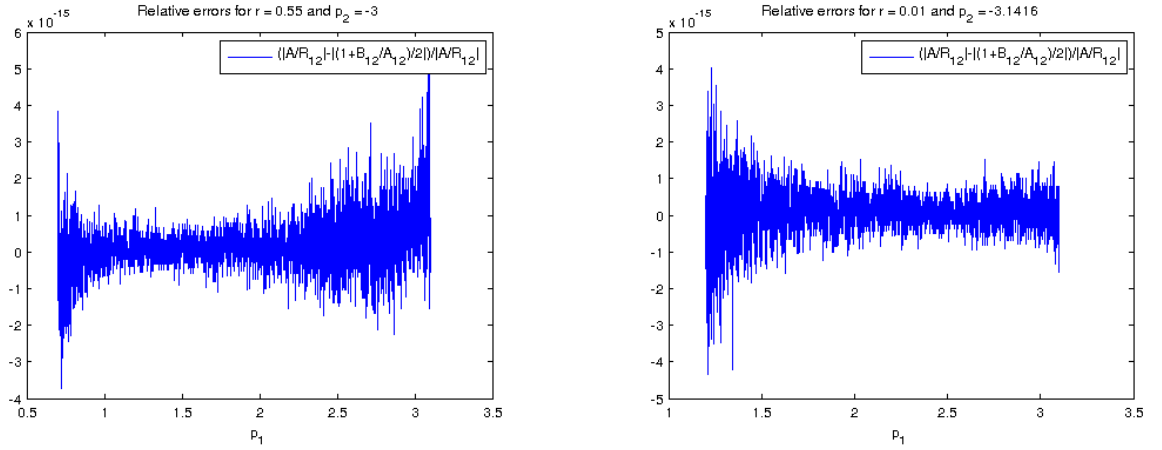
F.2.5 Relative errors in the magnitudes

We have studied the relative errors $\frac{\left| \frac{A}{R_{12}} \right| - \left| \left(1 + \frac{B_{12}}{A_{12}}\right)^{\frac{1}{2}} \right|}{\left| \frac{A}{R_{12}} \right|}$ for each of the above cases.

The size of the errors are due to the numerical precision offered by matlab. To see this, one can change the numerical precision. The relative errors decrease as we increase numerical precision. For example, fixing the matlab precision to be 10^{-16} we find the following numerical plots.



APPENDIX F. ANOTHER CHECK OF THE S -MATRIX



In this way, we confirm the S -matrix describing the scattering of a bulk and a boundary magnon.

Appendix G

No integrability

The (boundary) Yang-Baxter equation makes use of the boundary magnon (B) and two bulk magnons (1 and 2). For our purposes, it is enough to track only scattering between bulk and boundary magnons. The Yang-Baxter equation requires equality between the scattering¹ which takes $B + 1 \rightarrow B' + 1'$ and then $B' + 2 \rightarrow \tilde{B}' + \tilde{2}$ and the scattering which $B + 2 \rightarrow B' + 2'$ and then $B' + 1 \rightarrow \tilde{B}' + \tilde{1}$. For the first scattering, given the initial momenta p_1, p_2, p_B we need to solve

$$\begin{aligned} & \sqrt{1 + 8\lambda \sin^2 \frac{p_1}{2}} + \sqrt{1 + 8\lambda \left((1+r)^2 + 4r \sin^2 \frac{p_B}{2} \right)} \\ &= \sqrt{1 + 8\lambda \sin^2 \frac{p_1}{2}} + \sqrt{1 + 8\lambda \left((1+r)^2 + 4r \sin^2 \frac{p_B}{2} \right)} \end{aligned} \quad (\text{G.1})$$

$$\begin{aligned} & \sqrt{1 + 8\lambda \sin^2 \frac{p_2}{2}} + \sqrt{1 + 8\lambda \left((1+r)^2 + 4r \sin^2 \frac{q}{2} \right)} \\ &= \sqrt{1 + 8\lambda \sin^2 \frac{k_2}{2}} + \sqrt{1 + 8\lambda \left((1+r)^2 + 4r \sin^2 \frac{k_B}{2} \right)} \end{aligned} \quad (\text{G.2})$$

¹There are some bulk magnon scatterings that we are ignoring as they don't affect our argument.

for the final momenta k_1, k_2, k_B . For the second scattering we need to solve

$$\begin{aligned} & \sqrt{1 + 8\lambda \sin^2 \frac{p_2}{2}} + \sqrt{1 + 8\lambda \left((1+r)^2 + 4r \sin^2 \frac{p_B}{2} \right)} \\ &= \sqrt{1 + 8\lambda \sin^2 \frac{l_2}{2}} + \sqrt{1 + 8\lambda \left((1+r)^2 + 4r \sin^2 \frac{s}{2} \right)} \end{aligned} \quad (\text{G.3})$$

$$\begin{aligned} & \sqrt{1 + 8\lambda \sin^2 \frac{p_1}{2}} + \sqrt{1 + 8\lambda \left((1+r)^2 + 4r \sin^2 \frac{s}{2} \right)} \\ &= \sqrt{1 + 8\lambda \sin^2 \frac{l_1}{2}} + \sqrt{1 + 8\lambda \left((1+r)^2 + 4r \sin^2 \frac{l_B}{2} \right)} \end{aligned} \quad (\text{G.4})$$

for the final momenta l_1, l_2, l_B . It is simple to check that, in general, $k_1 \neq l_1$, $k_2 \neq l_2$ and $k_B \neq l_B$, so the two scatterings cant possibly be equal.

Appendix H

Double Coset background

The double coset ansatz was formulated in [20] by diagonalizing the one loop dilatation operator. In this section we will review those aspects of [20] that are crucial for our study

At the most basic level, the double coset ansatz follows from the fact that there are two ways to decompose $V_p^{\otimes m}$. To start, refine $V_p^{\otimes m}$ by the $U(1)^p$ charges measured by E_{ii} , as follows:

$$V_p = \bigoplus_{i=1}^p V_i \quad (\text{H.1})$$

The vector space V_i is a one-dimensional space. It is spanned by the eigenstate of E_{ii} with eigenvalue one. Consequently if $v_i \in V_i$ we have

$$\begin{aligned} E_{ii}v_j &= \delta_{ij}v_i \\ E_{ij}v_k &= \delta_{jk}v_i. \end{aligned} \quad (\text{H.2})$$

In the restricted Schur polynomial construction of [16] for long rows, a state in V_i corresponds to a Y -box in the i th row. The $U(1)$ charges of a restricted Schur polynomial can be collected into the vector \vec{m} , which corresponds to a vector with m_1 copies of v_1 , m_2 copies of v_2 etc.

$$|\bar{v}, \vec{m}\rangle = |v_1^{\otimes m_1} \otimes v_2^{\otimes m_2} \otimes \cdots \otimes v_p^{\otimes m_p}\rangle. \quad (\text{H.3})$$

A general state with these charges is given by acting with a permutation

$$|v_\sigma\rangle = \sigma |v_1^{\otimes m_1} \otimes v_2^{\otimes m_2} \otimes \cdots \otimes v_p^{\otimes m_p}\rangle. \quad (\text{H.4})$$

where

$$\sigma |v_{i_1} \otimes v_{i_2} \otimes \cdots \otimes v_{i_p}\rangle = |v_{i_{\sigma(1)}} \otimes v_{i_{\sigma(2)}} \otimes \cdots \otimes v_{i_{\sigma(p)}}\rangle. \quad (\text{H.5})$$

This description enjoys a symmetry under

$$H = S_{m_1} \times S_{m_2} \times \cdots \times S_{m_p} \quad (\text{H.6})$$

and as a consequence, not all σ give independent vectors

$$|v_\sigma\rangle = |v_{\sigma\gamma}\rangle \quad (\text{H.7})$$

if $\gamma \in H$. The restricted Schur polynomials are organized by reduction multiplicities of $U(p)$ to $U(1)^p$, which are counted by the Kotska numbers and resolved by the Gelfand-Tsetlin patterns. It is possible to prove the equality of Kotska numbers and the branching multiplicity of $S_m \rightarrow H$. This is a very direct indication that there are two possible ways to organize the local operators of the theory.

We can develop the steps above at the level of a basis for $V_p^{\otimes m}$. In terms of the branching coefficients, defined by

$$\frac{1}{|H|} \sum_{\gamma \in H} \Gamma_{ik}^{(s)}(\gamma) = \sum_{\mu} B_{i\mu}^{s \rightarrow 1_H} B_{k\mu}^{s \rightarrow 1_H} \quad (\text{H.8})$$

we have

$$\begin{aligned} |\vec{m}, s, \mu; i\rangle &\equiv \sum_j B_{j\mu}^{s \rightarrow 1_H} |v_{s,i,j}\rangle \\ &= \sum_j B_{j\mu}^{s \rightarrow 1_H} \sum_{\sigma \in S_m} \Gamma_{ij}^{(s)}(\sigma) |v_\sigma\rangle. \end{aligned} \quad (\text{H.9})$$

The μ index is a multiplicity for the reduction of S_m into H . We also have

$$\langle \vec{m}, s, \rho, j | = \frac{d_s}{m!|H|} \sum_{\sigma \in S_m, k} \langle \bar{v}, \vec{m} | \sigma^{-1} \Gamma_{jk}^{(s)}(\sigma) B_{k\rho}^{s \rightarrow 1_H}. \quad (\text{H.10})$$

which ensures the correct normalization

$$\langle \vec{m}, u, \nu; j | \vec{n}, s, \mu; i \rangle = \delta_{\vec{m}\vec{n}} \delta_{us} \delta_{ji} \delta_{\mu\nu}. \quad (\text{H.11})$$

Finally, the group-theoretic coefficients

$$C_{\mu_1 \mu_2}^s(\tau) = |H| \sqrt{\frac{d_s}{m!}} \Gamma_{kl}^{(s)}(\tau) B_{k\mu_1}^{s \rightarrow 1_H} B_{l\mu_2}^{s \rightarrow 1_H} \quad (\text{H.12})$$

provide an orthogonal transformation between double coset elements labeled by σ and the restricted Schur polynomials labeled by an irreducible representation $s \vdash m$ and a pair of multiplicities μ_1, μ_2 .

Appendix I

How to compute traces

In this appendix we will compute the traces needed to evaluate the action of $D_4^{(2)}$ in the Gauss graph basis. The generic form of the trace we need to evaluate is

$$\text{Tr}(Ap_{s\mu\nu}Bp_{u\gamma\delta}) \quad (\text{I.1})$$

with A and B any arbitrary product of the $E_{ij}^{(A)}$ s. If we are able to compute this trace, we are able to evaluate the action of any differential operator that does not change the number of Z or Y fields, on the Gauss graph operator in the displaced corners approximation. This therefore provides a general method to exploit the simplifications of the large N limit, for this class of operators.

The Fourier transform we want to consider maps between functions labeled by an irreducible representation s and a pair of multiplicity labels and functions that take values on the double coset $H \backslash S_m / H$. We can choose a permutation σ to represent each class of the coset $[\sigma]$. The transform is then

$$\tilde{f} = \sum_{s\alpha,\beta} \Gamma_s(\sigma)_{ab} B_{a\alpha}^{s \rightarrow 1_H} B_{b\beta}^{s \rightarrow 1_H} f(s, \alpha, \beta). \quad (\text{I.2})$$

For further details the reader is referred to [20].

I.1 Projector transformed

In this section we will Fourier transform the intertwining map used to define the restricted Schur polynomial. The projector that participates in the trace (I.1) can be expressed as

$$p_{u\mu\nu} = \sum_b |\vec{m}_2, u, \mu, b\rangle \langle \vec{m}_2, u, \nu, b| \quad (\text{I.3})$$

We will make use of the relations

$$\langle \vec{m}, s, \rho, j | = \frac{d_s}{m!|H|} \sum_{\sigma \in S_m, k} \langle \bar{v}, \vec{m} | \sigma^{-1} \Gamma_{jk}^{(s)}(\sigma) B_{k\rho}^{s \rightarrow 1_H}. \quad (\text{I.4})$$

and

$$|\vec{m}, s, \tau, i\rangle = \sum_{\sigma \in S_m, k} \Gamma_{ik}^{(s)}(\sigma) B_{k\tau}^{s \rightarrow 1_H} \sigma |\bar{v}, \vec{m}\rangle, \quad (\text{I.5})$$

as well as

$$\langle \bar{v}, \vec{m} | \sigma | \bar{v}, \vec{m} \rangle = \sum_{\gamma \in H} \delta(\sigma\gamma) \quad (\text{I.6})$$

and

$$\sum_{\rho} B_{c\rho}^{s \rightarrow 1_H} B_{d\rho}^{s \rightarrow 1_H} = \frac{1}{|H|} \sum_{\gamma \in H} \Gamma_{cd}^{(s)}(\gamma), \quad (\text{I.7})$$

We will use the notation $|v_{\sigma}\rangle = \sigma |\bar{v}\rangle$. It is then simple to show that

$$\begin{aligned} \sum_{s\mu\nu lm} p_{s\mu\nu} B_{l\mu}^{s \rightarrow 1_H} B_{m\nu}^{s \rightarrow 1_H} \Gamma_{ml}^{(s)}(\sigma) &= \sum_{s\mu\nu lma} |\vec{m}, s, \mu, a\rangle \langle \vec{m}, s, \nu, a| B_{l\mu}^{s \rightarrow 1_H} B_{m\nu}^{s \rightarrow 1_H} \Gamma_{ml}^{(s)}(\sigma) \\ &= \frac{1}{|H|^3} \sum_{\tau, \psi \in S_m} \sum_{\gamma_1, \gamma_2 \in H} |\bar{v}_{\tau}\rangle \langle \bar{v}_{\psi}| \delta(\psi^{-1} \tau \gamma_2 \sigma \gamma_1) \end{aligned} \quad (\text{I.8})$$

This last equation implies that the permutation applied to the ket and the permutation applied to the bra are related by multiplication by a permutation representing the double coset element.

I.2 Summing over H

We consider an intertwining map $p_{s\mu\nu}$ built on the state $|\bar{v}_1, \vec{m}_1\rangle$ with symmetry group H_1 and intertwining map $p_{t\gamma\delta}$ built on the state $|\bar{v}_2, \vec{m}_2\rangle$ with symmetry

group H_2 . We make no assumptions about H_1 and H_2 . In general they will be different groups and hence we Fourier transform $p_{s\mu\nu}$ and $p_{t\gamma\delta}$ to different double cosets. Using the result obtained above, the Fourier transform of

$$\text{Tr}(Ap_{s\mu\nu}Bp_{u\gamma\delta}) \quad (\text{I.9})$$

is

$$\begin{aligned} T &= \frac{1}{|H_1|^3|H_2|^3} \sum_{\gamma_i \in H_i} \sum_{\tau_i \in H_i} \sum_{\psi_i \in S_m} \langle v_2 | \gamma_2 \sigma_2^{-1} \tau_2 \psi_2^{-1} A \psi_1 | v_1 \rangle \langle v_1 | \gamma_1 \sigma_1^{-1} \tau_1 \psi_1^{-1} B \psi_2 | v_2 \rangle \\ &= \frac{1}{|H_1|^3|H_2|^3} \sum_{\gamma_i \in H_i} \sum_{\tau_i \in H_i} \sum_{\psi_i \in S_m} \langle v_2 | \gamma_2 \sigma_2^{-1} \tau_2 \psi_2^{-1} A \psi_1 | v_1 \rangle \langle v_2 | \psi_2^{-1} B^T \psi_1 \tau_1 \sigma_1 \gamma_1 | v_1 \rangle. \end{aligned} \quad (\text{I.10})$$

To get to the last line, we used the fact that the matrix element $\langle v_1 | \gamma_1 \sigma_1^{-1} \tau_1 \psi_1^{-1} B \psi_2 | v_2 \rangle$ is a real number and the permutations are represented by matrices with real elements. To make the discussion concrete, it is useful to make a specific choice for A and B . This will allow us to illustrate the argument in a very concrete setting. In the end we will state the general result. Choose, for example,

$$A = E_{ki}^{(1)} E_{ij}^{(2)} \quad B = E_{jl}^{(1)} E_{lk}^{(2)} \quad (\text{I.11})$$

Using the facts that

$$\begin{aligned} \gamma |v_1\rangle &= |v_1\rangle \quad \forall \gamma \in H_1 \\ \beta |v_2\rangle &= |v_2\rangle \quad \forall \beta \in H_2 \\ \psi^{-1} E_{qr}^{(a)} \psi &= E_{qr}^{\psi(a)} \quad \forall \psi \in S_m \end{aligned} \quad (\text{I.12})$$

we readily find

$$\begin{aligned} T &= \frac{1}{|H_1||H_2|} \sum_{\psi_i \in S_m} \langle v_2 | \sigma_2^{-1} E_{ki}^{\psi_2(1)} E_{ij}^{\psi_2(2)} \psi_1 | v_1 \rangle \langle v_1 | E_{lj}^{\psi_2(1)} E_{lk}^{\psi_2(2)} \psi_1 \sigma_1 | v_2 \rangle \\ &= \frac{1}{|H_1||H_2|} \sum_{\psi_i \in S_m} \langle v_2 | \sigma_2^{-1} \psi_2^{-1} A \psi_2 \psi_1 | v_1 \rangle \langle v_2 | \psi_2^{-1} B^T \psi_2 \psi_1 \sigma_1 \gamma_1 | v_1 \rangle. \end{aligned} \quad (\text{I.13})$$

where on the last line we have written the general result. Our next task is to compute the sums over ψ_1 and ψ_2 .

I.3 Summing over S_m

In this subsection we consider two increasing difficult examples before we state the general result. The first example is closely related to the trace needed to obtain the one loop dilatation operator. Since we know the result of this trace, this example is a nice test of our ideas. The second example is a simple but nontrivial example which will illustrate how the general case works. In the following section we will quote the result for the general case.

I.3.1 First evaluation

Choose $A = E_{ab}^{(1)}$ and $B = E_{ba}^{(1)}$ to get

$$\begin{aligned} T &= \frac{1}{|H_1||H_2|} \sum_{\psi_i \in S_m} \langle v_2 | \sigma_2^{-1} E_{ab}^{\psi_2(1)} \psi_1 | v_1 \rangle \langle v_1 | E_{ab}^{\psi_2(1)} \psi_1 \sigma_1 | v_2 \rangle \\ &= \frac{1}{|H_1||H_2|} \sum_{\psi_i \in S_m} \langle v_1 | \psi_1^{-1} E_{ba}^{\psi_2(1)} \sigma_2 | v_2 \rangle \langle v_2 | E_{ab}^{\psi_2(1)} \psi_1 \sigma_1 | v_1 \rangle. \end{aligned} \quad (\text{I.14})$$

We must turn a b vector in $|v_1\rangle$ into an a vector (and possibly permute) to get $|v_2\rangle$. Since the ordering of the slots in $|v_1\rangle$ and $|v_2\rangle$ is arbitrary, we can remove this possible permutation by declaring

$$|v_2\rangle = E_{ab}^{(1)}|v_1\rangle \quad |v_1\rangle = E_{ba}^{(1)}|v_2\rangle. \quad (\text{I.15})$$

Thus [in the computation below we denote by S_a^1 (S_a^2) the set of all slots in $|v_1\rangle(|v_2\rangle)$ that are filled with an a vector]

$$\begin{aligned} T &= \frac{1}{|H_1||H_2|} \sum_{\psi_i \in S_m} \langle v_1 | \psi_1^{-1} E_{ba}^{\psi_2(1)} \sigma_2 E_{ab}^{(1)} | v_1 \rangle \langle v_1 | E_{ba}^{(1)} E_{ab}^{\psi_2(1)} \psi_1 \sigma_1 | v_1 \rangle \\ &= \frac{1}{|H_1||H_2|} \sum_{\psi_i \in S_m} \langle v_1 | \psi_1^{-1} \sigma_2 E_{ba}^{\sigma_2 \psi_2(1)} \sigma_2 E_{ab}^{(1)} | v_1 \rangle \langle v_1 | E_{ba}^{(1)} E_{ab}^{\psi_2(1)} \psi_1 \sigma_1 | v_1 \rangle \\ &= \frac{1}{|H_1||H_2|} \sum_{\psi_i \in S_m} \sum_{\gamma_i \in H_1} \delta(\gamma_1 \psi_1^{-1} \sigma_2(1, \sigma_2 \psi_2(1))) \delta(\gamma_2 \sigma_1^{-1} \psi_1^{-1}(1, \psi_2(1))) \\ &\quad \times \sum_{x \in S_a^2} \delta(\sigma_2 \psi_2(1), x) \sum_{y \in S_a^2} \delta(\psi_2(1), y) \\ &= \frac{1}{|H_1||H_2|} \sum_{\psi_i \in S_m} \sum_{\gamma_i \in H_1} \delta(\gamma_1 \sigma_1 \gamma_2(1, \psi_2(1)) \sigma_2(1, \sigma_2 \psi_2(1))) \\ &\quad \times \sum_{x \in S_a^2} \delta(\sigma_2 \psi_2(1), x) \sum_{y \in S_a^2} \delta(\psi_2(1), y) \end{aligned} \quad (\text{I.16})$$

Now consider the final sum over ψ_2 , $\psi_2(1)$ is the start point of an oriented edge in Gauss graph σ_2 , $\sigma_2\psi_2(1)$ is the end point of the same edge. The delta functions on the last line ensure that both endpoints of this string are attached to node a in the Gauss graph. This is swapped with the edge labeled 1 (i.e. the edge in the first slot) and compared to σ_1 . According to (I.15), the edge in the first slot of $|v_1\rangle$ is attached to node b . Thus the above sum is ensuring that when a closed loop on node a of σ_2 is removed and reattached to node b of σ_2 we get σ_1 . The above sum is nonzero only when σ_1 and σ_2 are related in this way. The deltas only fix $\psi_2(1)$, so summing over S_m the remaining “unfixed” piece of ψ_2 gives $(m-1)!$. The first delta will, as usual, give the norm of Gauss graph σ_1 and we will get a nonzero contribution whenever $\psi_2(1)$ is one of the values in S_a^2 . There are $n_{aa}(\sigma_2)$ possible values. Thus, when T is nonzero it takes the value

$$T = (m-1)! n_{aa}(\sigma_2) |O(\sigma_1)|^2 \quad (\text{I.17})$$

where we have assumed that both σ_1 and σ_2 have a total of p nodes and we denote the number of oriented line segments stretching from node k to node l of σ by $n_{kl}(\sigma)$. We have denoted the “norm” of the Gauss graph operator by $|O(\sigma_1)|^2$. This is the value of the two point function of the Gauss operator

$$|O(\sigma_1)|^2 = \prod_{i,j=1}^p n_{ij}(\sigma_1)! = \langle O_{R,r}(\sigma_1)^\dagger O_{R,r}(\sigma_1) \rangle. \quad (\text{I.18})$$

The value of the trace (I.17) is in perfect agreement with the known result [?].

I.4 Second evaluation

For the second example we consider, we choose

$$A = E_{ki}^{(1)} E_{ij}^{(2)} \quad B = E_{jl}^{(1)} E_{lk}^{(2)} \quad (\text{I.19})$$

There is some freedom in the placement of the indices on A and B . To see why this is the case, recall that we are evaluating the Fourier transform of

$$\text{Tr}(Ap_{s\mu\nu}Bp_{u\gamma\delta}) \quad (\text{I.20})$$

The intertwining maps $p_{s\mu\nu}$ and $p_{u\gamma\delta}$ commute with any element of S_m . Consequently we have

$$\begin{aligned}\text{Tr}(Ap_{s\mu\nu}Bp_{u\gamma\delta}) &= \text{Tr}(A\sigma\sigma^{-1}p_{s\mu\nu}Bp_{u\gamma\delta}) \\ &= \text{Tr}(A\sigma p_{s\mu\nu}\sigma^{-1}Bp_{u\gamma\delta})\end{aligned}\quad (\text{I.21})$$

where σ is any element in S_m . Choosing $\sigma = (12)$ and using the representation $(12) = E_{ab}^{(1)}E_{ba}^{(2)}$ where a and b are summed from 1 to p , as well as the product rule

$$E_{ab}^{(A)}E_{cd}^{(B)} = E_{cd}^{(B)}E_{ab}^{(A)} \quad A \neq B \quad E_{ab}^{(A)}E_{cd}^{(A)} = \delta_{bc}E_{ad}^{(A)} \quad (\text{I.22})$$

we find

$$A(12) = E_{ki}^{(1)}E_{ij}^{(2)}(12) = E_{ki}^{(1)}E_{ij}^{(2)}E_{ab}^{(1)}E_{ba}^{(2)} = E_{kj}^{(1)}E_{ii}^{(2)} \quad (\text{I.23})$$

$$(12)B = (12)E_{jl}^{(1)}E_{lk}^{(2)} = E_{ab}^{(1)}E_{ba}^{(2)}E_{jl}^{(1)}E_{lk}^{(2)} = E_{ll}^{(1)}E_{jk}^{(2)} \quad (\text{I.24})$$

This implies that we can rather consider $A = E_{kj}^{(1)}E_{ii}^{(2)}$ and $B = E_{ll}^{(1)}E_{jk}^{(2)}$ without changing the value of the trace. In this case we have (argue as we did above and use $|v_2\rangle = E_{kj}^{(1)}|v_1\rangle$)

$$\begin{aligned}T &= \frac{1}{|H_1||H_2|} \sum_{\psi_i \in S_m} \langle v_2 | \sigma_2^{-1} E_{kj}^{\psi_2(1)} E_{ii}^{\psi_2(2)} \psi_1 | v_1 \rangle \langle v_2 | E_{ll}^{\psi_2(1)} E_{kj}^{\psi_2(2)} \psi_1 \sigma_1 | v_1 \rangle \\ &= \frac{1}{|H_1||H_2|} \sum_{\psi_i \in S_m} \langle v_1 | \psi_1^{-1} E_{jk}^{\psi_2(1)} E_{ii}^{\psi_2(2)} \sigma_2 | v_2 \rangle \langle v_2 | E_{ll}^{\psi_2(1)} E_{kj}^{\psi_2(2)} \psi_1 \sigma_1 | v_1 \rangle.\end{aligned}\quad (\text{I.25})$$

Notice that when $E_{ii}^{\psi_2(2)}$ acts on $|v_2\rangle$, it does not change the identity of any of the vectors appearing in $|v_2\rangle$. On the other hand, $E_{jk}^{\psi_2(1)}$ will turn an e_k into an e_j . Thus, again up to an arbitrary permutation which we can always remove, we must have

$$|v_2\rangle = E_{kj}^{(1)}|v_1\rangle \quad (\text{I.26})$$

The trace now takes the value

$$\begin{aligned}
 T &= \frac{1}{|H_1||H_2|} \sum_{\psi_i \in S_m} \langle v_1 | \psi_1^{-1} E_{kj}^{\psi_2(1)} E_{ii}^{\psi_2(2)} \sigma_2 E_{kj}^{(1)} | v_1 \rangle \langle v_1 | E_{jk}^{(1)} E_{ll}^{\psi_2(1)} E_{kj}^{\psi_2(2)} \psi_1 \sigma_1 | v_1 \rangle \\
 &= \frac{1}{|H_1||H_2|} \sum_{\psi_i \in S_m} \langle v_1 | \psi_1^{-1} \sigma_2 E_{kj}^{\sigma_2 \psi_2(1)} E_{ii}^{\sigma_2 \psi_2(2)} E_{kj}^{(1)} | v_1 \rangle \langle v_1 | E_{jk}^{(1)} E_{ll}^{\psi_2(1)} E_{kj}^{\psi_2(2)} \psi_1 \sigma_1 | v_1 \rangle \\
 &= \frac{1}{|H_1||H_2|} \sum_{\psi_i \in S_m} \sum_{\gamma_i \in H_1} \delta(\gamma_1 \psi_1^{-1} \sigma_2(\sigma_2 \psi_2(1), 1)) \delta(\gamma_2 \sigma_1^{-1} \psi_1^{-1}(1, \psi_2(2))) \\
 &\quad \sum_{x \in S_l^2} \delta(\psi_2(1), x) \sum_{y \in S_k^2} \delta(\psi_2(2), y) \sum_{W \in S_k^2} \delta(\sigma_2 \psi_2(1), w) \sum_{v \in S_i^2} \delta(\sigma_2 \psi_2(2), v) \\
 &= \frac{1}{|H_1||H_2|} \sum_{\psi_i \in S_m} \sum_{\gamma_i \in H_1} \delta(\gamma_1 \sigma_1 \gamma_2(1, \psi_2(1)) \sigma_2(1, \sigma_2 \psi_2(1))) \\
 &\quad \sum_{x \in S_l^2} \delta(\psi_2(1), x) \sum_{y \in S_k^2} \delta(\psi_2(2), y) \sum_{W \in S_k^2} \delta(\sigma_2 \psi_2(1), w) \sum_{v \in S_i^2} \delta(\sigma_2 \psi_2(2), v) \\
 &= \frac{(m-2)!}{|H_1||H_2|} n_{lk}(\sigma_2) n_{ki}(\sigma_2) \prod_{q=1}^p n_{qq}(\sigma_1)! \prod_{r,s=1, r \neq s}^p n_{rs}(\sigma_1)! \tag{I.27}
 \end{aligned}$$

whenever it is nonzero.

I.5 General result

Recall that both T and R have p long rows or columns. For the general result we consider

$$\begin{aligned}
 &\sum s_{\mu\nu} m \sum_{u\gamma\delta np} \text{Tr}(Ap_{s\mu\nu}Bp_{u\gamma\delta}) B_{m\mu}^{s \rightarrow 1_H} B_{l\nu}^{s \rightarrow 1_H} \Gamma_{ml}^{(s)}(\sigma_1) B_{p\gamma}^{u \rightarrow 1_H} B_{n\delta}^{u \rightarrow 1_H} \Gamma_{pn}^{(u)}(\sigma_2) \\
 &= \frac{1}{|H_1||H_2|} \sum_{\psi_i \in S_m} \langle v_2 | \sigma_2^{-1} (\psi_2^{-1} A \psi_2) \psi_1 | v_1 \rangle \langle v_2 | (\psi_2^{-1} B^T \psi_2) \psi_1 \sigma_1 \gamma_1 | v_1 \rangle \tag{I.28}
 \end{aligned}$$

where A and B are each products of a collection of the $E_{ab}^{(a)}$ s with $1 \leq a, b \leq p$ and $1 \leq \alpha \leq m$. We say that $E_{ab}^{(a)}$ occupies slot α . The sum over ψ_2 sums over the possible choices for the slots into which we place the factors of $E_{ab}^{(a)}$ in A and B . Thus, the specific slots chosen for the factors in A and B are arbitrary - we must simply respect the relative ordering of factors in A and B , i.e. factors sharing the same slot in one labeling share the same slot in all labelings. The sum over ψ_1 ensures that the relative labeling of the vectors appearing in $|v_1\rangle$ and $|v_2\rangle$ is arbitrary. Thus, the specific labeling of the directed edges in the

Gauss graph is arbitrary which ensures that the above sum is indeed defined on the relevant double cosets to which σ_1 and σ_2 belong. There are two pieces of information that we need to read from σ_1 and σ_2 , A and B :

- (1) When is the sum nonzero?
- (2) What is the value of the sum?

It is simplest to begin with the second question first. Towards this end, consider the expressions for A and B . After using the algebra for the $E_{ab}^{(a)}$ if needed, we know that at most a single $E_{ab}^{(a)}$ acts per slot in both A and B . By inserting factors of

$$\sum_{a=1}^p = E_{aa}^{(a)} = \mathbf{1} \quad (\text{I.29})$$

if necessary, we can ensure that the same set of occupied slots appears in A and B . For concreteness, assume that q slots are occupied in both. Use i_α^r (i_α^c) to denote the row (column) indices of the E_{ab} in the α th slot in B and use j_α^r (j_α^c) to denote the row (column) indices of the E_{ab} in the α th slot in A . Thanks to the lessons we have learned from the examples treated above, when the sum is nonzero it is given by

$$\begin{aligned} & \frac{1}{|H_1||H_2|} \sum_{\psi_i \in S_m} \langle v_2 | \sigma_2^{-1} (\psi_2^{-1} A \psi_2) \psi_1 | v_1 \rangle \langle v_2 | (\psi_2^{-1} B^T \psi_2) \psi_1 \sigma_1 \gamma_1 | v_1 \rangle \\ &= \frac{(m-q)! |O(\sigma_1)|^2}{|H_1||H_2|} \prod_{\alpha=1}^q n_{i_\alpha^c j_\alpha^r}(\sigma_2). \end{aligned} \quad (\text{I.30})$$

If any particular $n_{ij}(\sigma_2)$ appears more than once, each new factor in the product is to be reduced by 1. For example, $n_{12}(\sigma_2)^3$ would be replaced by $n_{12}(\sigma_2)(n_{12}(\sigma_2) - 1)(n_{12}(\sigma_2) - 2)$. By taking the transpose of (I.30), the value of the sum is not changed because it is a real number. However, the roles of σ_1 and σ_2 , as well as of A and B are reversed on the left-hand side of (I.30). Consequently, we must also have

$$\begin{aligned} & \frac{1}{|H_1||H_2|} \sum_{\psi_i \in S_m} \langle v_2 | \sigma_2^{-1} (\psi_2^{-1} A \psi_2) \psi_1 | v_1 \rangle \langle v_2 | (\psi_2^{-1} B^T \psi_2) \psi_1 \sigma_1 \gamma_1 | v_1 \rangle \\ &= \frac{(m-q)! |O(\sigma_2)|^2}{|H_1||H_2|} \prod_{\alpha=1}^q n_{j_\alpha^r i_\alpha^c}(\sigma_1). \end{aligned} \quad (\text{I.31})$$

The equality of (I.30) and (I.31) defines our delta function. We find that $\delta_{AB}([\sigma_1], [\sigma_2]) = 1$ if

$$\frac{(m-q)!|O(\sigma_1)|^2}{|H_1||H_2|} \prod_{\alpha=1}^q n_{i_\alpha^c j_\alpha^r}(\sigma_2) = \frac{(m-q)!|O(\sigma_2)|^2}{|H_1||H_2|} \prod_{\alpha=1}^q n_{j_\alpha^r i_\alpha^c}(\sigma_1) \quad (\text{I.32})$$

and it is zero otherwise.

We will sketch how the general result is proved. First, even if A and B straddle $q \leq m$ slots, by using (I.29) we can always introduce further $E^{(a)}$ s so that all m slots are straddled. Thus, without loss of generality we can now focus on the $q = m$ case. In this case, it is easy to prove that if $\prod_{\alpha=1}^q n_{i_\alpha^c j_\alpha^r}(\sigma_2)$ is nonzero, it is given by

$$\prod_{\alpha=1}^q n_{i_\alpha^c j_\alpha^r}(\sigma_2) = |O(\sigma_2)|^2 \quad (\text{I.33})$$

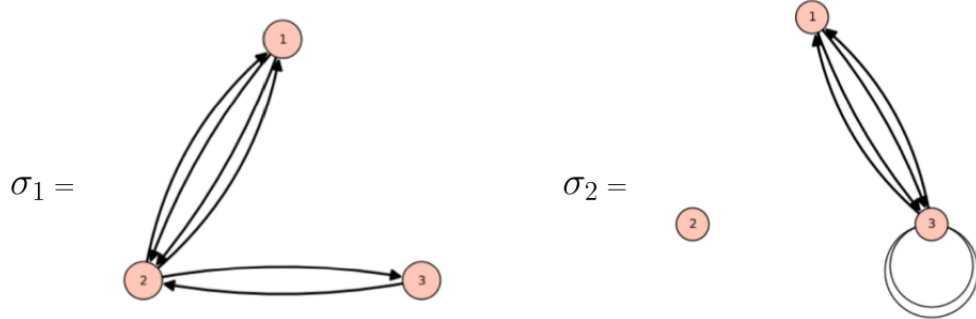
which again proves the general result.

I.6 Illustration of the general result

To illustrate the formula derived in the previous section consider computing the trace for the case that

$$\begin{aligned} A &= E_{2\mathbf{3}}^{(1)} E_{2\mathbf{3}}^{(2)} E_{1\mathbf{1}}^{(3)} E_{1\mathbf{3}}^{(4)} E_{3\mathbf{1}}^{(5)} E_{2\mathbf{3}}^{(6)} \\ B &= E_{\mathbf{3}1}^{(1)} E_{\mathbf{1}1}^{(2)} E_{\mathbf{3}2}^{(3)} E_{\mathbf{1}2}^{(4)} E_{\mathbf{3}2}^{(5)} E_{\mathbf{3}3}^{(6)} \end{aligned} \quad (\text{I.34})$$

For our example we have $m = 6$, $q = 6$ and $p = 3$, so that $(m-q)! = 1$. We choose σ_1 and σ_2 as illustrated below



From these Gauss graphs we easily read off $H_1 = S_2 \times S_3$ and $H_2 = S_4 \times S_2$. Consequently $|H_1| = 12$ and $|H_2| = 48$. If we choose the permutation

$$\sigma_1 = (13)(24)(56) \in H_1 \setminus S_6 / H_1 \quad (\text{I.35})$$

to represent the first Gauss graph, then we can choose the first factor in H_1 to permute 1 and 2 and the second factor to permute 3, 4 and 5. If we choose the permutation

$$\sigma_1 = (12)(45) \in H_2 \setminus S_6 / H_2 \quad (\text{I.36})$$

to represent the second Gauss graph, then we can choose the first factor to permute 2 and 5 and the last factor to permute 1, 3, 4 and 6.

From the row indices of A given by the ordered set $\{3, 1, 3, 1, 3, 3\}$ and the column indices of B given by the ordered set $\{3, 3, 1, 3, 1, 3\}$, we read off

$$\begin{aligned} \prod_{\alpha=1}^q n_{i_\alpha^c j_\alpha^r}(\sigma_2) &= n_{33}(\sigma_2) n_{31}(\sigma_2) n_{13}(\sigma_2) n_{31}(\sigma_2) n_{13}(\sigma_2) n_{33}(\sigma_2) \\ &\rightarrow n_{33}(\sigma_2)(n_{33}(\sigma_2) - 1) n_{31}(\sigma_2)(n_{31}(\sigma_2) - 1) n_{13}(\sigma_2)(n_{13}(\sigma_2) - 1) \\ &= |O(\sigma_2)|^2 = 8. \end{aligned} \quad (\text{I.37})$$

which indicates that the sum may indeed be nonzero. From the column indices of A given by the ordered set $\{1, 1, 2, 2, 2, 3\}$ and the row indices of B given by the ordered set $\{2, 2, 1, 1, 3, 2\}$, we read off

$$\begin{aligned} \prod_{\alpha=1}^q n_{j_\alpha^r i_\alpha^c}(\sigma_1) &= n_{12}(\sigma_1) n_{12}(\sigma_1) n_{21}(\sigma_1) n_{21}(\sigma_1) n_{23}(\sigma_1) n_{32}(\sigma_1) \\ &\rightarrow n_{12}(\sigma_1)(n_{12}(\sigma_1) - 1) n_{21}(\sigma_1)(n_{21}(\sigma_1) - 1) n_{23}(\sigma_1) n_{32}(\sigma_1) \\ &= |O(\sigma_1)|^2 = 4. \end{aligned} \quad (\text{I.38})$$

which indicates that the sum is indeed nonzero. We finally obtain

$$\frac{1}{|H_1||H_2|} \sum_{\psi_i \in S_m} \langle v_2 | \sigma_2^{-1} (\psi_2^{-1} A \psi_2) \psi_1 | v_1 \rangle \langle v_2 | (\psi_2^{-1} B^T \psi_2) \psi_1 \sigma_1 \gamma_1 | v_1 \rangle = \frac{32}{|H_1||H_2|} = \frac{1}{18}. \quad (\text{I.39})$$

I.7 Results for the 2-brane 4-string system

In this section we collect the operator valued coefficients that are relevant for the example described in Sec. III. The coefficients are

$$\begin{aligned}
 A = & \delta_{RT} \left(\frac{\delta_{r'_1 t'_1}}{R_2} + \frac{\delta_{r'_2 t'_2}}{R_1} \right) \delta_{R''_{12} T''_{12}} (N + R_1 - 1)(N + R_2 - 2) \\
 & + \delta_{RT} \frac{\delta_{r'_1 t'_1}}{R_1} \delta_{R''_{11} T''_{11}} (N + R_1 - 1)(N + R_1 - 2) \\
 & + \delta_{RT} \frac{\delta_{r'_2 t'_2}}{R_2} \delta_{R''_{22} T''_{22}} (N + R_2 - 2)(N + R_2 - 3) \\
 & - 2 \left(\delta_{RT} \delta_{r'_1 t'_1} \delta_{R'_1 T'_1} (N + R_1 - 1) + \delta_{RT} \delta_{r'_2 t'_2} \delta_{R'_2 T'_2} (N + R_2 - 2) \right) \\
 & - \delta_{R_{21}^+ T} \frac{\delta_{r'_1 t'_2}}{\sqrt{R_1(R_1 - 1)}} \delta_{R''_{11} T''_{12}} (N + R_1 - 2) \sqrt{(N + R_1 - 1)(N + R_2 - 1)} \\
 & - \delta_{R_{12}^+ T} \frac{\delta_{r'_2 t'_1}}{\sqrt{R_1(R_1 + 1)}} \delta_{R''_{12} T''_{11}} (N + R_1 - 1) \sqrt{(N + R_1)(N + R_2 - 2)} \\
 & - \delta_{R_{12}^+ T} \frac{\delta_{r'_2 t'_1}}{\sqrt{R_2(R_2 - 1)}} \delta_{R''_{22} T''_{12}} (N + R_2 - 3) \sqrt{(N + R_1)(N + R_2 - 2)} \\
 & - \delta_{R_{21}^+ T} \frac{\delta_{r'_1 t'_2}}{\sqrt{R_2(R_2 + 1)}} \delta_{R''_{12} T''_{22}} (N + R_2 - 2) \sqrt{(N + R_1 - 1)(N + R_2 - 1)} \\
 & + 2 \left(\delta_{R_{12}^+ T} \delta_{r'_2 t'_1} \delta_{R'_2 T'_1} \sqrt{(N + R_1)(N + R_2 - 2)} + \delta_{R_{21}^+ T} \delta_{r'_1 t'_2} \delta_{R'_1 T'_2} \sqrt{(N + R_1 - 1)(N + R_2 - 1)} \right)
 \end{aligned} \tag{I.40}$$

$$B = -8 \delta_{r'_2 t'_1} \delta_{RT} \delta_{R''_{12} T''_{12}} \sqrt{\frac{(N + R_1 - 1)(N + R_2 - 1)}{R_1 R_2}} \tag{I.41}$$

$$\begin{aligned}
 C = & 8 \left[\delta_{R_{21}^{++} T} \frac{\delta_{r'_1 t'_2}}{\sqrt{R_1(R_2 + 2)}} \delta_{R''_{11} T''_{22}} \sqrt{(N + R_1 - 1)(N + R_1 - 2)(N + R_2 - 1)(N + R_2)} \right. \\
 & - \delta_{R_{21}^+ T} \frac{\delta_{r'_1 t'_1}}{\sqrt{R_1(R_2 + 1)}} \delta_{R''_{11} T''_{12}} (N + R_1 - 2) \sqrt{(N + R_1 - 1)(N + R_2 - 1)} \\
 & \left. - \delta_{R_{21}^+ T} \frac{\delta_{r'_2 t'_2}}{\sqrt{R_1(R_2 + 1)}} \delta_{R''_{12} T''_{22}} (N + R_2 - 2) \sqrt{(N + R_1 - 1)(N + R_2 - 1)} \right]
 \end{aligned} \tag{I.42}$$

$$\begin{aligned}
 C^\dagger = 8 & \left[\delta_{R_{12}^{++} T} \frac{\delta_{r'_2 t'_1}}{\sqrt{R_2(R_1+2)}} \delta_{R''_{22} T''_{11}} \sqrt{(N+R_1)(N+R_1+1)(N+R_2-2)(N+R_2-3)} \right. \\
 & - \delta_{R_{12}^+ T} \frac{\delta_{r'_2 t'_2}}{\sqrt{R_2, (R_1+1)}} \delta_{R''_{22} T''_{12}} (N+R_2-3) \sqrt{(N+R_1)(N+R_2-2)} \\
 & \left. - \delta_{R_{12}^+ T} \frac{\delta_{r'_1 t'_1}}{\sqrt{R_2, (R_1+1)}} \delta_{R''_{12} T''_{11}} (N+R_1-1) \sqrt{(N+R_1)(N+R_2-2)} \right]. \tag{I.43}
 \end{aligned}$$

Appendix J

Gauss graph normalization

In this Appendix we prove the formula¹

$$\langle \mathcal{O}^\dagger(\sigma^{-1}) | \mathcal{O}(\sigma) \rangle \equiv |\mathcal{O}(\sigma)|^2 = \sum_{\gamma_1, \gamma_2 \in H} \delta(\gamma_1 \sigma \gamma_2 \sigma^{-1}) = \prod_{i,j=1}^p n_{ij}(\sigma)!, \quad (\text{J.1})$$

which is the magnitude squared of a Gauss graph $\mathcal{O}(\sigma)$. This formula is derived in [98]. Recall that $n_{ij}(\sigma)$ is the number of strings starting from the i 'th giant and ending on the j 'th giant. We also recall that $H \equiv S_{m_1} \times S_{m_2} \times \cdots \times S_{m_p}$ is the largest permutation group that leaves the Gauss graph label $\sigma \in H \backslash S_m / H$ invariant. In this discussion, consider a concrete example and use it to define our notation. Accordingly, consider the Gauss graph



Figure J.1: This Gauss graph is one of the double coset elements defined by the charge $\vec{m} = [2, 4]$. One possible label is $\sigma = (1, 4)(2, 3)$.

This Gauss graph corresponds to an element $\sigma \in H \backslash S_6 / H$, where $H = S_2 \times S_4$. It is useful to consider the following representation of a Gauss graph

¹Recall that $\delta(\rho) = 1$ if only if ρ is the identity of S_m otherwise it is equal to zero.

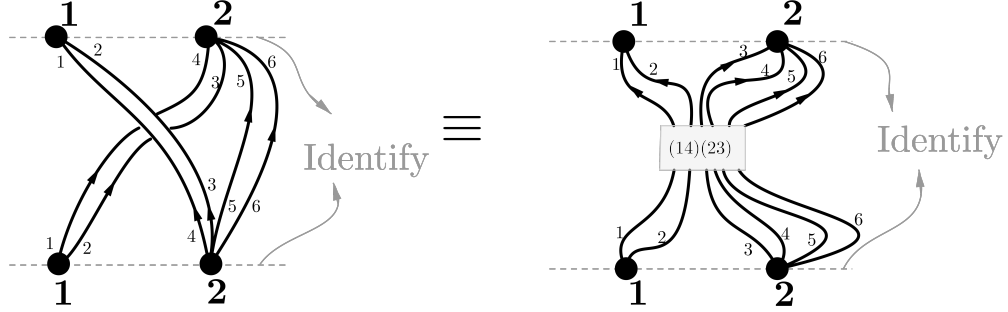


Figure J.2: Above, the two dashed horizontal lines are identified. In doing so, this Gauss graph is another graphic representation of the Gauss graph in Figure J.1

A generic Gauss graph, specified by the charge $\vec{m} = [m_1, m_2, \dots, m_p]^2$ is

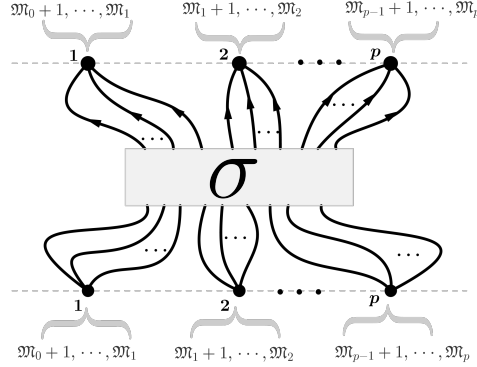


Figure J.3: Illustration of a generic Gauss graph label by $\sigma \in H \backslash S_m / H$. Again the two dashed horizontal lines are identified.

In figure J.3, there are a total of m strings stretching between the p - giant gravitons. The black nodes on the dashed-horizontal lines represent the giants. These two lines are identified. We label the giants by the integers in the range $\{1, \dots, p\}$. In this way, labels of the string end points attached to the I 'th giant

²Recall that, by definition $\sum_{i=1}^p m_i = m$.

take values in the set $\{\mathfrak{M}_{I-1} + 1, \dots, \mathfrak{M}_I\}$, where

$$\mathfrak{M}_0 \equiv 0, \quad \mathfrak{M}_K = \sum_{i=1}^K m_i. \quad (\text{J.2})$$

According to the above discussion, it follows that $\mathfrak{M}_p = m$. σ in Figure J.3 permutes the integers labeling the starting points of the strings and maps them to the integers labeling the ending points of the strings. For a concrete example see Figure J.2. We can now prove (J.1).

Proof. Note that the terms summed in (J.1) can be written as

$$\sum_{\gamma_i \in H} \delta_{\tilde{G}_{\gamma_i}, G_\sigma}. \quad (\text{J.3})$$

Trade the $\delta(\cdot)$ function in (J.1) for a Kronecker delta. The sum in (J.3) is counting how many times $\tilde{G}_{\gamma_i} = G_\sigma$. The Gauss graph has a symmetry that we now explain. If we fix the permutation $\gamma_i \in H$, the graph for \tilde{G}_{γ_i} is the same as the Gauss graph configuration labeled by $\gamma_1 \sigma \gamma_2$. In terms of pictures we manipulate the graph \tilde{G}_{γ_i} as follow

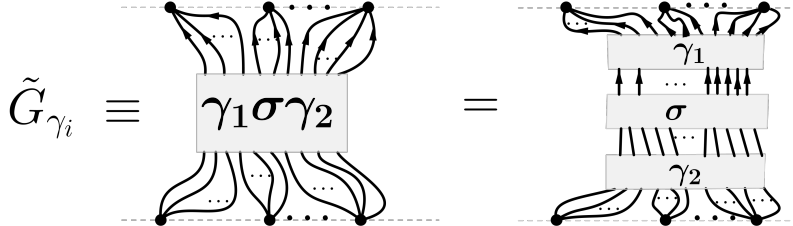


Figure J.4: Graphical manipulation of the Gauss graph labeled by $\gamma_1 \sigma \gamma_2$ and its relation to the Gauss graph labeled by σ .

Accordingly, the graph \tilde{G}_{γ_i} is the same configuration as that obtained from Gauss graph G_σ . The sum (J.3) is counting the elements $\gamma_i \in H$ that satisfy the graph equality $\tilde{G}_{\gamma_i} = G_\sigma$.

Recall that $n_{ij}(\sigma)$ counts the number of strings starting from the i 'th giant and end at the j 'th giant. Hence, the following cases are clear:

- Given a Gauss graphs $\mathcal{O}(\sigma)$ with

$$0 \leq n_{ij}(\sigma) \leq 1, \quad \forall i, j = 1, \dots, p \quad (\text{J.4})$$

the only element $\gamma_i \in H$ such that $G_{\gamma_i} = G_\sigma$ are $\gamma_1 = \gamma_2 = \mathbf{1}_H$. In this case the sum (J.3) is trivially equal to 1 and the magnitude of the corresponding Gauss graph is

$$|\mathcal{O}(\sigma)|^2 = \prod_{i,j=1}^p n_{ij}(\sigma)! = 1. \quad (\text{J.5})$$

- If a Gauss graph $\mathcal{O}(\sigma)$ has

$$n_{ij}(\sigma) \geq 1, \quad (\text{J.6})$$

then the $\gamma_1, \gamma_2 \in H$ that contribute to the sum in (J.3) belong to two isomorphic subgroups of H with order $n_{ij}(\sigma)!$.

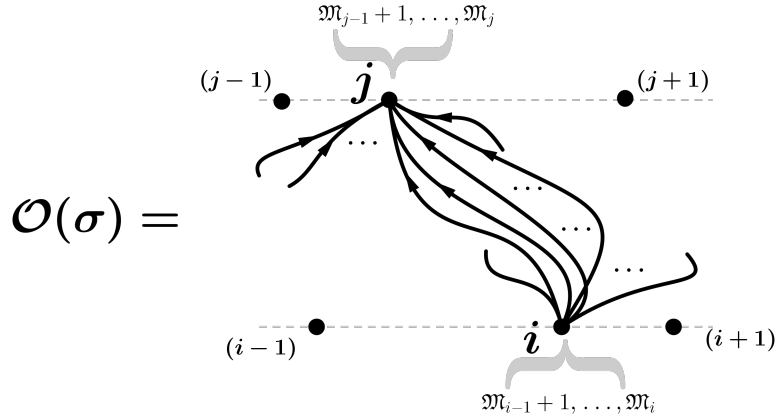


Figure J.5: Above, we have only illustrated the n_{ij} parallel strings stretching from the i 'th giant to the j 'th giant. The $n_{ij} + n_{ij}$ different integers labeling these strings belong respectively to $\{M_{i-1} + 1, \dots, M_i\}$ for the starting points and $\{M_{j-1} + 1, \dots, M_j\}$ for the ending points.

Accordingly, the permutation subgroups H_i and H_j are respectively constructed from the n_{ij} integers in $\{M_{i-1} + 1, \dots, M_i\}$ and the n_{ij} integers in $\{M_{j-1} + 1, \dots, M_j\}$, which label the end points of the n_{ij} strings visible in Figure J.5.

This is the only source of symmetry so that

$$|\mathcal{O}(\sigma)|^2 = \prod_{i,j=1}^p n_{ij}(\sigma)! \quad (\text{J.7})$$

□

A straightforward example illustrating (J.1) is the trivial Gauss graph $\sigma = \mathbf{1}_{S_M}$ which is a BPS state. Given $U(1)^p$ charge $\vec{m} = [m_1, m_2, \dots, m_p]$, the BPS state has

$$n_{ij} = \begin{cases} m_i & i = j, \\ 0 & i \neq j. \end{cases} \quad (\text{J.8})$$

It follows that

$$|\mathcal{O}(\mathbf{1})|^2 = |H| = \prod_{i=1}^p m_i!. \quad (\text{J.9})$$

This is indeed correct since H itself leaves the graph invariant.

Appendix K

The projective null cone in $D = 6$ and CFT in $\mathbb{R}^{1,3}$

We review the connection between conformal transformations in $\mathbb{R}^{1,3}$ and Lorentz rotations in $\mathbb{R}^{2,4}$. Our convention¹ for the metric of $\mathbb{R}^{2,4}$ is

$$\eta_{MN} \equiv \begin{bmatrix} -1 & 0 & 0 & 0 & 0 & 0 \\ 0 & 1 & 0 & 0 & 0 & 0 \\ 0 & 0 & 1 & 0 & 0 & 0 \\ 0 & 0 & 0 & 1 & 0 & 0 \\ 0 & 0 & 0 & 0 & 1 & 0 \\ 0 & 0 & 0 & 0 & 0 & -1 \end{bmatrix}_{MN}. \quad (\text{K.1})$$

The coordinates in $\mathbb{R}^{2,4}$ are X^M . The main idea of the projective null cone is to embed our physical 4-dimensional space $\mathbb{R}^{1,3}$ in $\mathbb{R}^{2,4}$. Let $x^\mu|_{\mu=0,\dots,3}$ be the coordinates of spacetime $\mathbb{R}^{1,3}$. There are two extra dimensions in the 6-dimensional space that we have to project out if we want to return to lower dimensional space. A simple way - due to Dirac [99] - to remove dimensions in an $\text{SO}(2,4)$ covariant way is to restrict to the subspace $\{X^M\}$ defined by

$$\eta_{MN} X^M X^N = 0. \quad (\text{K.2})$$

¹The indices $M, N \dots$ run from $0, \dots, 5$

The set of points $\{X^M\}$ satisfying (K.2) defines a light cone in $\mathbb{R}^{2,4}$. To build some geometrical intuition expand (K.2) as

$$(X^0)^2 + (X^5)^2 = (X^1)^2 + (X^2)^2 + (X^3)^2 + (X^4)^2. \quad (\text{K.3})$$

A geometrical representation of this light cone is given in the following figure.

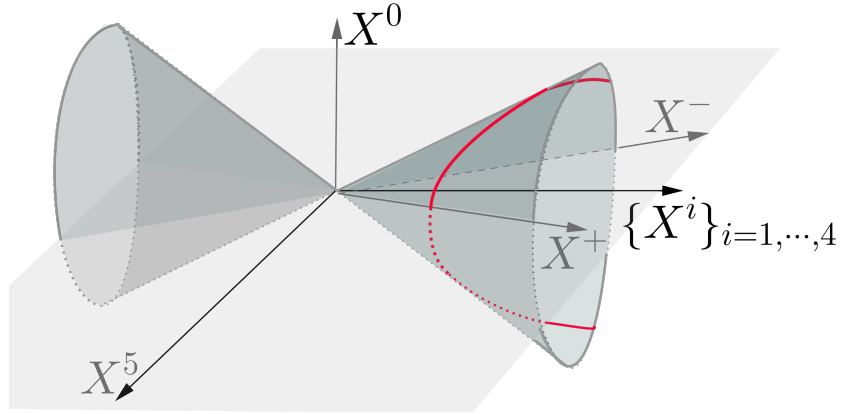


Figure K.1: This figure gives an illustration of the light cone of the spacetime $\mathbb{R}^{2,4}$. The red section line is identified with the 4-dimensional spacetime $\mathbb{R}^{1,3}$. X^\pm are light cone coordinates defined by $X^\pm = \frac{X^5 \pm X^4}{\sqrt{2}}$.

We will use the canonical basis² $\mathcal{B} \equiv \{\mathbf{e}_M\}_{M=0,\dots,5}$ for the spacetime $\mathbb{R}^{2,4}$. The \mathbf{e}_M 's are 6-dimensional column vectors with components

$$(\mathbf{e}_M)^N = \delta_M^N. \quad (\text{K.4})$$

An equivalent matrix representation suggested by the light cone is to use light cone coordinates. Toward this end, define the light cone basis vectors³ $\hat{\mathcal{B}} \equiv \{\hat{\mathbf{e}}_{\hat{M}}\}$ where

$$\hat{\mathbf{e}}_\mu = \mathbf{e}_\mu, \quad , \quad \hat{\mathbf{e}}_- = \frac{\mathbf{e}_5 - \mathbf{e}_4}{\sqrt{2}}, \quad \hat{\mathbf{e}}_+ = \frac{\mathbf{e}_5 + \mathbf{e}_4}{\sqrt{2}}. \quad (\text{K.5})$$

²More precisely, one also needs to consider the dual basis $\mathcal{B}^* \equiv \{\mathbf{e}_M^*\}_{M=0,\dots,5}$, where $\mathbf{e}_{0,5}^* = -\mathbf{e}_{0,5}^T$ and $\mathbf{e}_i^*|_{i=1,\dots,4} = \mathbf{e}_i^T|_{i=1,\dots,4}$ - with T : signifies taking the transpose.

³All hatted indices \hat{M}, \hat{N}, \dots take value in $\{0, 1, 2, 3, -, +\}$

In this light cone basis the metric of $\mathbb{R}^{2,4}$ becomes

$$\hat{\eta} \equiv [\hat{\eta}_{\hat{M}\hat{N}}] = \begin{bmatrix} -1 & 0 & 0 & 0 & 0 & 0 \\ 0 & 1 & 0 & 0 & 0 & 0 \\ 0 & 0 & 1 & 0 & 0 & 0 \\ 0 & 0 & 0 & 1 & 0 & 0 \\ 0 & 0 & 0 & 0 & 0 & -1 \\ 0 & 0 & 0 & 0 & -1 & 0 \end{bmatrix}. \quad (\text{K.6})$$

Indeed,

$$\begin{aligned} ds^2 &= \eta_{MN} dX^M dX^N \\ &= -(dX^0)^2 + (dX^1)^2 + (dX^2)^2 + (dX^3)^2 + (dX^4)^2 - (dX^5)^2, \\ &= -(dX^0)^2 + (dX^1)^2 + (dX^2)^2 + (dX^3)^2 - 2dX^+ dX^-, \\ &= \hat{\eta}_{\hat{M}\hat{N}} dX^{\hat{M}} dX^{\hat{N}}, \end{aligned}$$

where

$$X^\pm = \frac{X^5 \pm X^4}{\sqrt{2}}.$$

Following [100], define a section

$$\begin{cases} X^\mu = x^\mu, \\ X^- = \frac{x^2}{2}, \\ X^+ = 1, \end{cases} \quad (\text{K.7})$$

where $x^2 = \eta_{\mu\nu} x^\mu x^\nu$. Equation (K.7) gives the parametric equation of the section illustrated as a red curve in Figure K.1. x^μ are the coordinates of the 4-dimensional spacetime $\mathbb{R}^{1,3}$. A generic section on the light cone is obtained by fixing⁴ $X^+ = f(x^\mu) = \text{const}$. We choose $f(x^\mu) = 1$ for simplicity. The motivation for considering the section (K.7) is now explained. Following [100], the image of a point on the section with coordinate $x^\mu \in \mathbb{R}^{1,3}$ after the action of some Lorentz rotation $\Lambda \in SO(2, 4)$ is another point x'^μ on the section. This follows because the light cone has isometry group $SO(2, 4)$. It follows that any point x^μ on the section is mapped by $\Lambda \in SO(2, 4)$ back to the light cone

⁴ f is a function only depending on the coordinates $x^\mu \in \mathbb{R}^{1,3}$

but not necessarily on the section itself. One has to perform a rescaling $\lambda(X)$ to get back to the section. The two successive transformations reproduce the conformal transformations in $\mathbb{R}^{1,3}$. Consider the induced metric on the section

$$\hat{s}^2 = dx_\mu dx^\mu - 2dX^+ dX^- \Big|_{X^+ = f(x^\mu), X^- = \frac{x_\mu x^\nu}{2f(x^\mu)}}. \quad (\text{K.8})$$

For the moment allow $f(x^\mu) \neq 1$ so that our discussion is general.

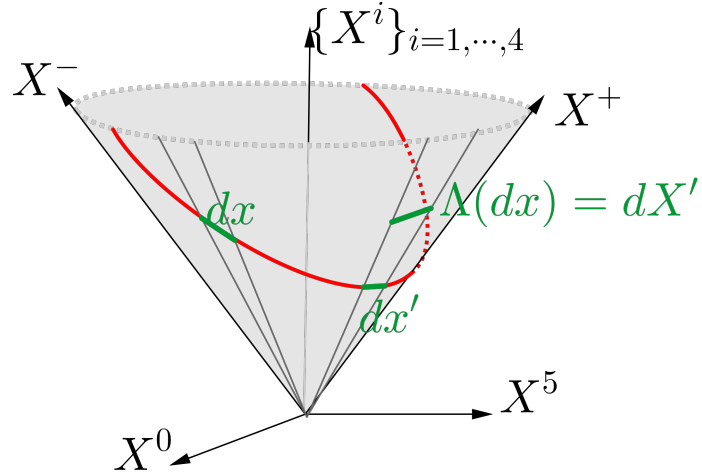


Figure K.2: Illustration of the action of $\Lambda \in SO(2, 4)$ followed by rescaling $\lambda(X)$ on a small displacement in the section of the light cone, which is identified to be the 4-dimensional space $\mathbb{R}^{1,3}$.

Assume that the action of Λ maps $x^\mu \rightarrow X'^\mu$, $X^+ \rightarrow X'^+ = f(X'^\rho)$ and $X'^- = \frac{X'_\mu X'^\mu}{2f(X'^\rho)}$. The point X' is not necessarily on the section $\mathbb{R}^{1,3}$. To return to the section $\mathbb{R}^{1,3}$ we have to perform a rescaling $\lambda(X')$. Performing a scale transformation $X' \rightarrow \lambda(X')X'$ at each point on the light cone is an homogeneous transformation. To understand this, consider

$$\begin{aligned} d[\lambda(X')X'] \cdot d[\lambda(X')X'] &= [\lambda(X')dX + (dX'_M \partial^M \lambda)X'] \cdot [\lambda(X')dX + (dX'_N \partial^N \lambda)X'], \\ &= \lambda^2 dX' \cdot dX', \end{aligned}$$

where we have used the fact that $X' \cdot dX' = X' \cdot X' = 0$ on the light cone. Using this homogeneity, we find

$$dX'_\mu dX'^\mu = (\lambda(X'))^2 dx'_\mu dx'^\mu, \quad (\text{K.9})$$

where x' are the coordinates of the section $\mathbb{R}^{1,3}$. To complete the argument, return to the original definition of the section $\mathbb{R}^{1,3}$ by setting $f(x^\mu) = 1$ so that $dX^+ = 0$. Summarizing the above idea, after an action of $\Lambda \in SO(2, 4)$ followed by a rescaling $\lambda(X)$, one finds

$$ds^2 = (\lambda(x))^2 d\hat{s}'^2. \quad (\text{K.10})$$

This is indeed the definition of conformal transformations in $\mathbb{R}^{1,3}$.

K.1 Reproducing conformal transformations in $\mathbb{R}^{1,3}$

In this section we will reproduce some conformal transformations in $\mathbb{R}^{1,3}$ using $\Lambda \in SO(2, 4)$ followed by a scaling $\lambda(X)$. The group $SO(2, 4)$ is the set of 6×6 matrices, that satisfy

$$\Lambda^T \eta \Lambda = \eta, \quad \det(\Lambda) = 1, \quad (\text{K.11})$$

where Λ^T is the matrix transpose of Λ . Work in the light cone basis. A point P in $\mathbb{R}^{2,4}$ has light cone coordinates $\hat{P}^{\hat{M}} \equiv (P^\mu, P^-, P^+)$. Furthermore, if we restrict to a point P on the section $\mathbb{R}^{1,3}$, it has the light cone coordinates

$$\begin{cases} \hat{P}^\mu = x^\mu, \\ \hat{P}^- = \frac{x^2}{2}, \quad x^2 \equiv \eta_{\mu\nu} x^\mu x^\nu, \\ \hat{P}^+ = 1. \end{cases} \quad (\text{K.12})$$

Introduce a four vector $b^\mu \equiv [b^0, b^1, b^2, b^3]^T$ and construct the matrix $\hat{\Lambda}_{\text{SCT}}$ such that

$$\hat{\Lambda}_{\text{SCT}} = \begin{bmatrix} \mathbb{1}_{4 \times 4} & b^\mu & 0 \\ 0 & 1 & 0 \\ b_\mu & \frac{b_\mu b^\mu}{2} & 1 \end{bmatrix} = \begin{bmatrix} 1 & 0 & 0 & 0 & b^0 & 0 \\ 0 & 1 & 0 & 0 & b^1 & 0 \\ 0 & 0 & 1 & 0 & b^2 & 0 \\ 0 & 0 & 0 & 1 & b^3 & 0 \\ 0 & 0 & 0 & 0 & 1 & 0 \\ -b^0 & b^1 & b^2 & b^3 & \frac{b_\mu b^\mu}{2} & 1 \end{bmatrix}. \quad (\text{K.13})$$

This matrix obeys

$$\det(\tilde{\Lambda}_{\text{SCT}}) = 1 \quad (\text{K.14})$$

and

$$(\hat{\Lambda}_{\text{SCT}})^T \hat{\eta} \hat{\Lambda}_{\text{SCT}} = \hat{\eta}.$$

and so it is an element of the group $SO(2, 4)$.

Consider the transformation of the point P on the section defined in (K.12).

We have

$$\begin{bmatrix} \hat{P}'^\mu \\ \hat{P}'^- \\ \hat{P}'^+ \end{bmatrix} = \begin{bmatrix} \mathbb{1}_{4 \times 4} & b^\mu & 0 \\ 0 & 1 & 0 \\ b_\mu & \frac{b_\mu b^\mu}{2} & 1 \end{bmatrix} \begin{bmatrix} x^\mu \\ \frac{x^2}{2} \\ 1 \end{bmatrix}, \quad (\text{K.15})$$

$$\Rightarrow \hat{P}'^{\hat{M}'} = \begin{cases} \hat{P}'^\mu = x^\mu + \frac{b^\mu}{2} x^2 \\ \hat{P}'^- = \frac{x^2}{2} \\ \hat{P}'^+ = 1 + b_\mu x^\mu + \frac{b_\mu b^\mu}{4} x^2. \end{cases} \quad (\text{K.16})$$

The point $\hat{P}'^{\hat{M}'} \equiv (\hat{\Lambda}_{\text{SCT}})_{\hat{N}}^{\hat{M}'} \hat{P}^{\hat{N}}$, is on the light cone but does not belong to the section $\mathbb{R}^{1,3}$. Indeed,

$$\begin{aligned} \hat{P}'_\mu \hat{P}'^\mu - 2\hat{P}'^- \hat{P}'^+ &= \left(x_\mu + \frac{b_\mu}{2} x^2 \right) \cdot \left(x^\mu + \frac{b^\mu}{2} x^2 \right) - 2 \frac{x^2}{2} \left(1 + b_\mu x^\mu + \frac{b_\mu b^\mu}{4} x^2 \right), \\ &= x^2 \left(1 + x \cdot b + \frac{b \cdot b x^2}{4} \right) - x^2 \left(1 + b_\mu x^\mu + \frac{b_\mu b^\mu}{4} x^2 \right) = 0. \end{aligned}$$

Knowing that $\hat{P}'^{\hat{M}'}$ lives on the light cone, we can rescale by $\lambda(\hat{P}')$ to recover $\mathbb{R}^{1,3}$. To do this

$$\lambda(\hat{P}') = \frac{1}{\hat{P}'^+}, \quad (\text{K.17})$$

to yield

$$\hat{P}''^\mu \equiv x'^\mu = \frac{x^\mu + \frac{b^\mu}{2} x^2}{1 + b \cdot x + x^2 \frac{b \cdot b}{4}} \quad (\text{K.18})$$

$$\hat{P}''^- = \frac{x^2}{2(1 + b \cdot x + x^2 \frac{b \cdot b}{4})} \quad (\text{K.19})$$

$$\hat{P}''^+ = 1. \quad (\text{K.20})$$

Define $a_\mu = \frac{b_\mu}{2}$, (K.18) becomes

$$x'^\mu = \frac{x^\mu + a^\mu}{1 + 2x \cdot a + a^2 x^2}. \quad (\text{K.21})$$

This is a special conformal transformation in $\mathbb{R}^{1,3}$.

Now, consider a translation. To reproduce a translation in $\mathbb{R}^{1,3}$ from an element $\hat{\Lambda} \in SO(2, 4)$ consider the matrix

$$\hat{\Lambda}_T = \begin{bmatrix} \mathbb{1}_{4 \times 4} & 0 & b^\mu \\ b_\mu & 1 & \frac{b_\mu b^\mu}{2} \\ 0 & 0 & 1 \end{bmatrix} = \begin{bmatrix} 1 & 0 & 0 & 0 & 0 & b^0 \\ 0 & 1 & 0 & 0 & 0 & b^1 \\ 0 & 0 & 1 & 0 & 0 & b^2 \\ 0 & 0 & 0 & 1 & 0 & b^3 \\ -b^0 & b^1 & b^2 & b^3 & 1 & \frac{b_\mu b^\mu}{2} \\ 0 & 0 & 0 & 0 & 0 & 1 \end{bmatrix}. \quad (\text{K.22})$$

$\hat{\Lambda}_T$ is an element of $SO(2, 4)$. After the action of this matrix on a point in the section

$$\begin{bmatrix} \hat{P}'^\mu \\ \hat{P}'^- \\ \hat{P}'^+ \end{bmatrix} = \begin{bmatrix} \mathbb{1}_{4 \times 4} & 0 & b^\mu \\ b_\mu & 1 & \frac{b_\mu b^\mu}{2} \\ 0 & 0 & 1 \end{bmatrix} \begin{bmatrix} x^\mu \\ \frac{x^2}{2} \\ 1 \end{bmatrix}, \quad (\text{K.23})$$

$$\Rightarrow \hat{P}'^{\hat{M}'} = \begin{cases} \hat{P}'^\mu \equiv x'^\mu &= x^\mu + b^\mu \\ \hat{P}'^- &= \frac{x^2}{2} + b_\mu x^\mu + \frac{b_\mu b^\mu}{2} = \frac{1}{2}(x_\mu + b_\mu) \cdot (x^\mu + b^\mu) \\ \hat{P}'^+ &= 1. \end{cases} \quad (\text{K.24})$$

It is straightforward to see that the above matrix $\hat{\Lambda}_T$ maps $\hat{P}^{\hat{M}} \in \mathbb{R}^{1,3}$ to another point $\hat{P}'^{\hat{M}'}$ which is already on the section $\mathbb{R}^{1,3}$. Moreover, if we restrict to the x^μ -direction then (K.24) tells us that $\hat{\Lambda}$ translates $x^\mu \in \mathbb{R}^{1,3}$ by b^μ on the section $\mathbb{R}^{1,3}$.

Finally, consider a dilatation in $\mathbb{R}^{1,3}$. Use

$$\hat{\Lambda}_D = \begin{bmatrix} 1 & 0 & 0 & 0 & 0 & 0 \\ 0 & 1 & 0 & 0 & 0 & 0 \\ 0 & 0 & 1 & 0 & 0 & 0 \\ 0 & 0 & 0 & 1 & 0 & 0 \\ 0 & 0 & 0 & 0 & e^{-\phi} & 0 \\ 0 & 0 & 0 & 0 & 0 & e^\phi \end{bmatrix}, \quad (K.25)$$

where ϕ is some real parameter. The action of this matrix on a point \hat{P} in the section $\mathbb{R}^{1,3}$ gives

$$\hat{P}'^{\hat{M}} = \begin{cases} \hat{P}'^\mu &= x^\mu \\ \hat{P}'^- &= e^{-\phi} \frac{x^2}{2} \\ \hat{P}'^+ &= e^\phi. \end{cases} \quad (K.26)$$

It follows that one has to rescale by

$$\lambda(\hat{P}') = \frac{1}{\hat{P}'^+} = e^{-\phi} \quad (K.27)$$

in order to get back to the section $\mathbb{R}^{1,3}$. After rescaling we find

$$\hat{P}''^{\hat{M}} = \begin{cases} x'^\mu &= e^{-\phi} x^\mu \\ \hat{P}''^- &= e^{-2\phi} \frac{x^2}{2} \\ \hat{P}''^+ &= 1. \end{cases} \quad (K.28)$$

Again, restricting to the x^μ -direction the action of $\hat{\Lambda}_D$ followed by rescaling produces dilatation transformations in $\mathbb{R}^{1,3}$. $\hat{\Lambda}_D$ takes a special form if we rotate back to the canonical basis representation using the matrix \mathcal{M} defined from the change of basis (K.5)

$$\Lambda_D = \mathcal{M}^{-1} \hat{\Lambda}_D \mathcal{M} = \begin{bmatrix} 1 & 0 & 0 & 0 & 0 & 0 \\ 0 & 1 & 0 & 0 & 0 & 0 \\ 0 & 0 & 1 & 0 & 0 & 0 \\ 0 & 0 & 0 & 1 & 0 & 0 \\ 0 & 0 & 0 & 0 & \cosh(\phi) & \sinh(\phi) \\ 0 & 0 & 0 & 0 & \sinh(\phi) & \cosh(\phi) \end{bmatrix}. \quad (K.29)$$

Since, the direction X^5 is timelike in $\mathbb{R}^{2,4}$, the relation (K.29) shows that a boost along the direction X^4 with parameter ϕ in the canonical basis gives rise to a scaling transformation in $\mathbb{R}^{1,3}$.

Appendix L

Review of the two point CFT correlation function

In this Appendix, we review the two point functions of primary operators in CFT. Concretely, we argue that given two spin-zero primary operators \mathcal{O}_1 and \mathcal{O}_2 with classical dimensions Δ_1 and Δ_2 ,

$$\langle \mathcal{O}_1(x) \mathcal{O}_2(y) \rangle = \frac{\delta_{\Delta_1, \Delta_2}}{|x - y|^{\Delta_1 + \Delta_2}}. \quad (\text{L.1})$$

The action of a conformal transformation g on a primary field with non-trivial spin in D -dimensional spacetime is

$$U(g) \mathcal{O}^A(x) U^\dagger(g) = L_B^A(g) \left| \frac{\partial x}{\partial x'} \right|^{\frac{2}{D}} \mathcal{O}_1^B(g^{-1}x) = \mathcal{O}'^A(x'), \quad (\text{L.2})$$

where $U(g)$ is an unitary representation of the conformal group. $L_B^A(g)$ is a finite dimensional matrix. More precisely, $L_B^A(g)$ is an irreducible representation specifying the spin transformation under the orbital transformation $x^\mu \rightarrow [g^{-1}]^\mu{}_\nu x^\nu$. Close to the identity this transformation take the form

$$\mathcal{O}'^A(x') = \mathcal{O}^A(x) + \delta \mathcal{O}^A(x). \quad (\text{L.3})$$

In addition, we assume that conformal symmetry is not spontaneously broken, i.e. the vacuum state is invariant under conformal transformations

$$U(g)|0\rangle = |0\rangle. \quad (\text{L.4})$$

With the above assumptions, the statement of conformal invariance of correlation functions is

$$\begin{aligned}
\langle 0 | \mathcal{O}_1^{A_1}(x_1) \mathcal{O}_2^{A_2}(x_2) \cdots \mathcal{O}_n^{A_n}(x_n) | 0 \rangle &= \langle 0 | \mathcal{O}'_1^{A_1}(x'_1) \mathcal{O}'_2^{A_2}(x'_2) \cdots \mathcal{O}'_n^{A_n}(x'_n) | 0 \rangle, \\
&= \langle 0 | U^\dagger(g) U(g) \mathcal{O}_1^{A_1}(x_1) U^\dagger(g) U(g) \mathcal{O}_2^{A_2}(x_2) U^\dagger(g) \cdots U(g) \mathcal{O}_n^{A_n}(x_n) U^\dagger(g) U(g) | 0 \rangle, \\
&= \langle 0 | \mathcal{O}_1^{A_1}(x_1) \mathcal{O}_2^{A_2}(x_2) \cdots \mathcal{O}_n^{A_n}(x_n) | 0 \rangle + \langle 0 | \delta \mathcal{O}_1^{A_1}(x_1) \mathcal{O}_2^{A_2}(x_2) \cdots \mathcal{O}_n^{A_n}(x_n) | 0 \rangle \\
&\quad \langle 0 | \mathcal{O}_1^{A_1}(x_1) \delta \mathcal{O}_2^{A_2}(x_2) \cdots \mathcal{O}_n^{A_n}(x_n) | 0 \rangle + \cdots + \langle 0 | \mathcal{O}_1^{A_1}(x_1) \mathcal{O}_2^{A_2}(x_2) \cdots \delta \mathcal{O}_n^{A_n}(x_n) | 0 \rangle.
\end{aligned}$$

It follows that

$$\begin{aligned}
\langle 0 | \delta \mathcal{O}_1^{A_1}(x_1) \mathcal{O}_2^{A_2}(x_2) \cdots \mathcal{O}_n^{A_n}(x_n) | 0 \rangle + \langle 0 | \mathcal{O}_1^{A_1}(x_1) \delta \mathcal{O}_2^{A_2}(x_2) \cdots \mathcal{O}_n^{A_n}(x_n) | 0 \rangle + \cdots \\
+ \cdots + \langle 0 | \mathcal{O}_1^{A_1}(x_1) \mathcal{O}_2^{A_2}(x_2) \cdots \delta \mathcal{O}_n^{A_n}(x_n) | 0 \rangle = 0. \tag{L.5}
\end{aligned}$$

Now we use (L.5) to prove (L.1). First, simplify our notation as

$$\langle \mathcal{O}_1^{A_1}(x_1) \mathcal{O}_2^{A_2}(x_2) \cdots \mathcal{O}_n^{A_n}(x_n) \rangle \equiv \langle 0 | \mathcal{O}_1^{A_1}(x_1) \mathcal{O}_2^{A_2}(x_2) \cdots \mathcal{O}_n^{A_n}(x_n) | 0 \rangle. \tag{L.6}$$

Using the above identities, we start by requiring translation invariance. Focus on the two point function. The translation invariance coming from (L.5) is

$$\langle \delta \mathcal{O}_1(x) \mathcal{O}_2(y) \rangle + \langle \mathcal{O}_1(x) \delta \mathcal{O}_2(y) \rangle = a^\mu \left(\frac{\partial}{\partial x^\mu} + \frac{\partial}{\partial y^\mu} \right) \langle \mathcal{O}_1(x) \mathcal{O}_2(y) \rangle = 0. \tag{L.7}$$

This equation implies that $\langle \mathcal{O}_1(x) \mathcal{O}_2(y) \rangle$ must be a function of the difference $x^\mu - y^\mu$, i.e.

$$\langle \mathcal{O}_1(x) \mathcal{O}_2(y) \rangle \sim f(x^\mu - y^\mu). \tag{L.8}$$

Next, by requiring Lorentz invariance, it is not difficult to argue that f is a function of the magnitude of the distance

$$\langle \mathcal{O}_1(x) \mathcal{O}_2(y) \rangle \sim f(|x - y|). \tag{L.9}$$

Scaling invariance implies

$$\lambda^{\Delta_1 + \Delta_2} f(\lambda|x - y|) = f(|x - y|). \tag{L.10}$$

Thus

$$f(|x - y|) = \frac{\text{const.}}{|x - y|^{\Delta_1 + \Delta_2}}. \tag{L.11}$$

To determine the constant in the numerator we require invariance under a special conformal transformation (SCT) of this function. Recall that a SCT is a composition of an inversion followed by a translation and then a second inversion. The constraints following from invariance under special conformal transformations are most easily obtained by requiring invariance under inversion. The inversion transformation is

$$x^\mu \rightarrow x'^\mu = \frac{x^\mu}{x \cdot x}.$$

Thus, the action of an inversion on the field is

$$\mathcal{O}'_\Delta(x') = \left| \frac{\partial x}{\partial x'} \right|^{\frac{\Delta}{D}} \mathcal{O}_\Delta(x) = \frac{1}{(x'^2)^\Delta} \mathcal{O}_\Delta(x). \quad (\text{L.12})$$

The implication of this for the two point functions is

$$\langle \mathcal{O}'_1(x') \mathcal{O}'_2(y') \rangle = \frac{1}{(x'^2)^{\Delta_1}} \frac{1}{(y'^2)^{\Delta_2}} \langle \mathcal{O}_1(x) \mathcal{O}_2(y) \rangle. \quad (\text{L.13})$$

In terms of the function f in (L.11), the equation (L.13) becomes

$$\frac{(x'^2)^{\Delta_1} (y'^2)^{\Delta_2}}{|x' - y'|^{\Delta_1 + \Delta_2}} = \frac{1}{|x - y|^{\Delta_1 + \Delta_2}}. \quad (\text{L.14})$$

It is possible to verify the identity

$$\frac{1}{|x - y|^{\Delta_1 + \Delta_2}} = \left(\frac{x'^2 y'^2}{|x' - y'|^2} \right)^{\frac{\Delta_1 + \Delta_2}{2}} \quad (\text{L.15})$$

Hence, invariance under inversion implies

$$\frac{(x'^2)^{\Delta_1} (y'^2)^{\Delta_2}}{|x' - y'|^{\Delta_1 + \Delta_2}} = \left(\frac{x'^2 y'^2}{|x' - y'|^2} \right)^{\frac{\Delta_1 + \Delta_2}{2}}. \quad (\text{L.16})$$

This equation is only true if $\Delta_1 = \Delta_2$. Thus, after a normalization of the operators \mathcal{O}_i , we conclude that

$$\langle \mathcal{O}_1(x) \mathcal{O}_2(y) \rangle = \frac{\delta_{\Delta_1, \Delta_2}}{|x - y|^{\Delta_1 + \Delta_2}}. \quad (\text{L.17})$$

References

- [1] David Berenstein. On the central charge extension of the $\mathcal{N} = 4$ SYM spin chain. *JHEP*, 05:129, 2015, 1411.5921.
- [2] Gerard 't Hooft. A Planar Diagram Theory for Strong Interactions. *Nucl. Phys.*, B72:461, 1974.
- [3] Steve Corley, Antal Jevicki, and Sanjaye Ramgoolam. Exact correlators of giant gravitons from dual N=4 SYM theory. *Adv. Theor. Math. Phys.*, 5:809–839, 2002, hep-th/0111222.
- [4] John McGreevy, Leonard Susskind, and Nicolaos Toumbas. Invasion of the giant gravitons from Anti-de Sitter space. *JHEP*, 06:008, 2000, hep-th/0003075.
- [5] Akikazu Hashimoto, Shinji Hirano, and N. Itzhaki. Large branes in AdS and their field theory dual. *JHEP*, 08:051, 2000, hep-th/0008016.
- [6] Marcus T. Grisaru, Robert C. Myers, and Oyvind Tafjord. SUSY and goliath. *JHEP*, 08:040, 2000, hep-th/0008015.
- [7] Robert de Mello Koch, Jelena Smolic, and Milena Smolic. Giant Gravitons - with Strings Attached (I). *JHEP*, 06:074, 2007, hep-th/0701066.
- [8] Robert de Mello Koch, Jelena Smolic, and Milena Smolic. Giant Gravitons - with Strings Attached (II). *JHEP*, 09:049, 2007, hep-th/0701067.
- [9] David Bekker, Robert de Mello Koch, and Michael Stephanou. Giant Gravitons - with Strings Attached. III. *JHEP*, 02:029, 2008, 0710.5372.

REFERENCES

- [10] Rajsekhar Bhattacharyya, Storm Collins, and Robert de Mello Koch. Exact Multi-Matrix Correlators. *JHEP*, 03:044, 2008, 0801.2061.
- [11] Rajsekhar Bhattacharyya, Robert de Mello Koch, and Michael Stephanou. Exact Multi-Restricted Schur Polynomial Correlators. *JHEP*, 06:101, 2008, 0805.3025.
- [12] Niklas Beisert. The $SU(2-2)$ dynamic S-matrix. *Adv. Theor. Math. Phys.*, 12:948–979, 2008, hep-th/0511082.
- [13] Niklas Beisert. The Analytic Bethe Ansatz for a Chain with Centrally Extended $su(2-2)$ Symmetry. *J. Stat. Mech.*, 0701:P01017, 2007, nlin/0610017.
- [14] Vincent De Comarmond, Robert de Mello Koch, and Katherine Jefferies. Surprisingly Simple Spectra. *JHEP*, 02:006, 2011, 1012.3884.
- [15] Warren Carlson, Robert de Mello Koch, and Hai Lin. Nonplanar Integrability. *JHEP*, 03:105, 2011, 1101.5404.
- [16] Robert de Mello Koch, Matthias Dessein, Dimitrios Giataganas, and Christopher Mathwin. Giant Graviton Oscillators. *JHEP*, 10:009, 2011, 1108.2761.
- [17] Robert de Mello Koch, Gareth Kemp, and Stephanie Smith. From Large N Nonplanar Anomalous Dimensions to Open String Theory. *Phys. Lett.*, B711:398–403, 2012, 1111.1058.
- [18] Robert de Mello Koch, Gareth Kemp, Badr Awad Elseid Mohammed, and Stephanie Smith. Nonplanar integrability at two loops. *JHEP*, 10:144, 2012, 1206.0813.
- [19] Robert de Mello Koch, Stuart Graham, and Ilies Messamah. Higher Loop Nonplanar Anomalous Dimensions from Symmetry. *JHEP*, 02:125, 2014, 1312.6227.
- [20] Robert de Mello Koch and Sanjaye Ramgoolam. A double coset ansatz for integrability in AdS/CFT. *JHEP*, 06:083, 2012, 1204.2153.

REFERENCES

- [21] Diego M. Hofman and Juan Martin Maldacena. Reflecting magnons. *JHEP*, 11:063, 2007, 0708.2272.
- [22] Diego M. Hofman and Juan Martin Maldacena. Giant Magnons. *J. Phys.*, A39:13095–13118, 2006, hep-th/0604135.
- [23] Paolo Di Vecchia. Large N gauge theories and AdS / CFT correspondence. In *Superstrings and related matters. Proceedings, Spring Workshop, Trieste, Italy, March 22-30, 1999*, 1999, hep-th/9908148.
- [24] Anton Kapustin and Edward Witten. Electric-Magnetic Duality And The Geometric Langlands Program. *Commun. Num. Theor. Phys.*, 1:1–236, 2007, hep-th/0604151.
- [25] Ofer Aharony, Steven S. Gubser, Juan Martin Maldacena, Hirosi Ooguri, and Yaron Oz. Large N field theories, string theory and gravity. *Phys. Rept.*, 323:183–386, 2000, hep-th/9905111.
- [26] Edward Witten. Chern-Simons gauge theory as a string theory. *Prog. Math.*, 133:637–678, 1995, hep-th/9207094.
- [27] S.S. Gubser, I.R. Klebanov, and A.M. Polyakov. Gauge theory correlators from non-critical string theory. *Physics Letters B*, 428(12):105 – 114, 1998.
- [28] Edward Witten. Perturbative gauge theory as a string theory in twistor space. *Commun. Math. Phys.*, 252:189–258, 2004, hep-th/0312171.
- [29] G. C. Wick. The evaluation of the collision matrix. *Phys. Rev.*, 80:268–272, Oct 1950.
- [30] Kenneth G. Wilson. The renormalization group: Critical phenomena and the kondo problem. *Rev. Mod. Phys.*, 47:773–840, Oct 1975.
- [31] Philippe Di Francesco, P. Mathieu, and D. Sénéchal. *Conformal Field Theory*. Graduate Texts in Contemporary Physics. Springer, 1997.
- [32] R. Blumenhagen and E. Plauschinn. *Introduction to Conformal Field Theory: With Applications to String Theory*. Lecture Notes in Physics. Springer Berlin Heidelberg, 2009.

REFERENCES

- [33] F. A. Dolan and H. Osborn. Conformal four point functions and the operator product expansion. *Nucl. Phys.*, B599:459–496, 2001, hep-th/0011040.
- [34] F. A. Dolan and H. Osborn. Conformal partial waves and the operator product expansion. *Nucl. Phys.*, B678:491–507, 2004, hep-th/0309180.
- [35] Robert de Mello Koch and Sanjaye Ramgoolam. CFT_4 as $SO(4,2)$ -invariant TFT_2 . *Nucl. Phys.*, B890:302–349, 2014, 1403.6646.
- [36] Robert de Mello Koch and Sanjaye Ramgoolam. Interactions as a conformal intertwiners in 4D QFT. *JHEP*, 03:165, 2016, 1512.00652.
- [37] Riccardo Rattazzi, Vyacheslav S. Rychkov, Erik Tonni, and Alessandro Vichi. Bounding scalar operator dimensions in 4D CFT. *JHEP*, 12:031, 2008, 0807.0004.
- [38] Vyacheslav S. Rychkov and Alessandro Vichi. Universal Constraints on Conformal Operator Dimensions. *Phys. Rev.*, D80:045006, 2009, 0905.2211.
- [39] Riccardo Rattazzi, Slava Rychkov, and Alessandro Vichi. Bounds in 4D Conformal Field Theories with Global Symmetry. *J. Phys.*, A44:035402, 2011, 1009.5985.
- [40] F. A. Dolan and H. Osborn. Conformal Partial Waves: Further Mathematical Results. 2011, 1108.6194.
- [41] Slava Rychkov. Conformal Bootstrap in Three Dimensions? 2011, 1111.2115.
- [42] Duccio Pappadopulo, Slava Rychkov, Johnny Espin, and Riccardo Rattazzi. OPE Convergence in Conformal Field Theory. *Phys. Rev.*, D86:105043, 2012, 1208.6449.
- [43] Slava Rychkov and Pierre Yvernay. Remarks on the Convergence Properties of the Conformal Block Expansion. *Phys. Lett.*, B753:682–686, 2016, 1510.08486.

REFERENCES

- [44] Matthijs Hogervorst and Slava Rychkov. Radial Coordinates for Conformal Blocks. *Phys. Rev.*, D87:106004, 2013, 1303.1111.
- [45] Matthijs Hogervorst, Hugh Osborn, and Slava Rychkov. Diagonal Limit for Conformal Blocks in d Dimensions. *JHEP*, 08:014, 2013, 1305.1321.
- [46] David Eliecer Berenstein, Juan Martin Maldacena, and Horatiu Stefan Nastase. Strings in flat space and pp waves from N=4 superYang-Mills. *JHEP*, 04:013, 2002, hep-th/0202021.
- [47] Niklas Beisert et al. Review of AdS/CFT Integrability: An Overview. *Lett. Math. Phys.*, 99:3–32, 2012, 1012.3982.
- [48] David Berenstein, Diego H. Correa, and Samuel E. Vazquez. All loop BMN state energies from matrices. *JHEP*, 02:048, 2006, hep-th/0509015.
- [49] David Berenstein. A Toy model for the AdS / CFT correspondence. *JHEP*, 07:018, 2004, hep-th/0403110.
- [50] Hai Lin, Oleg Lunin, and Juan Martin Maldacena. Bubbling AdS space and 1/2 BPS geometries. *JHEP*, 10:025, 2004, hep-th/0409174.
- [51] Vijay Balasubramanian, Micha Berkooz, Asad Naqvi, and Matthew J. Strassler. Giant gravitons in conformal field theory. *JHEP*, 04:034, 2002, hep-th/0107119.
- [52] Steven Corley and Sanjaye Ramgoolam. Finite factorization equations and sum rules for BPS correlators in N=4 SYM theory. *Nucl. Phys.*, B641:131–187, 2002, hep-th/0205221.
- [53] Thomas William Brown, P. J. Heslop, and S. Ramgoolam. Diagonal multi-matrix correlators and BPS operators in N=4 SYM. *JHEP*, 02:030, 2008, 0711.0176.
- [54] Thomas William Brown, P. J. Heslop, and S. Ramgoolam. Diagonal free field matrix correlators, global symmetries and giant gravitons. *JHEP*, 04:089, 2009, 0806.1911.

REFERENCES

- [55] Yusuke Kimura and Sanjaye Ramgoolam. Branes, anti-branes and brauer algebras in gauge-gravity duality. *JHEP*, 11:078, 2007, 0709.2158.
- [56] Yusuke Kimura and Sanjaye Ramgoolam. Enhanced symmetries of gauge theory and resolving the spectrum of local operators. *Phys. Rev.*, D78:126003, 2008, 0807.3696.
- [57] Yusuke Kimura. Non-holomorphic multi-matrix gauge invariant operators based on Brauer algebra. *JHEP*, 12:044, 2009, 0910.2170.
- [58] Yusuke Kimura, Sanjaye Ramgoolam, and David Turton. Free particles from Brauer algebras in complex matrix models. *JHEP*, 05:052, 2010, 0911.4408.
- [59] Yusuke Kimura. Quarter BPS classified by Brauer algebra. *JHEP*, 05:103, 2010, 1002.2424.
- [60] Yusuke Kimura and Hai Lin. Young diagrams, Brauer algebras, and bubbling geometries. *JHEP*, 01:121, 2012, 1109.2585.
- [61] Yusuke Kimura. Correlation functions and representation bases in free N=4 Super Yang-Mills. *Nucl. Phys.*, B865:568–594, 2012, 1206.4844.
- [62] Yusuke Kimura. Non-planar operator mixing by Brauer representations. *Nucl. Phys.*, B875:790–807, 2013, 1302.6404.
- [63] Vijay Balasubramanian, David Berenstein, Bo Feng, and Min-xin Huang. D-branes in Yang-Mills theory and emergent gauge symmetry. *JHEP*, 03:006, 2005, hep-th/0411205.
- [64] Robert de Mello Koch, Grant Mashile, and Nicholas Park. Emergent Threebrane Lattices. *Phys. Rev.*, D81:106009, 2010, 1004.1108.
- [65] Pawel Caputa, Robert de Mello Koch, and Pablo Diaz. A basis for large operators in N=4 SYM with orthogonal gauge group. *JHEP*, 03:041, 2013, 1301.1560.
- [66] Pawel Caputa, Robert de Mello Koch, and Pablo Diaz. Operators, Correlators and Free Fermions for SO(N) and Sp(N). *JHEP*, 06:018, 2013, 1303.7252.

- [67] Pablo Diaz. Orthogonal Schurs for Classical Gauge Groups. *JHEP*, 10:228, 2013, 1309.1180.
- [68] Gareth Kemp. $SO(N)$ restricted Schur polynomials. *J. Math. Phys.*, 56(2):022302, 2015, 1405.7017.
- [69] Gareth Kemp. Restricted Schurs and correlators for $SO(N)$ and $Sp(N)$. *JHEP*, 08:137, 2014, 1406.3854.
- [70] Pablo Diaz. Novel charges in CFT's. *JHEP*, 09:031, 2014, 1406.7671.
- [71] David Berenstein. Giant gravitons: a collective coordinate approach. *Phys. Rev.*, D87(12):126009, 2013, 1301.3519.
- [72] David Berenstein and Eric Dzienkowski. Open spin chains for giant gravitons and relativity. *JHEP*, 08:047, 2013, 1305.2394.
- [73] David Berenstein. Sketches of emergent geometry in the gauge/gravity duality. *Fortsch. Phys.*, 62:776–785, 2014, 1404.7052.
- [74] David Berenstein and Eric Dzienkowski. Giant gravitons and the emergence of geometric limits in beta-deformations of $\mathcal{N} = 4$ SYM. *JHEP*, 01:126, 2015, 1408.3620.
- [75] Yusuke Kimura and Ryo Suzuki. Negative anomalous dimensions in $\mathcal{N} = 4$ SYM. *Nucl. Phys.*, B900:603–659, 2015, 1503.06210.
- [76] Vijay Balasubramanian, Min-xin Huang, Thomas S. Levi, and Asad Naqvi. Open strings from $N=4$ superYang-Mills. *JHEP*, 08:037, 2002, hep-th/0204196.
- [77] Sumit R. Das, Antal Jevicki, and Samir D. Mathur. Vibration modes of giant gravitons. *Phys. Rev.*, D63:024013, 2001, hep-th/0009019.
- [78] Ofer Aharony, Yaron E. Antebi, Micha Berkooz, and Ram Fishman. 'Hooley sheets': Pfaffians and subdeterminants as D-brane operators in large N gauge theories. *JHEP*, 12:069, 2002, hep-th/0211152.
- [79] David Berenstein. Shape and holography: Studies of dual operators to giant gravitons. *Nucl. Phys.*, B675:179–204, 2003, hep-th/0306090.

REFERENCES

- [80] David Berenstein, Diego H. Correa, and Samuel E. Vazquez. A Study of open strings ending on giant gravitons, spin chains and integrability. *JHEP*, 09:065, 2006, hep-th/0604123.
- [81] David Berenstein and Samuel E. Vazquez. Integrable open spin chains from giant gravitons. *JHEP*, 06:059, 2005, hep-th/0501078.
- [82] David Berenstein, Diego H. Correa, and Samuel E. Vazquez. Quantizing open spin chains with variable length: An Example from giant gravitons. *Phys. Rev. Lett.*, 95:191601, 2005, hep-th/0502172.
- [83] David Garner, Sanjaye Ramgoolam, and Congkao Wen. Thresholds of large N factorization in CFT_4 : exploring bulk spacetime in AdS_5 . *JHEP*, 11:076, 2014, 1403.5281.
- [84] J. A. Minahan and K. Zarembo. The Bethe ansatz for $N=4$ superYang-Mills. *JHEP*, 03:013, 2003, hep-th/0212208.
- [85] N. Beisert, C. Kristjansen, and M. Staudacher. The Dilatation operator of conformal $N=4$ superYang-Mills theory. *Nucl. Phys.*, B664:131–184, 2003, hep-th/0303060.
- [86] Robert C. Myers. Dielectric branes. *JHEP*, 12:022, 1999, hep-th/9910053.
- [87] Romuald A. Janik. The $AdS(5) \times S^{*5}$ superstring worldsheet S-matrix and crossing symmetry. *Phys. Rev.*, D73:086006, 2006, hep-th/0603038.
- [88] D. H. Correa and C. A. S. Young. Asymptotic Bethe equations for open boundaries in planar AdS/CFT . *J. Phys.*, A43:145401, 2010, 0912.0627.
- [89] Hai Lin. Relation between large dimension operators and oscillator algebra of Young diagrams. *Int. J. Geom. Meth. Mod. Phys.*, 12(04):1550047, 2015, 1407.7815.
- [90] Frederik Denef. Supergravity flows and D-brane stability. *JHEP*, 08:050, 2000, hep-th/0005049.
- [91] Abdelhamid Mohamed Adam Ali, Robert de Mello Koch, Nirina Hasina Tahiridimbisoa, and Augustine Larweh Mahu. Interacting Double Coset Magnons. *Phys. Rev.*, D93(6):065057, 2016, 1512.05019.

REFERENCES

- [92] Juan Martin Maldacena. The Large N limit of superconformal field theories and supergravity. *Int. J. Theor. Phys.*, 38:1113–1133, 1999, hep-th/9711200. [Adv. Theor. Math. Phys.2,231(1998)].
- [93] Jurgis Pasukonis and Sanjaye Ramgoolam. Quivers as Calculators: Counting, Correlators and Riemann Surfaces. *JHEP*, 04:094, 2013, 1301.1980.
- [94] Robert de Mello Koch, Nirina Hasina Tahiridimbisoa, and Christopher Mathwin. Anomalous Dimensions of Heavy Operators from Magnon Energies. *JHEP*, 03:156, 2016, 1506.05224.
- [95] Eric Dzienkowski. Excited States of Open Strings From $\mathcal{N} = 4$ SYM. *JHEP*, 12:036, 2015, 1507.01595.
- [96] Matthias Staudacher. The Factorized S-matrix of CFT/AdS. *JHEP*, 05:054, 2005, hep-th/0412188.
- [97] L. Freyhult, C. Kristjansen, and T. Mansson. Integrable spin chains with $U(1)^{**3}$ symmetry and generalized Lunin-Maldacena backgrounds. *JHEP*, 12:008, 2005, hep-th/0510221.
- [98] Robert de Mello Koch, Rocky Kreyfelt, and Stephanie Smith. Heavy Operators in Superconformal Chern-Simons Theory. *Phys. Rev.*, D90(12):126009, 2014, 1410.0874.
- [99] P. A. M. Dirac. Wave equations in conformal space. *Annals of Mathematics*, 37(2):429–442, 1936.
- [100] Slava Rychkov. EPFL Lectures on Conformal Field Theory in $D \geq 3$ Dimensions. 2016, 1601.05000.